

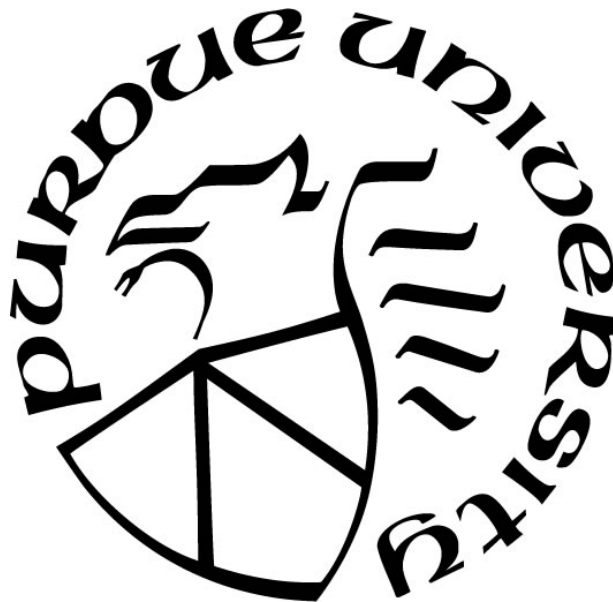
**PURIFICATION OF BRINE AND PRODUCED WATER USING
ACTIVATED CARBON COATED POLYURETHANE FOAM**

by
Ashreet Mishra

A Thesis

*Submitted to the Faculty of Purdue University
In Partial Fulfillment of the Requirements for the degree of*

Master of Science in Mechanical Engineering



Department of Mechanical and Civil Engineering

Hammond, Indiana

August 2019

**THE PURDUE UNIVERSITY GRADUATE SCHOOL
STATEMENT OF COMMITTEE APPROVAL**

Dr. George Nnanna, Chair

Department of Mechanical and Civil Engineering

Dr. Harvey Abramowitz, Co-Chair

Department of Mechanical and Civil Engineering

Dr. Chandramouli Viswanatha Chandramouli

Department of Mechanical and Civil Engineering

Dr. Xiuling Wang

Department of Mechanical and Civil Engineering

Approved by:

Dr. Chen Zhou

Head of the Graduate Program

This project is dedicated to my late grandfather Sri Purna Chandra Mishra, my late maternal grandfather Lakshmi Narayan Nanda who have inspired me along every step in my childhood. I would also like to dedicate this project to one of my very first teachers' late Shri Ranjan Behera who never lost faith in me and kept inspiring me in every step of my early education.

ACKNOWLEDGMENTS

I profoundly express my deepest gratitude to a lot of people that contributed to the success of this academic program. I do not think I could have been able to undertake this rigorous academic and research works without their immense support and encouragement.

Most importantly, I would like to thank Professor George Nnanna for giving me this great and rare opportunity to pursue my Master's degree program and to work under his supervision at Purdue University and Purdue Water Institute respectively. I am appreciative of his insightful guidance, encouragement, and unalloyed support throughout the process. The best gift he ever gave me was to believe in my intellectual capability to accomplish my research objectives in the midst of all the challenges I encountered. I also want to thank Purdue Water Institute for the financial support.

I am indebted to my committee members Prof. Harvey Abramowitz, Prof. Chandramouli Viswanathan and Prof. Xiuling Wang. I also would like to thank Prof. Kim Hansung and my colleagues (Michael Ozeh, Emekwo Ukoha, Uzumma Ozeh, David Okposio and Kingsley Obinna) and Williams Oged for their helpful contribution in my research projects and in mechanical engineering labs.

I also thank my parents (Dr.Rabindranath Mishra and Dr.Puspalata Mishra), my siblings (Dr.Aparajita Mishra and Anindita Mishra), for their unreserved love and immeasurable support, for which I would not have persevered in this rigorous and advanced program.

I would also like to thank the members at the Sikh religious society in Crown Point, Indiana and the Hindu society in Crown Point, Indiana for their religious support to me and finally my friends Preemy Nayak, Pratik Samal, Ahijeet Das, Vishist Verma, Sandeep Kumar, Bhushan Manjari, Tanuj Karia, Amarjeet Jena, Saaransh Saxena, Avinash Jeyaram and Harshil Gadhia for their assistance and encouragement throughout this work.

TABLE OF CONTENTS

LIST OF FIGURES	7
ABBREVIATIONS	10
ABSTRACT.....	11
CHAPTER 1. INTRODUCTION	13
CHAPTER 2. LITERATURE REVIEW	18
2.1 Produced water	18
2.2 Present technologies to purify produced water	18
2.3 Solar energy and use.....	19
2.4 Nanoparticles	20
2.5 Surface Plasmon resonance	20
2.6 Solar steam generation via nanoparticles	21
2.7 Activated carbon.....	21
CHAPTER 3. METHODOLOGY.....	22
3.1 Materials used.....	22
3.2 Preparation of the activated carbon nanofluid.....	22
3.3 Preparation of the activated carbon nanoparticle immobilized polyurethane foam	23
3.4 Preparation of produced water.....	23
3.5 SEM characterization	24
3.6 Analytical Measurement of oil and contaminants	25
CHAPTER 4. EVAPORATION AND ADSORPTION EXPERIMENTS SETUP	27
4.1 Steam generation from saline water using solar simulator.....	27
4.2 Steam generation from saline water using electronic heat source.....	28
4.3 Distillation of saline water using solar simulator	29
4.4 Determination of stability of the nanofluid	31
4.5 Steam generation from produced water using solar simulator	31
4.6 Steam generation from produced water using fresnel lens.....	32
4.7 Oil adsorbance by polyurethane foam	33

4.8 Distillation experiments using polyurethane foam under simulated solar light and natural solar light.....	34
CHAPTER 5. RESULTS AND DISCUSSION.....	36
5.1 Physics and calculations.....	36
5.2 Characterization of activated carbon.....	37
5.3 Evaporation performance of activated carbon nanofluids versus CNT nanofluids.....	41
5.4 Photo thermal evaporation performance of activated carbon nano-fluids with varying concentration.....	42
5.5 Thermal Evaporation performance of Activated Carbon Nano-Fluids.....	45
5.6 Efficiency analysis of photo-thermal unit.....	45
5.7 Effect of turbidity on the evaporation performance.....	46
5.8 Photo-thermal evaporation performance of the distillation unit.....	47
5.9 Temperature variation of the distillation unit.....	48
5.10 Performance variation of the unit due to variation in fluid height.....	50
5.11 Performance variation due to an induced wind speed.....	51
5.12 Water quality analysis of the distillate obtained.....	53
5.13 Efficiency analysis of distillation unit.....	54
5.14 Stability of nanofluid.....	55
5.15 Economic analysis of the setup.....	55
5.16 Produced water proof of concept of evaporation and adsorption.....	56
5.17 Temperature variance.....	57
5.18 Oil absorbance by polyurethane foam.....	59
5.19 Oil recovery.....	60
5.20 Comparison with ongoing methods.....	61
5.21 Distillation experiments using natural and simulated solar light.....	63
5.22 Evaporation with fresnel lens and temperature variance.....	65
5.23 Evaporation rates with impurities and effect of foam thickness.....	67
CHAPTER 6. CONCLUSION.....	70
REFERENCES.....	71

LIST OF FIGURES

Figure 1 Water use in Texas.	13
Figure 2 Produced water uses and treatment process.	14
Figure 3 Produced Water samples.	15
Figure 4 Produced water treatment technique.	19
Figure 5 UP 200 s Ultraschallprozessor. (Source-Hielscher.com)	23
Figure 6 Synthetic Produced Water.	24
Figure 7 SEM Microscope for microstructure characterization.	24
Figure 8 UV-Vis spectrometer step for analysis of Filtrate and Condensate.	25
Figure 9 TOC Analyzer for analysis of oil mixture.	26
Figure 10 Schematic of the steam generation system.	28
Figure 11 Schematic for steam generation via electric heater.	29
Figure 12 Experimental setup used for the distillation experiments.	30
Figure 13 Placement of thermocouples in the setup.	31
Figure 14 TES 2000 solar meter.	32
Figure 15 Steam generation using fresnel lens.	33
Figure 16 Produced water filtration by Polyurethane Foam.	34
Figure 17 Produced Water evaporation using natural solar light.	35
Figure 18 Process of steam generation and oil adsorption.	37
Figure 19 Relationship between absorbance and concentration at low concentration.	38
Figure 20 Relationship between transmission and concentration.	39
Figure 21 The tri linkage structure of the PU foam and visible porosity.	39
Figure 22 The immobilized black activated carbon nanoparticles on the tri linkage structures.	40
Figure 23 The high surface area of the activated carbon which is embedded on the tri linkage structures.	40
Figure 24 Relationship between absorbance and concentration at high concentrations.	41
Figure 25 Comparison between CNT and Activated Carbon nanoparticles evaporation performance.	42
Figure 26 Evaporation performance for Activated Carbon at different concentrations.	43
Figure 27 Comparison of mass evaporated at T=25 minutes for different concentration values.	44

Figure 28 Difference between top surface and bulk temperatures showing effect of the surface evaporation.	44
Figure 29 Evaporation performance with a heating source.	45
Figure 30 Comparison of efficiency for different concentration values.	46
Figure 31 Effect of turbidity on evaporation performance.	47
Figure 32 Temporal evolution of water with time for different types of fluids.	48
Figure 33 Temperature profile for saline water obtained at the top surface of the fluid and the bulk fluid.	49
Figure 34 Temperature profile for activated carbon nanofluid in saline water obtained at the top surface of the fluid and the bulk fluid.	50
Figure 35 Variation of distillate obtained with fluid column height.	51
Figure 36 Variation of distillate obtained due to different induced wind speeds along with still air.	52
Figure 37 Temperature variations due to different induced wind speeds versus still air.	52
Figure 38 Quality analysis of distillate obtained.	53
Figure 39 Efficiency values of the system for 1. Saline water, 2. Nanofluid, 3. Foam, 4. Nanofluid with forced air.	54
Figure 40 The comparison of stability of nanofluids sonicated for different time intervals.	55
Figure 41 Cost analysis.	56
Figure 42 Steam generation results with activated carbon nanofluid and activated carbon foam.	57
Figure 43 Heat localization in produced water.	58
Figure 44 Heat localization in produced water and foam.	58
Figure 45 Comparison of different volume % of oil used.	59
Figure 46 Produced water before and after treatment.	60
Figure 47 Oil recovery unit.	61
Figure 48 Air diffuser oil removal.	62
Figure 49 Centrifuge for oil removal.	62
Figure 50 Comparison of oil absorbance between the three methods.	63
Figure 51 Comparison between the evaporation performances of the three methods.	63
Figure 52 Distillation results in natural sunlight.	64

Figure 53 Water characteristics of obtained water compared with D.I water.	64
Figure 54 Evaporation performance of different methods.....	66
Figure 55 Before and after pictures after concentrated solar experiment.	66
Figure 56 Heat localization on top of the foam due to concentrated solar light.	67
Figure 57 Temperature variation due to concentrated solar light.	67
Figure 58 Evaporation performance due to various thickness of foam.	68
Figure 59 Evaporation performance due to organic impurities.	69

ABBREVIATIONS

Ag- Silver

Au- Gold

CNT- Carbon Nanotubes

US EPA- United States Environmental Protection Agency

D.I.- De-ionized

NTU-Nephelometric Turbidity Units

TOC- Total Organic Carbon

PU- Polyurethane Foam

SEM- Scanning Electron Microscope

LSPR- Local Surface Plasmon Resonance

ABSTRACT

Author: Mishra, Ashreet. MSME

Institution: Purdue University

Degree Received: August 2019

Title: Purification of Brine and Produced Water using Activated Carbon coated Polyurethane

Committee Co-Chairs: A.G Agwu Nnanna, Harvey Abramowitz.

There is an increased discharge of produced water in the USA, which is causing decrease in the amount of usable water and is being rendered useless by refinery and extraction operations. Produced water that is obtained from these activities is usually not feasible to be used in any form. So, it becomes necessary to get the water to a quality standard, as per the US EPA, which will make this water suitable for both commercial as well as household purposes.

There have been a number of studies on Au, Ag and Carbon Nanotubes solar enabled steam generation with potential applications in water purification, distillation and sterilization of medical equipment. The key challenge with these nanoparticles is cost of production, hence limiting its wide application for clean water production. This work, for the first time, reports on activated carbon enabled steam generation hence addressing the cost limitations of metallic nanoparticles. Activated carbon has high solar absorptivity at various wavelengths of visible light.

This work uses Activated Carbon coated Polyurethane foam to simultaneously adsorb oil from the produced water and also yield surface vapors under application of solar light to get a clean distillate which can be used in various ways be it commercial or household. The given fabricated system will be an inexpensive and simple method to get clean water. The temporal evolution of the distillate has been measured as well as the temperature characteristics. Experiments were carried out using activated carbon and CNT nanofluids and polyurethane membrane with immobilized activated carbon and CNT. A simulated solar light of 1 KW ~1 Sun was used. The rate of evaporation, temporal and spatial evolution of bulk temperature in the water were monitored automatically and recorded for further data reductions. Parametric studies of the effect of nanoparticle concentration, water quality and salinity were performed. Experimental evidence showed that activated carbon has potential. Previous work reported for the first time that optimal

activated carbon concentration for maximum steam generation is 60 % vol. There was a 160 % increase in steam production rate at 60 % concentration of activated carbon when compared with D.I. water. Different atmospheric conditions were varied and the concentration of the sun to see the effects on the production of water. The recovery capacity of the foam was also tested so as to determine the waste oil that can be obtained from the foam and if the foam can be reused without being disposed of. More than 95% oil can be recovered The quality analysis has been performed and is an integral focus of the work as the comparison with the USA EPA (Environmental Protection Agency) will make it more robust and real world ready. The inclusion of Polyurethane foam, which is a major accumulating waste in the environment because of its use in packaging industry, and solar light as the energy source, to drive the distillation process, makes this a very clean and green process to treat produced water.

CHAPTER 1. INTRODUCTION

Freshwater is an ever-increasing need in industrial, household and agricultural sectors [1, 2]. Due to this overconsumption, that there has been an increase in the demand for more water because of the excessive consumption [3, 4]. The fresh water resources are fast declining and we need to recycle water instead of using more freshwater [5, 6]. Freshwater is very essential for human life and wasting it on industrial and energy purposes is not a wise choice [7-9].

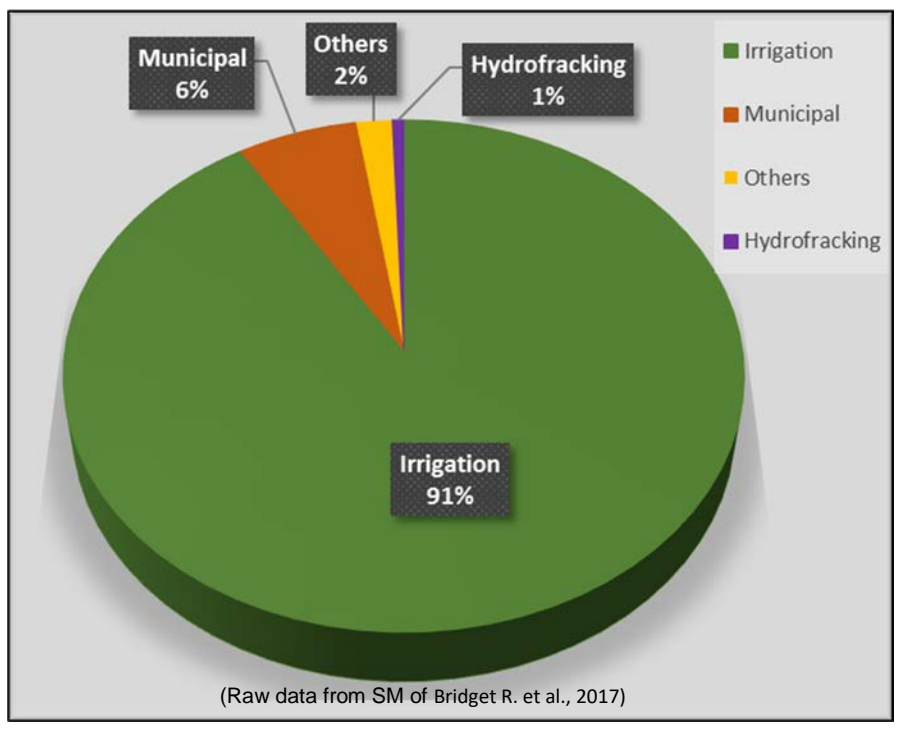


Figure 1 Water use in Texas.

There is an ever increasing need for oil and natural gas because of the population and the demands for vehicles, factories and machines [10-16]. Like water, oil and natural gas have become much required necessities for us. In the last decade there has been a very sharp increase in demand which has simultaneously caused an increase in extraction of oil [17, 18]. There is a large amount of oil being extracted in USA right now and most of it comes from the Permian Basin in Texas, the most active oil producing area in the USA accounting for more than 70 % of the oil being produced [19,20]. This high demand of water because of extraction causes requirements for a lot of

freshwater resources, which is almost 8 million gallons per oil well [20, 21]. About 50% of this water cannot be used after its first use cycle and hence needs to be replaced with new freshwater [22].

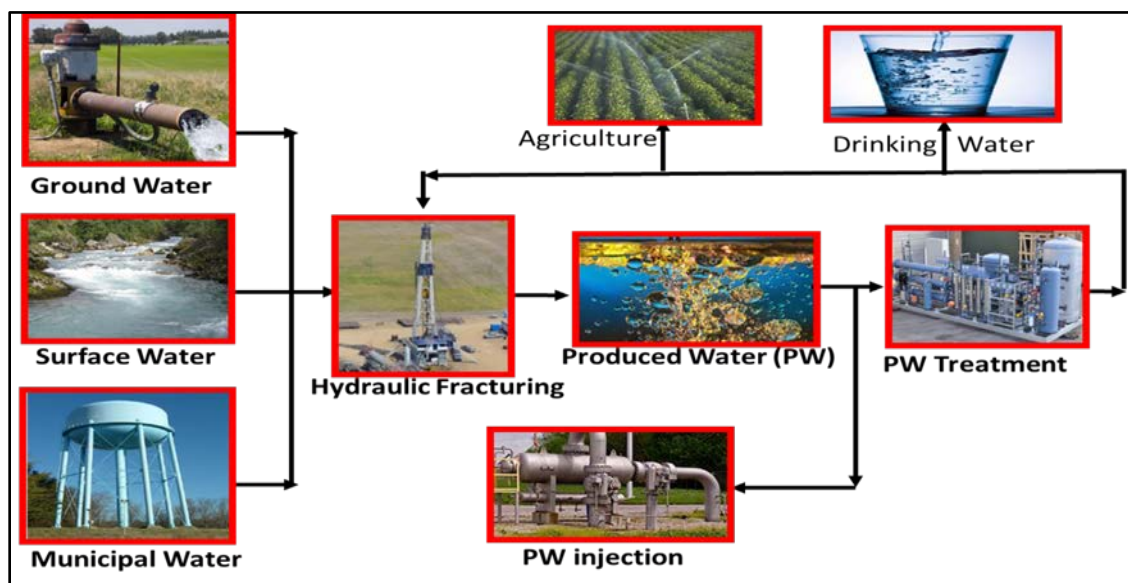


Figure 2 Produced water uses and treatment process.

Produced water is a product of the flow-back and residue water obtained after hydraulic fracturing and drilling operations to extract oil and natural gas. The physical and chemical characteristics of produced water vary with different geographical formations from which it is extracted, the location of its formation and the type of petro product being extracted [23-25]. The lifetime of the reservoir also plays a part in the composition of the produced water that is obtained. The major components that are present in produced water are salts, oil and grease, dissolved solids, naturally occurring radioactive material, heavy metals, dissolved gases and organic compounds [26-30]. The salts are defined by salinity, electrical conductivity and total dissolved solids [31]. Analytical methods measure the organic compounds and the hydrocarbons present in the formation [32-35]. Oil is found in different forms like free oil/ large droplets, dispersed oil / small oil droplets and dissolved hydrocarbons which are very difficult to remove. There are different organic and inorganic compounds that are added to the oil extraction process to enhance the process. In addition to these compounds there are also constituents that occur naturally in the produced water formation [36].

So there is a need to monitor the water quality to keep track of these characteristics for their treatment [37-40].



Figure 3 Produced Water samples.

There is a greater consumption of energy in the recent times because of modernization. [41]. There is an ever-increasing need for renewable resources / alternative sources of energy so that we do not run out of energy [42]. There needs to be an increase in the utilization of solar energy to make sure that some pressure can be taken off the grids. At an individual point of view we should be trying to reduce the dependence on other sources of renewable energy almost on the verge of running out of the non- renewable sources of energy and also cause a lot of harm to the environment which has been a known fact. The drive to go green should be a priority [43, 44]. Solar energy systems are being employed variedly in several different fields so as to utilize and improvise a clean, free and never-ending source of energy [45]. They are being used in many energy systems, storage systems and very intricate processes like generation of hydrogen, which is also possible now due to rapid technological advances [46]. The light energy of the sun can be used to generate steam using a varied number of nanoparticles that can harvest the light from the sun because of their optical absorption properties [47, 48].

In the recent times a very interesting and potent topic like nanoparticles is emerging [49]. The applications and opportunities are limitless for nanoparticles. Modern nanotechnology can produce

metallic or non-metallic particles of nanometer dimensions which have unique mechanical, optical, electrical, magnetic, and thermal properties [50]. Studies in this field indicate that exploiting nanofluid in solar systems, offers unique advantages over conventional fluids which cannot offer the same properties and advantages. They are being implemented in solar collectors, evacuated solar collectors, photovoltaic thermal systems, thermal energy storage, solar thermoelectric and solar cells [51]. They also decrease the operating temperatures of various applications. These additions also are responsible to change the different thermo-physical properties of the fluids which can be used in different ways. Nanofluids are the next generation in heat transfer fluids and are used as a substitute in various fields for traditional heat transfer fluids and phase change materials [52]. Different physical properties like specific heat, thermal conductivity and viscosity can be affected by nanoparticles [53].

Carbon is one of the materials that is very versatile in nature and has been used in a varied number of fields for its effectiveness for solar steam generation at a low-cost point of view [54-56]. A cheap but very effective nanoparticle is activated carbon that can be used and implemented in the process of water purification because of its high surface area, which allows it to absorb contaminants [57, 58] and also generate steam efficiently. Polyurethane foam is a waste that is generated in the industrial and household sector [59-61]. This foam is very effective at adsorbing oil and can be an effective tool to treat produced water in terms of removal of emulsified and non-emulsified oils [62-65].

For the first time, based on literature review, this work uses Activated Carbon coated Polyurethane foam to simultaneously adsorb oil from the produced water and also yield surface vapors under application of solar light to get a clean distillate, which can be used in various ways, either commercial or household. There was a need for the development of a low-cost system which can generate steam with the same effectiveness as the commonly used nanoparticles. Different parametric studies have been conducted to get the optimal concentration of activated carbon for steam generation. The temporal evolution of the distillate has been measured, as well as the temperature characteristics. Different atmospheric conditions and the concentration of the sun are varied to see the effects on the production of water. The recovery capacity of the foam was also tested so as to determine the waste oil that can be obtained from the foam and if the foam can be

reused. The quality analysis has been performed and is an integral focus of the work as the comparison with the US EPA standards. The inclusion of polyurethane foam, which is a major accumulating waste in the environment, and solar light as the energy source to drive the distillation process makes this a very clean and green process to treat produced water.

CHAPTER 2. LITERATURE REVIEW

2.1 Produced water

The composition of produced water obtained are not fixed with its geographical location [66, 67]. The composition typically varies from place-to-place with different physical and chemical properties. The variation also depends on the age and the formation of the hydrocarbon source. The main components of produced water are different dissolved salts, oil, grease, benzene, toluene, xylene, organic acids, phenol, organic impurities and additives during hydraulic fracturing [68, 69]. There is dissolved oil and large particles of oil floating on the surface, which is a major source of concern and removal [70]. This oil causes the most problems in the present purification systems of produced water. The second most important aspect of purification is the dissolved salts in the produced water, which is present in a very high quantity of about 300000 mg/L [71]. The salinity present in produced water can sometimes be higher than the salinity that is seen in seawater. The major contributors to the Total Dissolved Solids (TDS) are Na^+ , Cl^- , HCO_3^- and SO_4^{2-} ions which cause an increase in the TDS of the water that is obtained [72-78]. There are also metal ions like Ba^{2+} , Ni^{2+} , Fe^{2+} , Zn^{2+} and Cr^{2+} present and have higher concentration in produced water than in seawater [79, 80]. There is also presence of total suspended solids (TSS) like silt, sand and clay which can be suspended in the produced water extracted from the formations. Organic impurities like algae and plankton can also be found in produced water [81, 82]. Total organic carbon (TOC) is also present which can range up to 11000 mg/L. Organic acids, benzene, toluene, xylene and ethylene are some of the organic compounds present in the water according to studies [82]. Chemicals like methane hydrate are found in the oil formations along with emulsions and emulsion breakers to make the produced water usable [83].

2.2 Present technologies to purify produced water

Methods like microfiltration, nano-filtration, UV treatment, electrochemical and adsorption are currently employed to treat produced water [84-86]. Produced water is also stored in wells and is reused again in the fracking process [87]. Usually a multi-step approach is required to purify produced water, since it is difficult to remove all the contaminants with different concentrations in one step [88]. If the water can be treated to a certain quality then it can be reused for various

industrial, household and commercial applications without the need for new fresh water resources [89]. A combination of physical, chemical and biological methods are optimal to remove most contaminants from produced water [90]. Physical treatment processes like filtration, electro dialysis, electro dialysis reversal, floatation and adsorption are used to remove the oil, salts and organic impurities [91-98]. Chemical treatment processes like precipitation, chemical oxidation, electrochemical technologies, and biological treatment processes like activated sludge, aerated filters, microbial capacitive desalination cell and Microalgae based treatment is being employed to treat produced water [99-105].

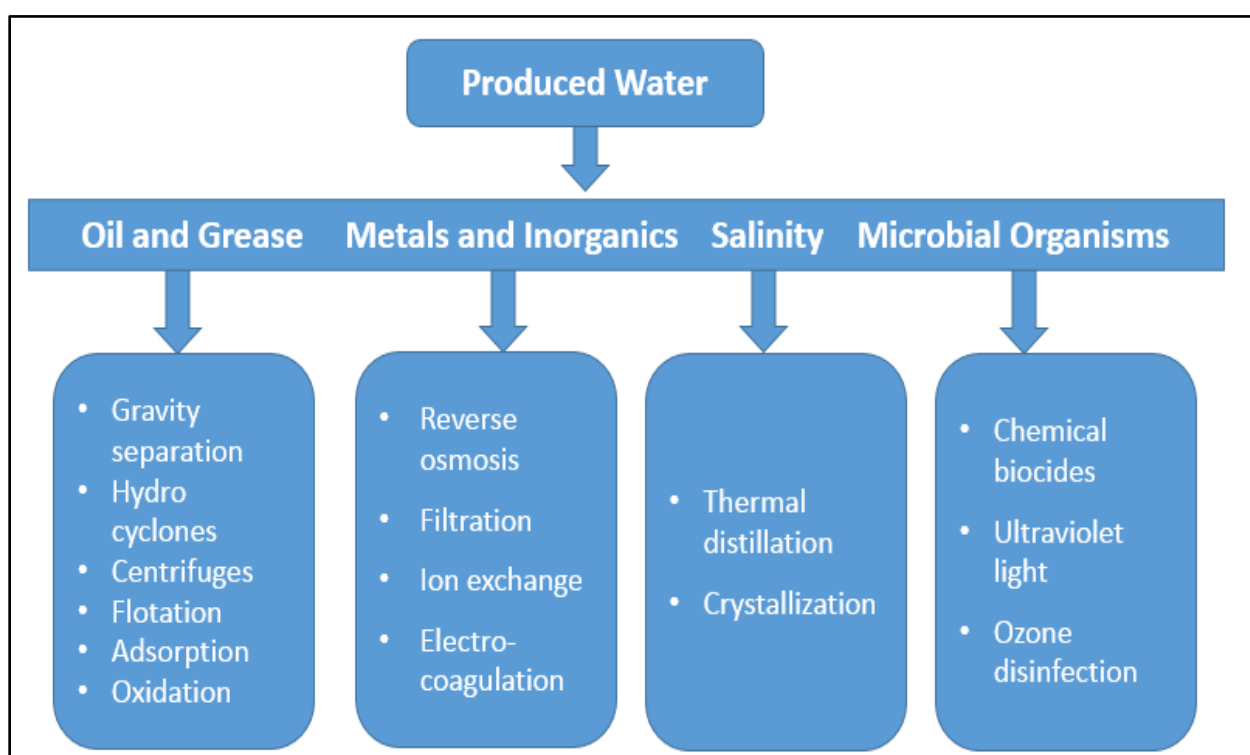


Figure 4 Produced water treatment technique.

2.3 Solar energy and use

Solar energy systems are being employed variedly in several different fields so as to utilize and improvise a clean, free and never-ending source of energy [106]. They are being used in many energy systems, storage systems and very intricate processes like generation of hydrogen [107]. The light energy of the sun can be used to generate steam using a varied number of nanoparticles that can harvest the light from the sun [108]. Nanoparticles in conjunction with solar energy are

being used as it's a renewable source of energy which can help us take pressure off the grid [109]. Nanofluids are being currently integrated with solar energy systems to generate steam and get pure water [110].

2.4 Nanoparticles

Nanoparticles have been used to generate steam under a solar simulator [111-113]. The particles have been varied with concentration and size to study the effects on the rate of steam generation [114-116]. The nanoparticles help localize the heat to the surface of the nano-fluid hence, the solar energy that is received is not wasted in increasing the overall bulk fluid temperature. Various nanoparticles like CNT, Au, Ag, TiO₂, Graphene, and Carbon black have been used as the nanoparticle options to perform the experiments [117-120]. The efficiency of the systems and the overall temperature rise in the fluid was determined. Ag and Au nanoparticles are very effective but expensive. When used in very small amounts, CNT can almost give the same results of steam generation. However, it has the problem of agglomeration which settles to the bottom of the solution, which calls for re-sonication. Graphene is a good alternative but needs to be used with other nanoparticles to become effective and produce efficient results. In summary, these are the nanoparticles that are very effective and produce a good rate of steam generation [121, 122].

2.5 Surface Plasmon resonance

The optical properties of nano-fluids play a very critical role in their application. These particles are able to absorb light at different wavelengths and are responsible for a phenomenon known as Local Surface Plasmon Resonance, which is the excitation of these particles from a level of lower energy to a level of higher energy which causes transfer of energy from the nanoparticles to the fluids in which they are suspended [123]. This transfer of energy is used to vaporize the fluid surrounding it and aids in evaporation [124]. This phenomenon takes place at a specific wavelength which excites the nanoparticle. The other phenomenon that is used for steam generation is light absorbance of the nanoparticles, the extinction coefficients of the fluids are measured which help us in determining the optimal absorption of light by the fluid [125, 126]. Moreover the optical properties also help us determine the transmittance of the solution which plays a very vital and

crucial role in the solar steam generation process. The transmittance can also be used to determine the stability of the nano-fluid [127].

2.6 Solar steam generation via nanoparticles

The nanoparticles like Au, Ag and CNT are very efficient in the process of photo thermal conversion where the reported efficiencies for these systems are 300-400 % increase in evaporation performance of the system which cannot be achieved by conventional methods [128-135]. Although the nanoparticles are efficient in generating steam in nano-fluid form, when the nanoparticles are used in conjunction with a membrane then the solar efficiency obtained is higher than the ones used in the base nano-fluid [136-138]. The membranes are very efficient in localizing the solar energy on the surface of the fluid and hence prevent the bulk heating to a very large extent so are more efficient [139-141].

2.7 Activated carbon

One of the emerging candidates in the field of nanomaterials is carbon [142-144]. Carbon has always been there around us having a lot of potential to be applied in different fields like adsorption , water purification and gas cleaning purposes very efficiently [145, 146]. Owing to its different forms, carbon is a very versatile material and very cost effective as well. Carbon nanotubes, nanohorns, graphite, graphene and carbon fiber are some of the few allotropes which are scaling new heights in research as well as in the industry [147].

CHAPTER 3. METHODOLOGY

3.1 Materials used

The activated carbon was purchased from charcoalhouse.com USA. Dopamine, sodium chloride (NaCl) buffer solution (pH=8) and ethyl alcohol was obtained from Sigma Aldrich USA. PU foam was obtained from generalplastics.com USA. Multi-walled carbon nano-tubes were obtained from cheaptubes.com USA. Motor oil (SAE- 5W 30) was obtained from Amazon, USA. All the chemicals obtained were used as provided by the supplier. Acrylic Glass, plastic tubes and other fittings were procured from ACE Hardware, Hammond, USA. Other materials include 500 W halogen lamps bulb, halogen lamp setup, and magnetic stirrer and Hielscher UP200 ultrasonic processor. Distilled water was used for the produced water preparation and the nanofluid preparation.

3.2 Preparation of the activated carbon nanofluid

The activated carbon nanofluid was prepared by sonicating the activated carbon nanoparticles in 500 ml D.I water for 30 minutes using UP 200 s Ultraschallprozessor (amplitude = 50 and frequency 0.5) as shown in figure 5. It was then magnetically stirred at 1000 rpm for 60 minutes to make sure all the nanoparticles are well dispersed. Different concentrations ranging from 1% to 100 % by volume were prepared.



Figure 5 UP 200 s Ultrasonic processor. (Source-Hielscher.com)

3.3 Preparation of the activated carbon nanoparticle immobilized polyurethane foam

The PU Foam was first sonicated (amplitude = 50 and frequency 0.5) for 60 minutes to remove all the impurities in the foam. It was then washed thoroughly with ethyl alcohol. The nanofluid used was mixed with 2mg of dopamine solution prepared in the pH=8 buffer solution. It was then magnetically stirred for 60 minutes in 200 ml of nanofluid. After that it was dried in an electrical oven for 15 hours at 60^oC.

3.4 Preparation of produced water

The Produced Water was prepared by magnetically stirring tap water, NaCl (25000 mg/L) and SAE- 5W 30 (10 %- 25 % by volume) for 60 minutes so as to create an oil water emulsion with dissolved impurities. This is the synthetic version of the effluent that has been prepared to imitate real produced water as shown in figure 6.

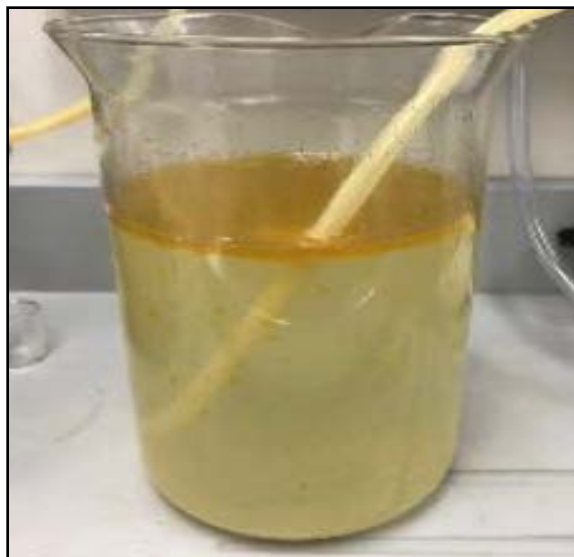


Figure 6 Synthetic Produced Water.

3.5 SEM characterization

The activated carbon nanoparticles were analyzed using a SEM microscope (figure 7) to observe the size uniformity and porous structure. The morphology and the microstructure of the given nanoparticles were also obtained for analysis. The structure of the PU foam was also observed using a SEM Microscope (JEOL JSM-6010LA) before immobilization and after immobilization.



<https://www.jeol.co.jp/en/products/detail/JSM-7800FPRIME.html>

Figure 7 SEM Microscope for microstructure characterization.

3.6 Analytical Measurement of oil and contaminants

The water samples were analyzed using UV-Vis spectrometer (Ocean optics HR 4000 series) by measuring the absorbance of the oil and nanofluid solution as seen in figure 8. Halogen and deuterium tungsten bulbs provide the light sources for illumination for the light source. Three readings were taken and the average value was used.

Total organic carbon analysis is a good estimation of the total concentration of organic carbon compounds/oil in the produced water. The reduction in TOC depicts the extent at which the oil is removed from the system. The TOC was measured using high sensitive TOC analyzer (Shimadzu TOC-LCSH) and a standalone computer for monitoring result. A standard air at a pressure of 29 PSI was used to operate the TOC equipment. 2ml samples were ejected into the TOC-L sample chamber. The UV-Vis spectrometer and TOC Analyzer is shown in figure 9.

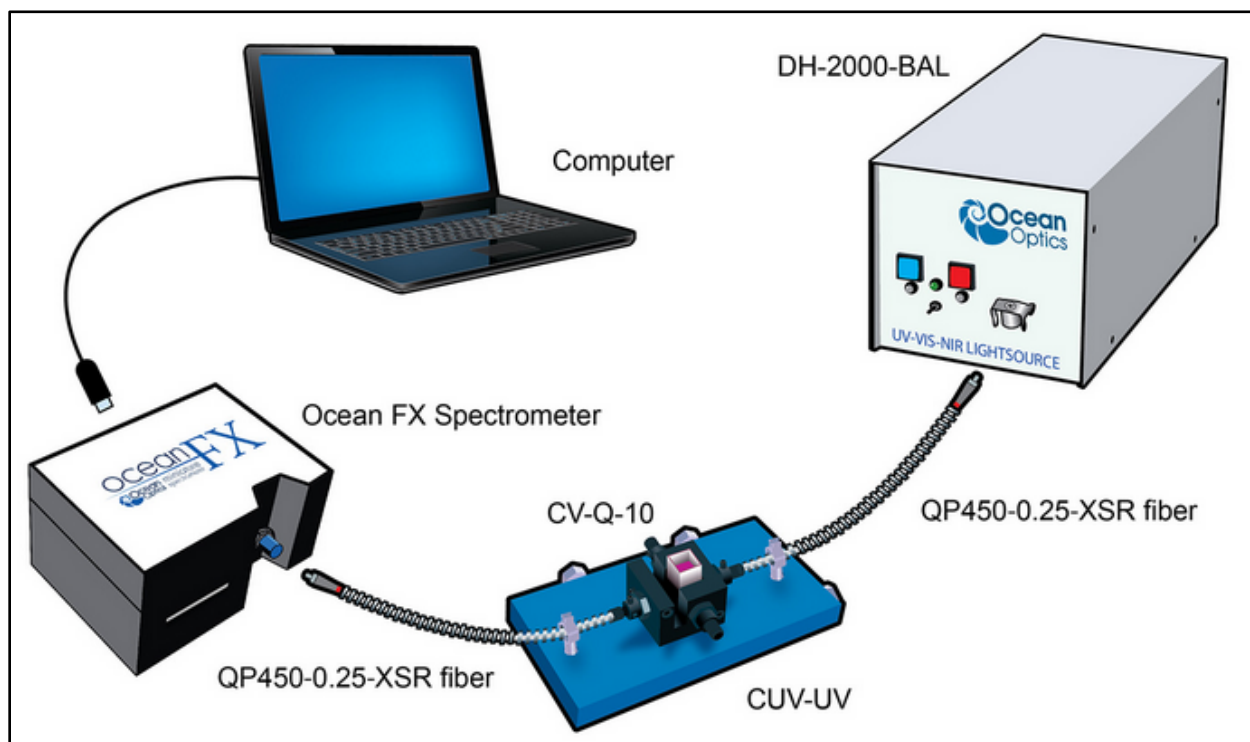


Figure 8 UV-Vis spectrometer step for analysis of Filtrate and Condensate.



Figure 9 TOC Analyzer for analysis of oil mixture.

CHAPTER 4. EVAPORATION AND ADSORPTION EXPERIMENTS SETUP

4.1 Steam generation from saline water using solar simulator

The experimental setup as depicted in figure 10 was used for the solar steam generation using activated carbon nanofluids and PU foam immobilized with activated carbon. The setup consists of a quartz glass beaker (diameter=75mm, height =150mm, thickness=3mm) which was placed on an electronic weighing scale (AND GX-8000) which recorded the weight loss of the sample in 1 minute intervals. It was connected to a computer, which gave the output for the scale. The light source is a 500 W lamp that has uniform flux output. The intensity of the light on the top surface of the container was measured by a solar meter (TES 2000) as shown in figure 13 and the value obtained was $1000 \text{ W}/\text{m}^2$. This was kept constant for all the experiments. Then the thermocouples were attached to a PVC pipe that was 3D printed and placed in the beaker. It held the 5 thermocouples (T-type) each at a distance of 20 mm from each other. The thermocouples were connected to the data acquisition unit (Agilent-34970A) which was in turn connected to the computer which recorded the data for temperature in intervals of 1 minute. Each trail was conducted for a time of 30 minutes each.

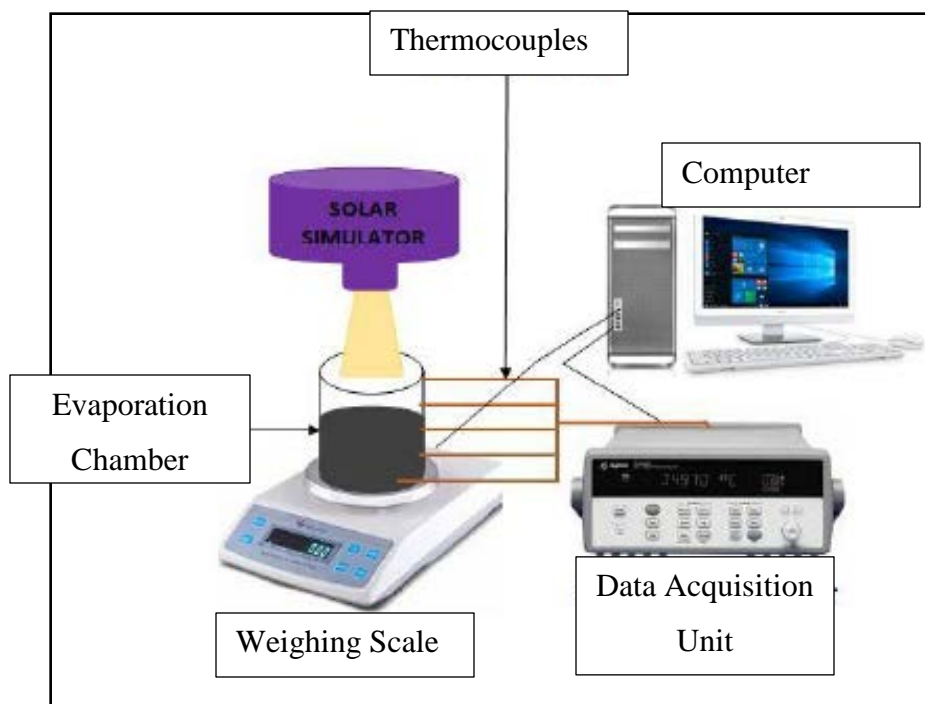


Figure 10 Schematic of the steam generation system.

4.2 Steam generation from saline water using electronic heat source

In this setup as shown by figure 11 the container was placed in an enclosure which was airtight and the heating source was placed on the top of the enclosure. The container was placed just below the heating source and it was made sure that the intensity of heat was analogous to the light source used in figure 10. This experiment served as the control to show contribution of ambient evaporation. The container was placed on the weighing scale and the thermocouples were attached as well. The mass loss and the change in temperature from the container were observed simultaneously every 1 minute for 30 minutes in total for each trail.

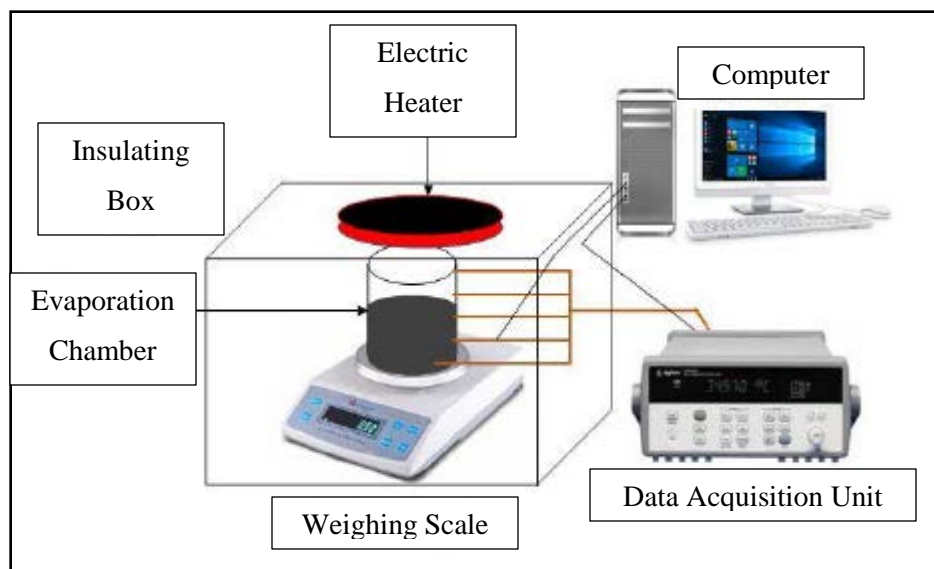


Figure 11 Schematic for steam generation via electric heater.

4.3 Distillation of saline water using solar simulator

The experimental figure 12 shows the setup that was used for water distillation from the activated carbon nanofluid and the activated carbon coated polyurethane foam. The given setup consists of an acrylic glass container that was fabricated to be the steam generation compartment which housed the nanofluid in it. The cover of the container was the area where majority of the condensation was taking place in the setup. The cover was placed on the setup in an inclined manner at an angle of to the horizontal which was the optimum value as mentioned and determined from previous literature review. A baffle was placed at the end of inclination of the glass cover to collect the condensed water droplets. Baffles were also attached to the side walls on all the three walls around the main baffle so as to collect condensate from the walls as well, so as to increase the collection efficiency of the system. Inlet, outlet and waste removal valves were attached to the evaporation chamber where the inlet valve was used to get in the nanofluid. The outlet was used to get the condensate out to the collection chamber and the waste valve to remove concentrated solution after the experiment. The outlet valve had a pipe connected from it to the collecting container which was placed on an electronic weighing scale (AND GX-8000) which recorded the mass of the distillate obtained in intervals of 5 minutes each for a total time of 10 hours and after 10 hours the light source was turned off and the setup was left for 30 minutes more so as to collect more distillate from the after-heating effects of water. The light source used was a 500 W lamp

with a uniform light output. The intensity on the top surface of the container, 1000 W/m^2 , was measured by solar meter (TES 2000). The T-type thermocouples were attached at different locations to measure the temperature effects as shown in figure 13. Two were attached at the bottom surface, two were attached at the top surface at the brim of the nanofluid and two were attached to the top condensing surface. The thermocouples were attached to the data acquisition unit (Agilent-34970A) which is connected to a computer and the data is collected for the same time interval as the mass measurement.

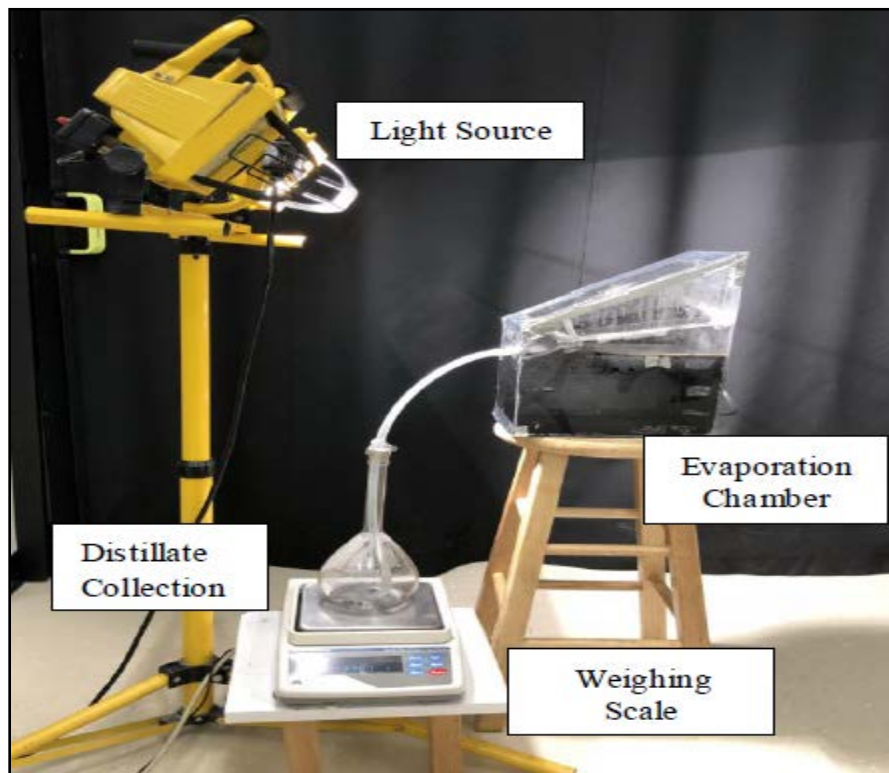


Figure 12 Experimental setup used for the distillation experiments.

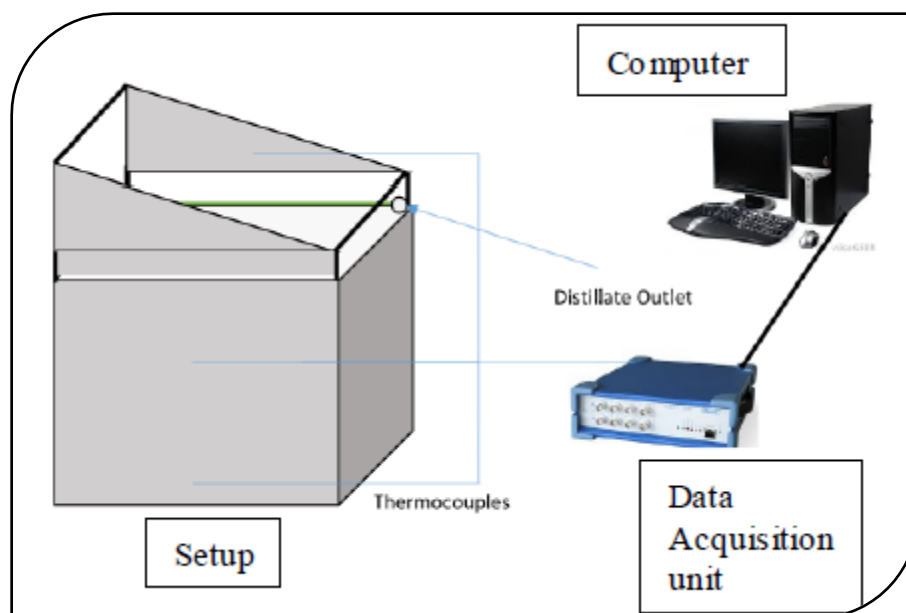


Figure 13 Placement of thermocouples in the setup.

4.4 Determination of stability of the nanofluid

To determine the stability of the nanofluid first the nanoparticles were dispersed in D.I. water (60 % by volume) and sonicated for a total time of 4 hours. Samples were collected after 1 hour each, amounting to 4 samples in 4 hours. Then the absorbance of the samples was measured with (Ocean Optics HR 4000) once every 24 hours to see the variance of the absorbance values which is directly related to the stability of the nanofluid. The containers the nanofluids were kept in and not disturbed whatsoever to make sure the sample obtained each time is the upper liquid and none of the settled nanoparticles so as to not deter the absorbance values.

4.5 Steam generation from produced water using solar simulator

To test the feasibility of the setup for purifying Produced water initial experiments were done in an insulated beaker. The setup consisted of a quartz glass beaker (diameter=75mm, height =150mm, thickness=3mm) which was placed on an electronic weighing scale (AND GX-8000) which recorded the weight loss of the sample in 1minute intervals. It was connected to a computer which gives the output for the scale. The light source was a 500 W lamp which has uniform flux output. The intensity of the light on the top surface of the container was measured by a solar meter

(TES 2000) as shown in figure 14 and the value obtained was $1000 \text{ W}/\text{m}^2$. This was kept constant for all the experiments. It is depicted in Fig.10

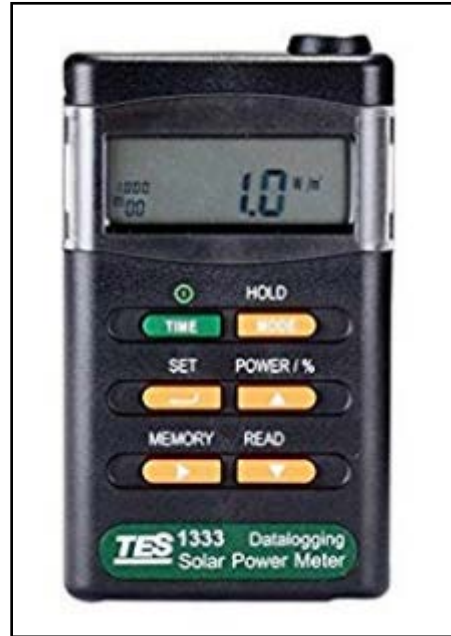


Figure 14 TES 2000 solar meter.

4.6 Steam generation from produced water using fresnel lens

The produced water was irradiated with concentrated solar light using a fresnel lens. The thermocouples were attached to multiple areas to measure the temperature changes. The electronic weighing scale (AND GX-8000) which recorded the weight loss of the sample in 1minute intervals. It was connected to a computer which gives the output for the scale. It is depicted in figure 15. The temperature changes were measured by a thermal camera.



Figure 15 Steam generation using fresnel lens.

4.7 Oil adsorbance by polyurethane foam

The oil water mixture was passed through Polyurethane foam to check the amount of oil and dissolved solids that can be absorbed by the foam. The oil water mixture was put into the inlet and the outlet was obtained at the other end via the outlet. The absorbance values were measured by using UV-Vis spectroscope (Ocean Optics HR 4000) to observe the variation of absorbance. The change in absorbance was given by $\frac{Initial\ Absorbance - Final\ Absorbance}{Initial\ Absorbance} \times 100$, where initial absorbance was the absorbance of the produced water and final absorbance was the absorbance obtained at the outlet and was measured once every 10 minutes to see the variation of absorbance. The setup is depicted in figure 16.

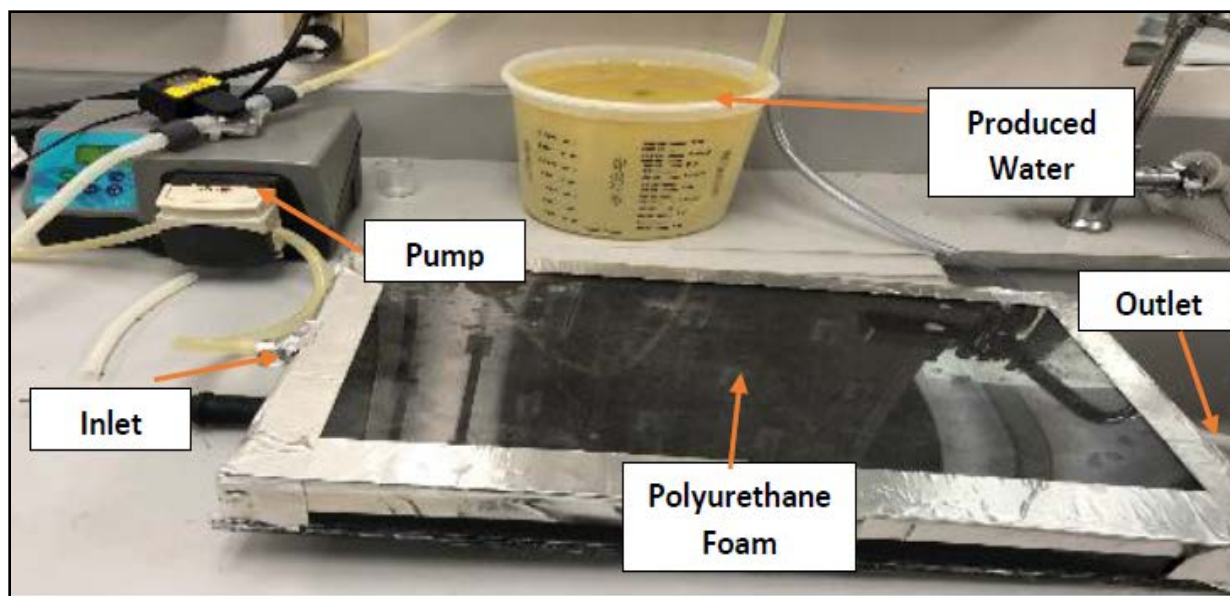


Figure 16 Produced water filtration by Polyurethane Foam.

4.8 Distillation experiments using polyurethane foam under simulated solar light and natural solar light.

The obtained filtrate from the polyurethane filter was then added to the evaporation chamber where it was irradiated with simulated solar light. The distillate was obtained and the temporal evolution was obtained from the weighing scale. The steam generated was condensed on the surfaces and then collected. The experimental setup is depicted in Fig. 12. The same experiments that were performed using natural solar light and the evolution of the steam was monitored. It is depicted in Fig 17.



Figure 17 Produced Water evaporation using natural solar light.

CHAPTER 5. RESULTS AND DISCUSSION

5.1 Physics and calculations

The steam generation that takes place is due to two major contributors, solar light which is absorbed effectively by the activated carbon nanoparticles and the heat which is absorbed by the polyurethane foam from the incoming solar light. The solar light that is incident on the activated carbon coated polyurethane foam causes the top surface of the foam to get heated, which causes a temperature differential as seen in figure 18. This temperature differential is the cause for the process that is happening. The manual holes that are made, serve as capillary tubes through which the produced water flows up because of the temperature differential. As the produced water flows up the oil present in it is filtered by the oleophilic nature of the foam and the clean water reached the top surface of the foam, where it is turned into vapors because of the high temperature localization. The process continues as the water is evaporated and the new water coming to the surface from the capillary tubes and the process continues because of the temperature differential.

The amount of heat absorbed by the foam can be given by Stefan Boltzmann Law $Q = \epsilon \sigma T^4 A$, where ϵ = emissivity = 1 (assuming integrated PU Foam is a black body), A = area of the foam = 0.0177 m^2 , T = ambient temperature, $\sigma = 5.6703 \times 10^{-8} \text{ (W/(m}^2 \cdot \text{K}^4))$. We get $Q = 7.7 \text{ W}$ which is the heat absorbed by the foam. Conversely, we get 13 grams of steam at the end of the experiment (, from which the necessary heat used is obtained as $Q = mL$, where m = mass evaporated and L = latent heat of vaporization of water = 2258000 J/kg . We get $Q = 16.3 \text{ W}$, so there is a disparity between the wattage actually obtained and the wattage due to heating alone. Hence we can say that the remaining wattage that is obtained is due to the light interaction effects of the nanoparticles with solar light. Heat localization is created around the immobilized nanoparticles which enhance evaporation at the surface of the foam which is further proved by experiments showing that nanoparticles play a major role in enhancing the efficiency and effectiveness of the process.

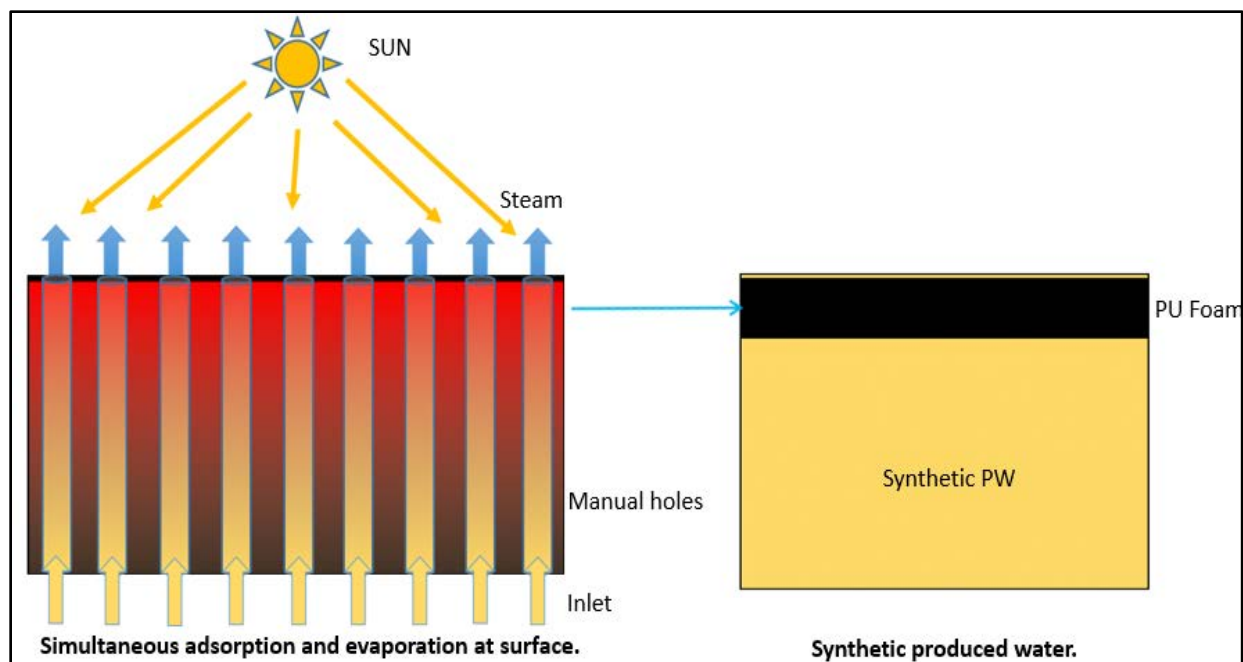


Figure 18 Process of steam generation and oil adsorption.

5.2 Characterization of activated carbon

The activated carbon nanoparticle was analysed with SEM and the high surface areas with irregularities on the surface were observed as can be seen in figure 23. For the PU foam there was a porous structure and tri linkage bonds were observed which were repeated throughout the framework. This tri linkage bonds made up the whole foam as observed in Figure 21. After the activated carbon was immobilized on the foam it was attached on the surface of the tri linkage bonds of the foam as there were irregularities observed after immobilization on the linkage structures which were smooth before immobilization as seen in Figure 22.

The absorbance of the activated carbon nano-fluid solution was observed with increase in concentration from 1% to 5% where it was linear (figure 19) according to Beer Lambert's law but as the concentration was increased from 10% to 100 % the increase in absorbance was not linear to the increase in concentration as observed in figure 25 which is in violation of Beer Lambert's law suggesting that the law is applicable to a low concentration of nanofluids and not to the higher concentrations because at higher concentration due to the presence of a large number of particles there is inter particle interaction which causes deviation from the actual law. The higher

absorbance at high concentrations suggests that more light can be absorbed by the nanoparticles and hence there is more photo thermal conversion which results in better performance. The peak absorbance was observed at 390 nm. This is the wavelength of light at which the phenomenon of LSPR takes place. In this phenomenon usually at this wavelength of light the electrons in the conduction band absorb energy from the incident flux and then move to a higher state. These electrons at a higher state provide energy to the water molecules surrounding them and hence cause immediate vaporization of water molecule and formation of a nanobubble around the nanoparticle. Since all this is taking place at the nano level so the flux incident on the nanoparticles gives them very high energy and temperature which is the driving force of the vapour generation process.

The transmission was also observed with respect to concentration which showed a logarithmic trend. The lower transmission at higher concentration also sheds light to the fact that these higher concentration values can prevent the phenomenon of bulk heating in the nanofluids which is very necessary to limit the unnecessary loss of energy from the Sun. We can see the trend in figure 20.

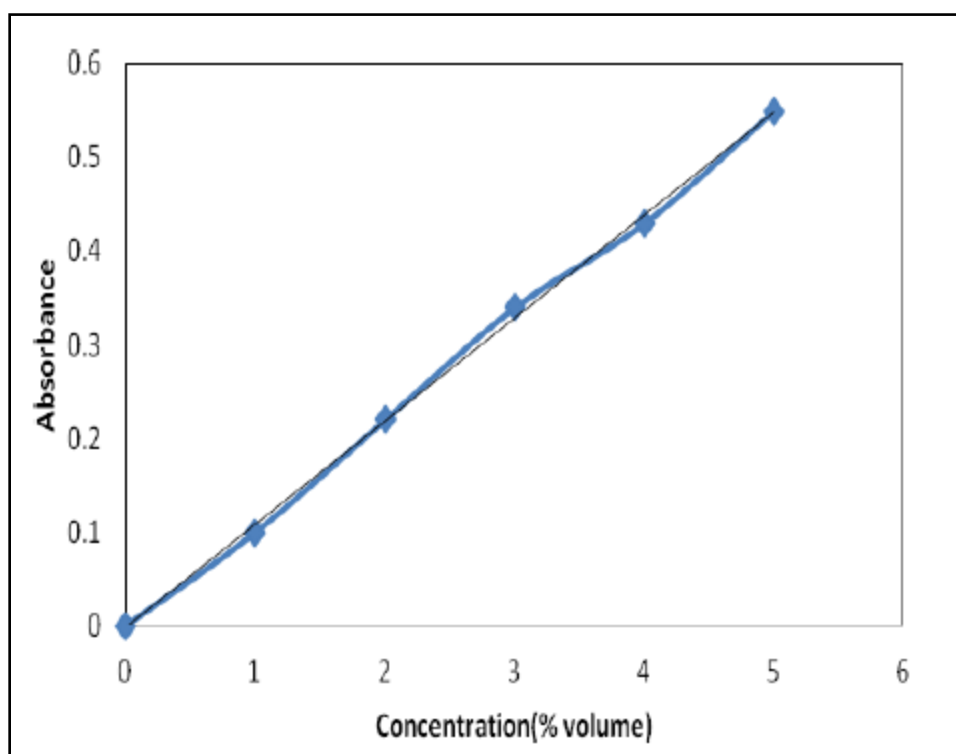


Figure 19 Relationship between absorbance and concentration at low concentration.

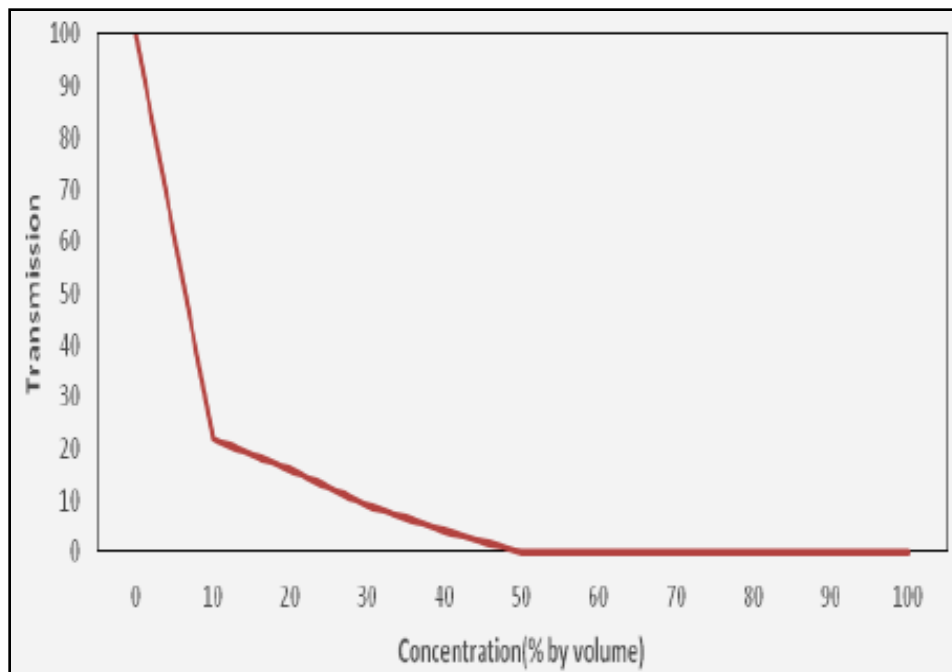


Figure 20 Relationship between transmission and concentration.

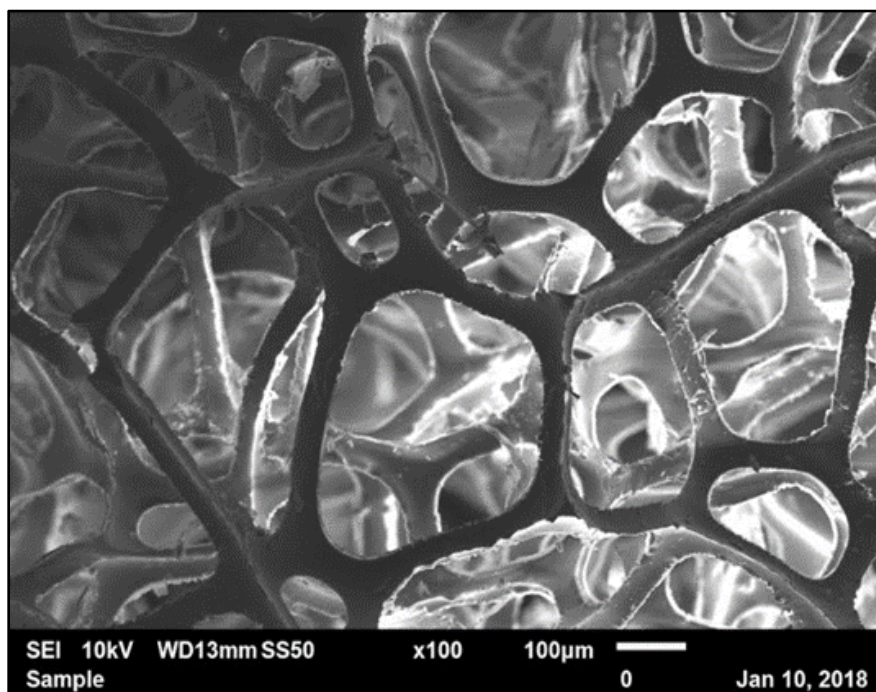


Figure 21 The tri linkage structure of the PU foam and visible porosity.

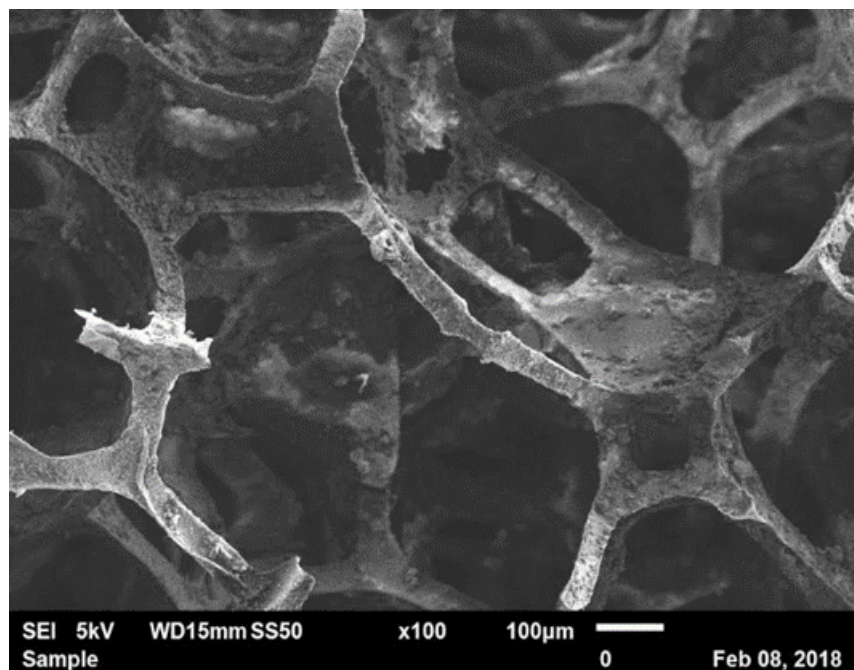


Figure 22 The immobilized black activated carbon nanoparticles on the tri linkage structures.

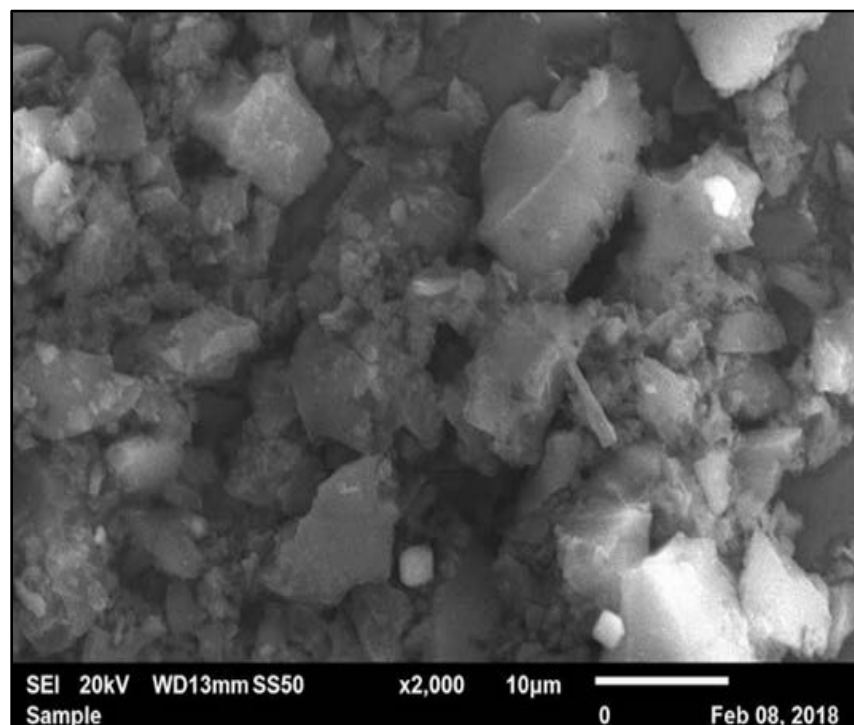


Figure 23 The high surface area of the activated carbon which is embedded on the tri linkage structures.

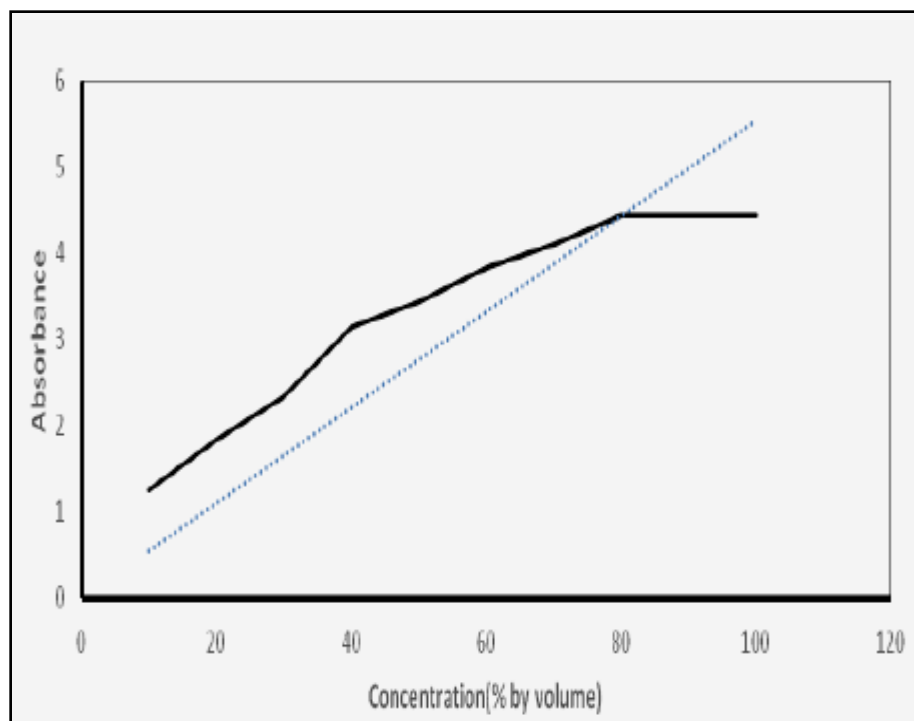


Figure 24 Relationship between absorbance and concentration at high concentrations.

5.3 Evaporation performance of activated carbon nanofluids versus CNT nanofluids

This trial was conducted with activated carbon nanofluid, activated carbon foam, CNT nanofluid and CNT foam to observe performance of the individual types of nanofluids and membranes. As depicted in Figure 25 it was observed that the CNT nanofluid gave the better performance when compared with the activated carbon nanofluid. Likewise CNT coated foam was better than the activated carbon coated counterpart. This is because of the fact that the CNT nanoparticle has better photo thermal conversion characteristics than activated carbon nanoparticles because of their lower band gap between the conduction and valence band than the activated carbon. So it takes a lower amount of energy to achieve the phenomenon of LSPR in CNT rather than in activated carbon. Moreover the thermal conductivity of CNT is better than that of activated carbon so it is better able to absorb the incoming heat and use it more effectively. But this comes at a price; the CNT nano-particle is very expensive and moreover is difficult to fabricate which can be a challenge in the developing and third world countries so activated carbon can be used as an alternative which is inexpensive and gives an acceptable performance when compared to CNT as we are looking to develop a cost effective system.

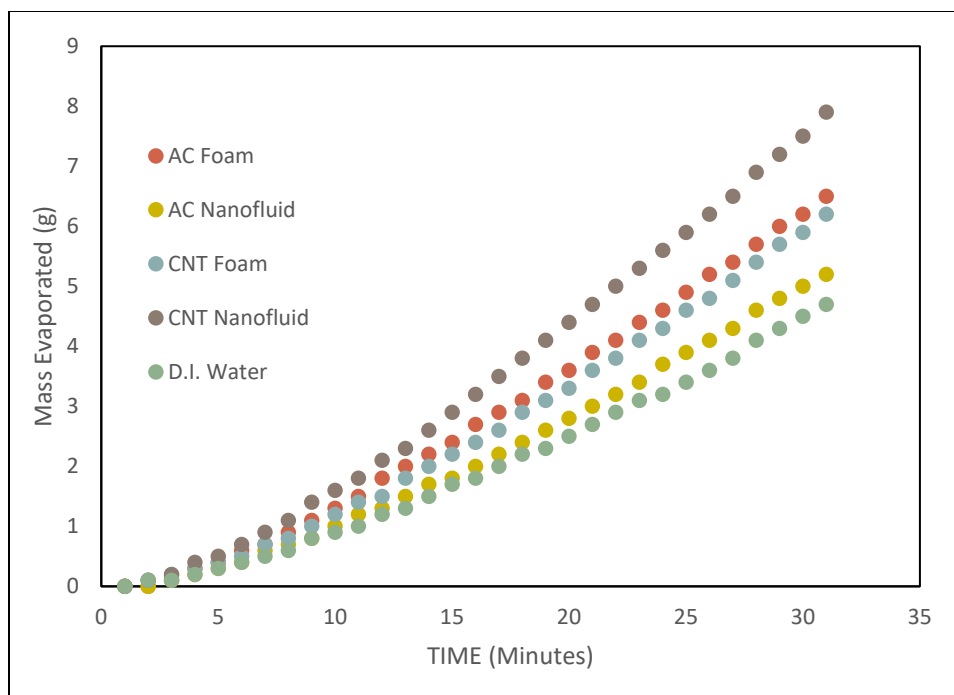


Figure 25 Comparison between CNT and Activated Carbon nanoparticles evaporation performance.

5.4 Photo thermal evaporation performance of activated carbon nano-fluids with varying concentration

The effect of concentration on the evaporation performance was observed from this experiment. The evaporation performance as seen in Figure 26 increases as the concentration increases from 0% until 60% concentration after which it starts decreasing until 100 % at intervals of 10 % showing that the optimal value of concentration is 60% at which the maximum evaporation (9.3 grams/30minutes) takes place in the nano-fluid. The temperature difference at the top surface and bulk of the nano-fluid shows an increase with increasing concentration showing similarity with the results of transmission studies that were conducted .For a small sample size (30 minutes) a polynomial trend is observed but when the experiment is carried out for a larger time frame (180 minutes) we observe that the trend slowly becomes linear in nature which shows linearity of mass of water evaporated with time which can be used to obtain the evaporation rate by extrapolation. Studies conducted in the past have a very small sample space and an ambiguity regarding better evaporation performance values at higher concentrations. There has not been any optimal concentration usually specified in them which is one of the major focus of this work as we see in figure 26. Figure 28 for the temperature difference also shows the difference between the top

surface temperature and the bulk temperature indicating that there is not a lot of energy that is wasted in bulk heating and the phenomenon is strictly at the surface only. The evaporation at $t=25$ minutes was observed which showed us a bell curve relationship of mass evaporated with concentration where it increases to an optimum value (60%) and then decreases as seen in Figure 27.

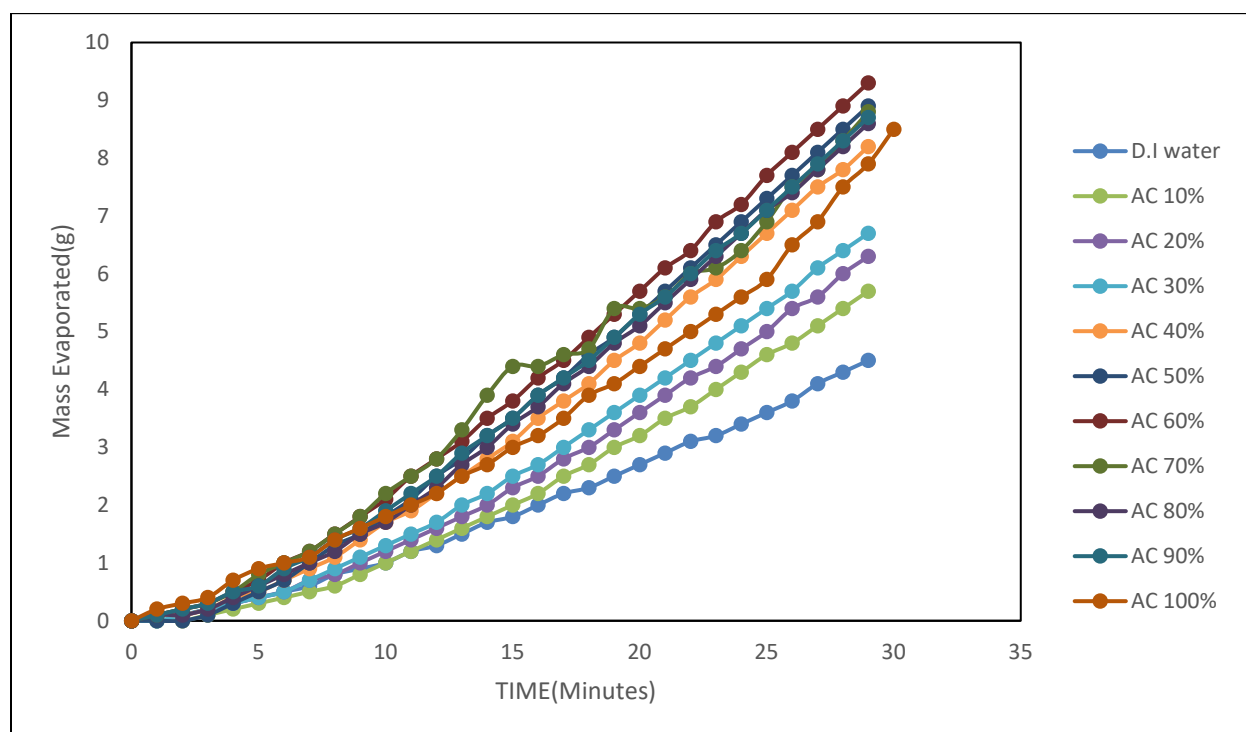


Figure 26 Evaporation performance for Activated Carbon at different concentrations.

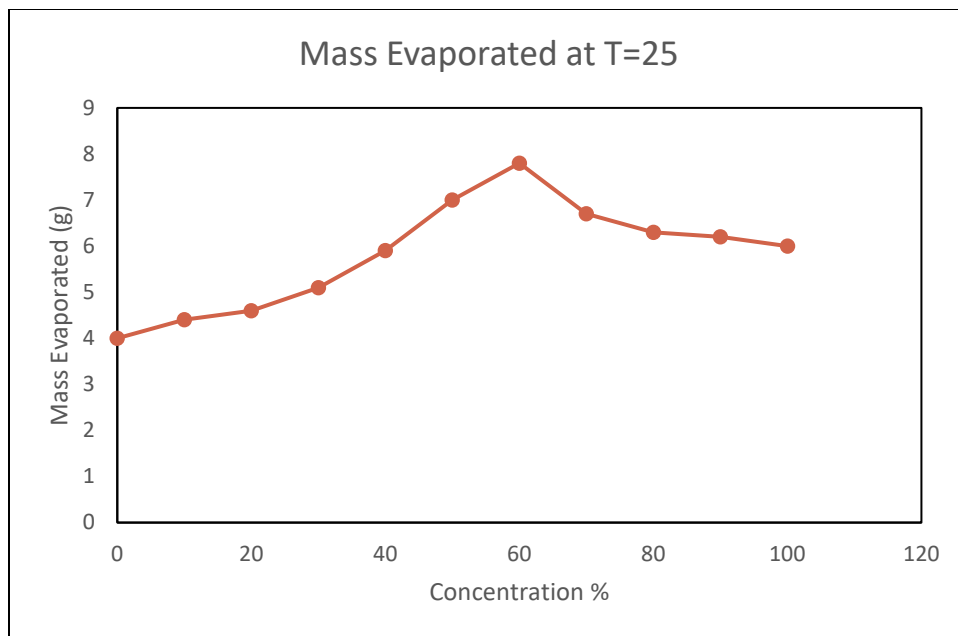


Figure 27 Comparison of mass evaporated at T=25 minutes for different concentration values.

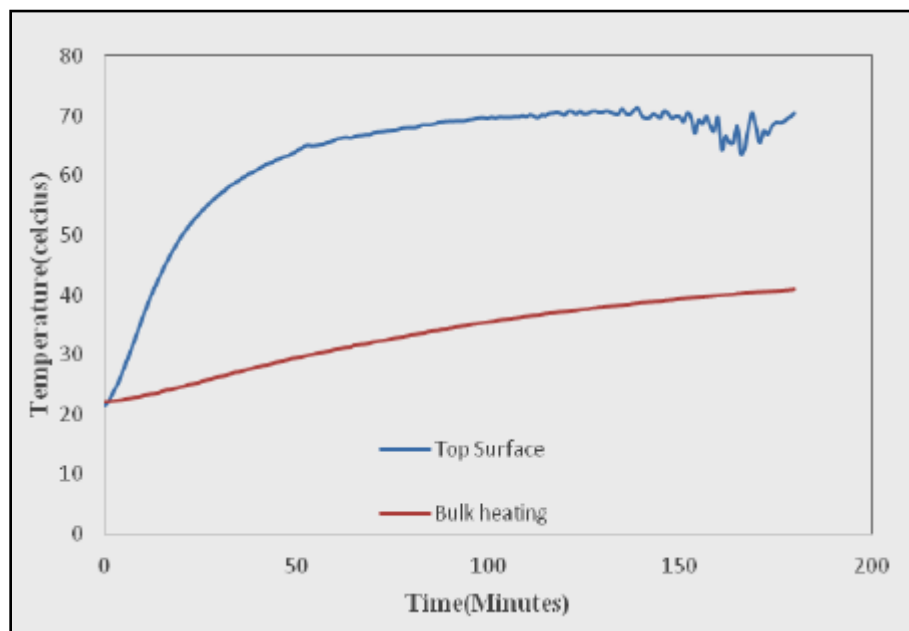


Figure 28 Difference between top surface and bulk temperatures showing effect of the surface evaporation.

5.5 Thermal Evaporation performance of Activated Carbon Nano-Fluids

The evaporation performance for increase in concentration for thermal energy $1000 \text{ W}/\text{m}^2$ remains more or less the same for concentrations ranging from 0% to 100%. This shows that there is not much effect of concentration in increase of evaporation rate which stays around 1.5g -2g/30 minutes as observed in Figure 29. The observed phenomenon brings to our notice that the mass obtained for the optimal concentration 60% under solar light is 9.3 grams whereas for the one using just a heat source we observe it is around 2.2 grams which proves and brings to life the fact that the evaporation takes places majorly as a result of LSPR and not due the heat from the sunlight which has a small contribution to make in evaporation. It is a photo thermal dominated phenomenon rather than just a thermal process.

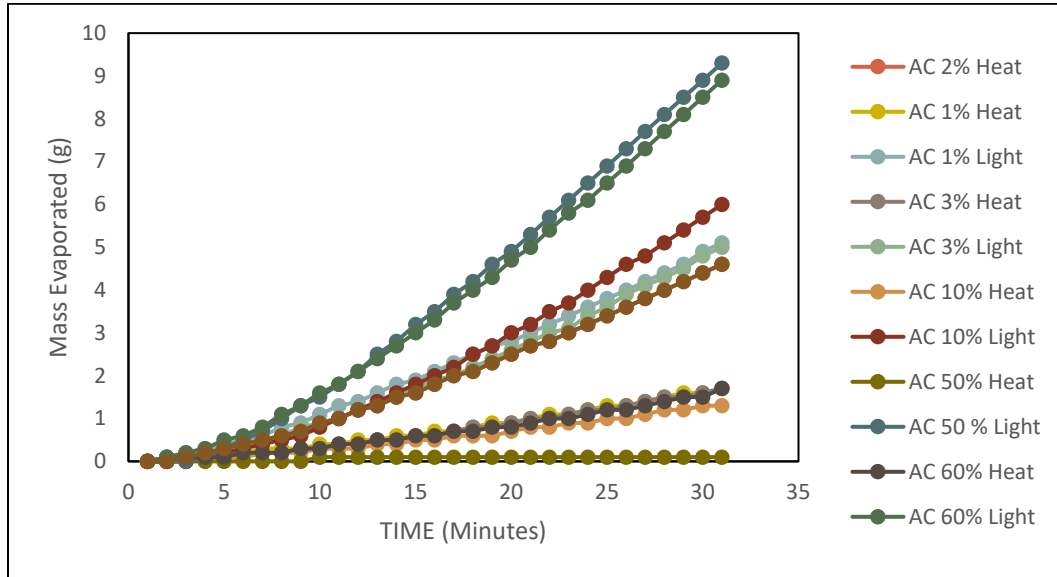


Figure 29 Evaporation performance with a heating source.

5.6 Efficiency analysis of photo-thermal unit

The efficiency of the system here is determined for each value of concentrations. The evaporation efficiency is defined as $\eta_{Evaporation} = \frac{m_g L}{I A t}$. Where m_g = mass of water evaporated (kg), $L = 2257$ kJ/kg, $I =$ incident flux = $1000 \text{ W}/\text{m}^2$, $A =$ area of the container on which the flux is incident (m^2), $t = 1800$ s. The heating efficiency is defined as $\eta_{heating} = \frac{m_{rem} c_p \Delta T}{I A t}$, where m_{rem} is mass

remaining after evaporation(kg), C_p is specific heat capacity of water = 4200 , temperature increase in the bulk fluid is ΔT , I = incident flux = $1000 \text{ W}/\text{m}^2$, A = area of the container on which the flux is incident(m^2), t = 1800 s. The total efficiency is defined as $\eta_{heating} + \eta_{avaporation}$. The total efficiency of the system is the efficiency with which vapor is produced from the system .From Figure 30 we observe that the efficiency increases up-to the optimum value of 60% and then decreases, the same trend that is observed with the concentration trend. The highest evaporation efficiency obtained was 66.75 % which is ~ 160 % increase in steam production than that from that of D.I water (27.9 %). The heating efficiency is highest for D.I. water and lowest for concentration 60%. This shows that the presence of the nano-particles helps in reducing the bulk heating phenomenon. The best system here is the one with 60% concentration of activated carbon with a total efficiency of 85%.

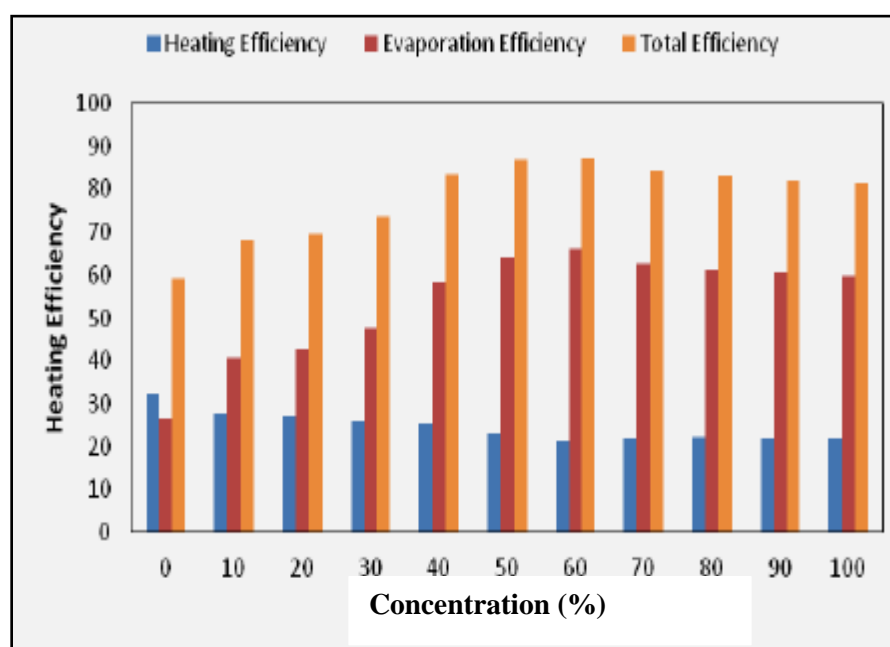


Figure 30 Comparison of efficiency for different concentration values.

5.7 Effect of turbidity on the evaporation performance

The effect of turbidity on the evaporation performance was determined by using D.I water (0.04 NTU), tap water (4.85 NTU), brine (12.86 NTU) and mud water (145.06 NTU). Figure 31 shows that the evaporation performance was almost similar in all these cases showing that there is no

pronounced effect of turbidity on the evaporation rates of the nanofluid. So the evaporation performance is independent of the turbidity of the water that is being used.

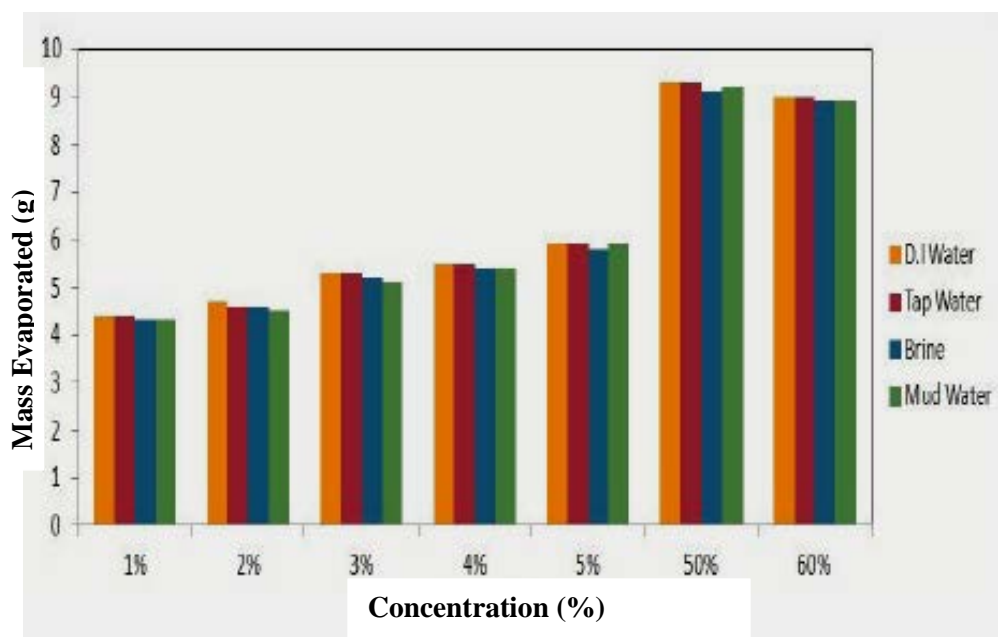


Figure 31 Effect of turbidity on evaporation performance.

5.8 Photo-thermal evaporation performance of the distillation unit

To determine the evaporation performance of the given fabricated system three different trials were run for the given setup with saline water, activated carbon nanofluid in saline water and activated carbon embedded foam. We observe from figure 32 that the highest obtained distillate is for the one which has activated carbon nanofluids mixed with the saline water which is roughly 240 grams of water for 10 hours of experiment. We also observe there is a decrease in the production when the solar simulator is turned off at the 10 hour mark but there is steam generation after that also for some time and distillate can be obtained with the sensible heat that was added to the water by the light source suggesting that the system can be used after the sun actually goes down to still collect steam from all the heat that has been imparted to the water. The activated carbon coated foam comes in after the nanofluid showing that the foam is also an effective method to obtain distilled water but works a little less efficiently giving about 150 grams of water in 10 hours of operation. This shows that the micro channels in the foam are effective enough to wick water from the bottom surface to their top. Although these are not as productive as the nanofluids

but still utilize much less nanoparticles to coat them and hence if there is a cost constraint then these can be used instead of nanofluids, the use of which may be extravagant but in this case activated carbon is a very inexpensive nanoparticle so there are no such constraints. Lastly the saline water gives around 80 grams of distilled water which serves as the control for the experiment. So we observe a very notable increase in the mass of the distillate that is obtained that is about 200 % increase for the one with activated carbon nanofluid and about 90 % increase for the one with the activated carbon coated foam showing their effectiveness.

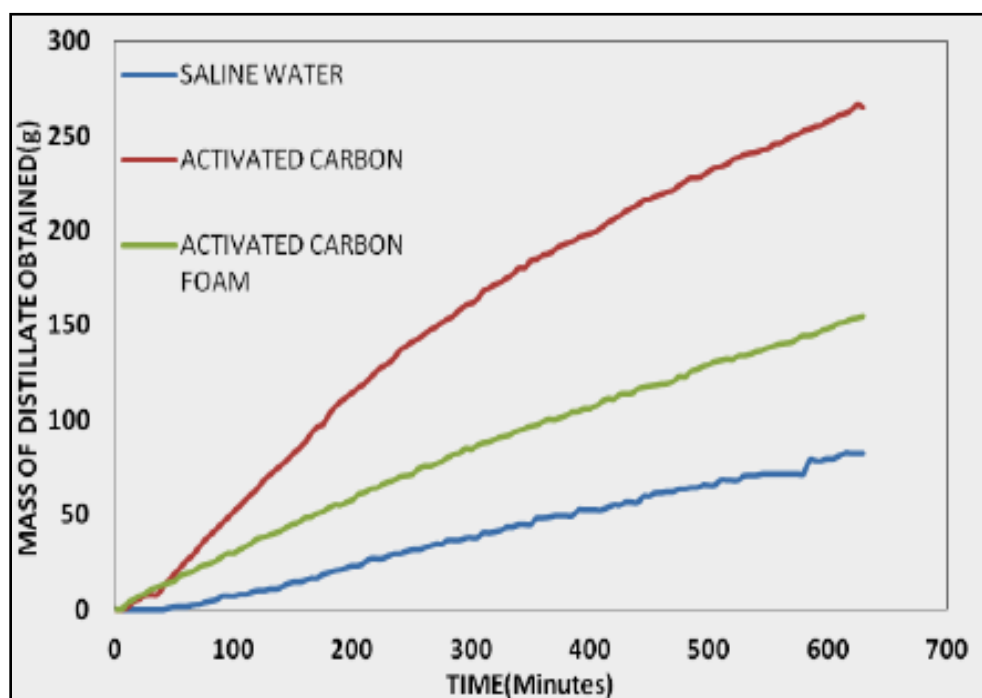


Figure 32 Temporal evolution of water with time for different types of fluids.

5.9 Temperature variation of the distillation unit

The temperature variation at the top surface of the fluid and the bulk temperature was measured using the thermocouples and there was a difference in temperatures that was observed in both the saline water which was the control fluid and in the activated carbon nanofluid in saline water. For the saline water in figure 33 we observe that the difference in temperature of the top and the bulk is not too much and hence we see that most of the energy that is incident on the top surface of the water is dissipated due to the inability of the fluid to restrict this energy loss hence it is not preferred. For the activated carbon nanofluid in saline water as shown in figure 34 we observe that the

temperature difference for the top surface and bulk is much more than the one observed in the control experiment. So this suggests that the energy that is incident on the top surface of the nanofluid is not dissipated much into the bulk fluid which in turn correlates to less amount of energy used to heat the overall fluid but only concentrated at the top which increases the rate of evaporation. This suggests that it can be a much more efficient process than conventional boiling where bulk heating is the major contributor for evaporation unlike nanofluids. One more interesting observation that we make is the difference in top surface temperatures between the nanofluid and the control. The surface temperature for the control is higher than that of the nanofluid which points out to the fact and correlates with the earlier observation that is made of a higher amount of water being evaporated from the nanofluid. So the higher amount of fluid that is being evaporated from the nanofluid causes a decrease in the surface temperature owing to the fact that it is a surface phenomenon. Due to the less amount of water being evaporated from the surface the temperature is higher in the control as observed.

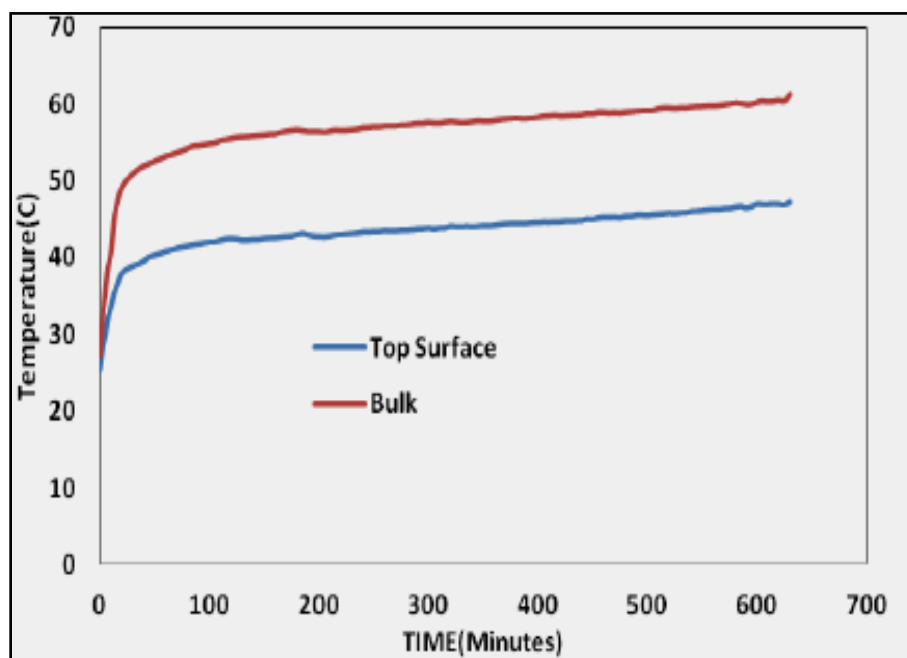


Figure 33 Temperature profile for saline water obtained at the top surface of the fluid and the bulk fluid.

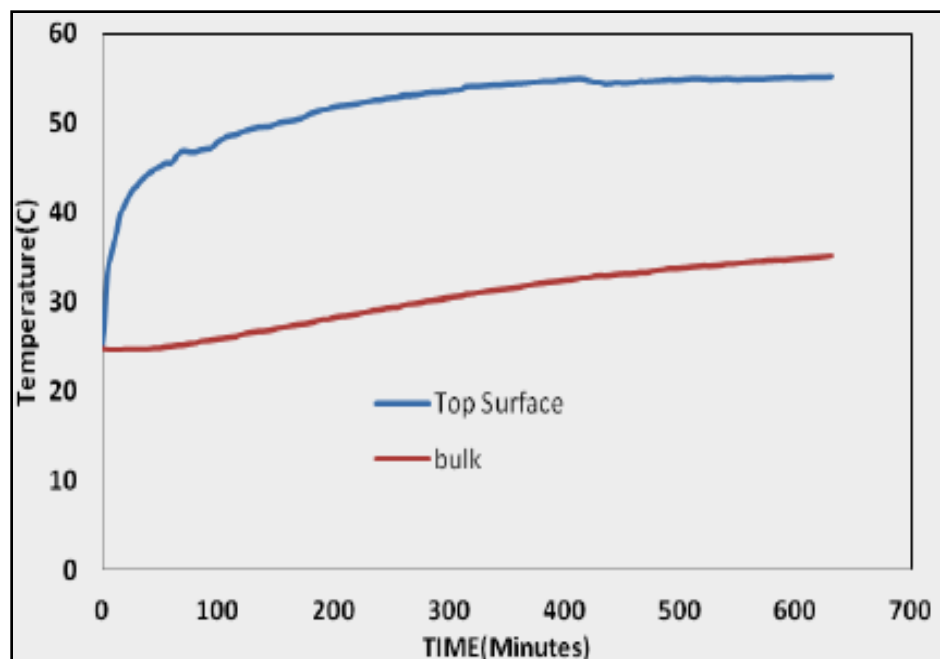


Figure 34 Temperature profile for activated carbon nanofluid in saline water obtained at the top surface of the fluid and the bulk fluid.

5.10 Performance variation of the unit due to variation in fluid height

The variation in the distillate production was observed in the system from figure 35 by varying the height of the fluid from 5 cm from the bottom to 15 cm from the bottom. There was a steep increase in the production of the condensate at the higher height of 15 cm because of the fact that the vapors that were produced could easily travel to the top condensing surface as well as the baffles that were placed in the sides. Hence, it was easy for them to be recovered but when we start decreasing the height of the fluid column then it becomes increasingly difficult for the vapors to get to the top surface of the condensing cover or the side walls with the baffles. Most of the vapors are seen condensing on the walls which are well below the baffles. Hence, there is a very sharp decline in the distillate output as majority of the distillate cannot reach the top surface. Thus, a higher height is desired for the best performance of this type of system so as to benefit the full benefits of the top condensing surface as well as the baffles that are located on the walls in the side.

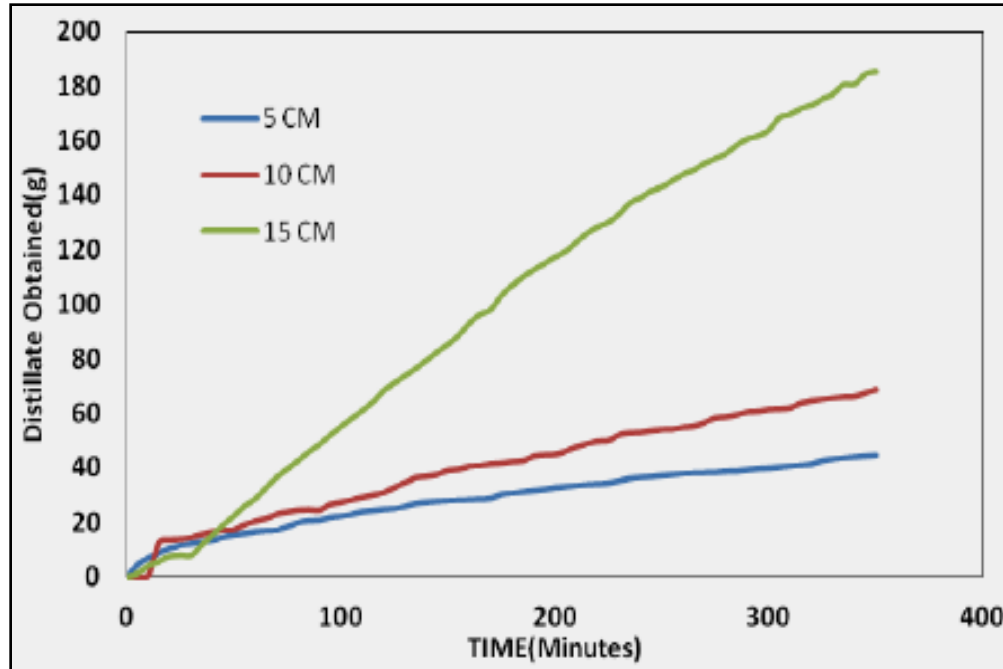


Figure 35 Variation of distillate obtained with fluid column height.

5.11 Performance variation due to an induced wind speed

The performance of the system was observed from figure 36 when an induced wind speed was applied to the condensing areas of the system (the top cooling surface and baffles) there was an increased rate of condensation in these areas as the speed of the wind that was applied increased. These were compared with the performance of the system with that given by still air. Three wind speeds 1 m/s, 2 m/s and 5 m/s were applied. The one with wind velocity 10 m/s gave the best result (the maximum amount of distillate) when compared with the ones of 5 m/s, 2 m/s and still air. As the wind speed increases on the condensing areas which simultaneously causes increase in the Reynolds number of the surrounding area (turbulent flow) which causes an increase in the heat transfer coefficient of the condensing areas and hence there is better dissipation of heat as the velocity of the wind increases as compared to the one in which the velocity of the wind is low or is still air condition. From figure 36 we observe the temperature variation of the condensing areas of the system where we observe that the temperature of the surface which is operating under still air conditions is very high than the one that is under the influence of forced air. Here we see that the effects of the change in the heat transfer coefficient of the areas. For the one of still air we see that there is a lower heat transfer coefficient and hence the heat dissipation to the surroundings is

much less and hence the higher temperature that is observed. For the one with the induced air we see that the temperature at the condensing surface is much less because of the fact that the heat transfer coefficient is much higher due to the forced convection that is setup because of the fan and hence the heat dissipation process is much higher in this giving a lower temperature.

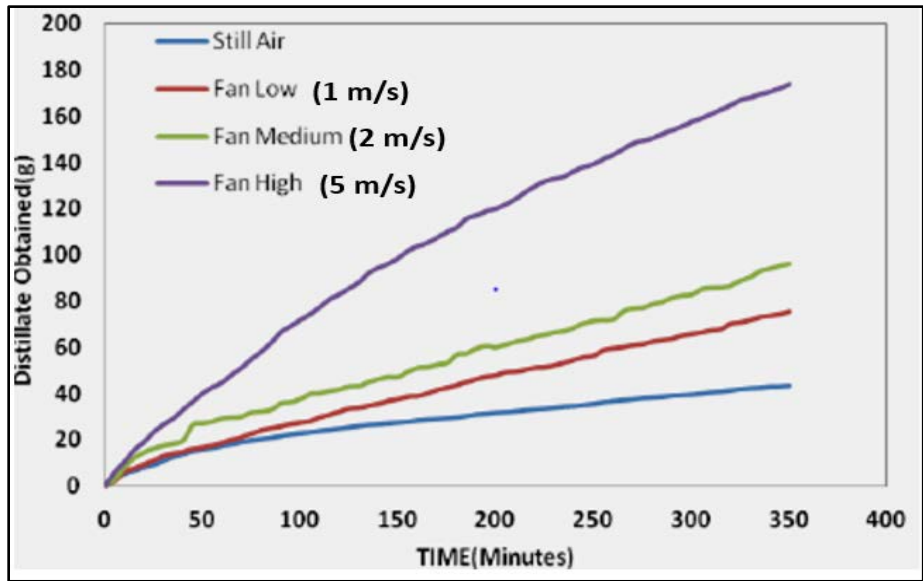


Figure 36 Variation of distillate obtained due to different induced wind speeds along with still air.

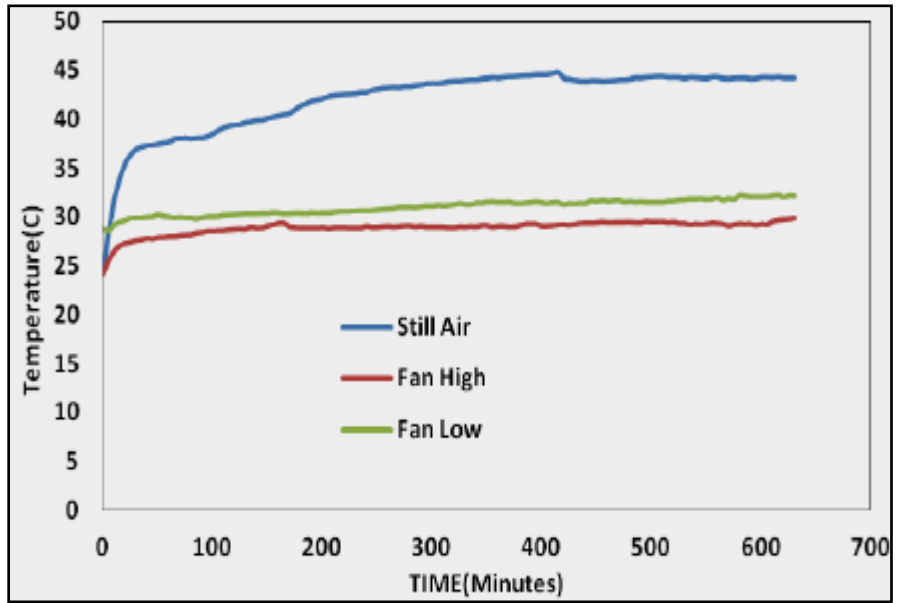


Figure 37 Temperature variations due to different induced wind speeds versus still air.

5.12 Water quality analysis of the distillate obtained

The water quality of the obtained distillate was checked and compared with the one of D.I. water as the control quality as shown in figure 38. The initial turbidity, pH and absorbance values were measured for the D.I water. In the UV-Vis spectrophotometer the D.I. water was the control and assigned 0 absorbance. Then the distillate qualities were measured and compared with the control. The usual drinking water standards by WHO are pH of 8.2 to 8.8 at 25°C, the turbidity less than 1.5 NTU. The results show that the quality of the water that was obtained was almost at par with the distilled water. There was no objectionable taste and odor. So this shows that the quality of the water that was obtained from the process can be a reliable source of water that can be used for either drinking purposes or either for commercial purposes. So even without very complicated equipment there can be high quality distilled water obtained from this setup at a very low initial investment.

Sample	Turbidity (NTU)	pH	Absorbance
D.I Water	0.020	7.01	0
Saline water	0.100	6.95	0.15
Nanofluid	0.105	7.05	0.20
Foam	0.105	7.04	0.20
Mud water	0.107	7.20	0.25

Figure 38 Quality analysis of distillate obtained.

5.13 Efficiency analysis of distillation unit

The efficiency of the system here is determined for each value of concentration. The evaporation efficiency is defined as $\eta_{Evaporation} = \frac{m_g L}{I A t}$. Where m_g = mass of water evaporated (kg), L = 2257 kJ/kg, I = incident flux = 1000 W/m^2 , A = area of the container on which the flux is incident (m^2), t = 36000 s. The heating efficiency is defined as $\eta_{heating} = \frac{m_{rem} c_p \Delta T}{I A t}$, where m_{rem} is mass remaining after evaporation (kg), C_p is specific heat capacity of water = 4200, temperature increase in the bulk fluid is ΔT , I = incident flux = 1000 W/m^2 , A = area of the container on which the flux is incident (m^2), t = 36000 s. The total efficiency is defined as $\eta_{heating} + \eta_{avaporation}$. Here we observe in figure 39 that the efficiency of the system increases from 41 % in the saline water to 73 % in the nanofluids which shows a viable increase in performance due to addition of the nanoparticles. The foam also gives an efficiency of 60 % which is more than the one with the control of saline water. The best result is obtained with the one of nanofluid used with forced air (6 m/s) which is 84 % showing the increased effect of the air in enhancing the condensation of the system.

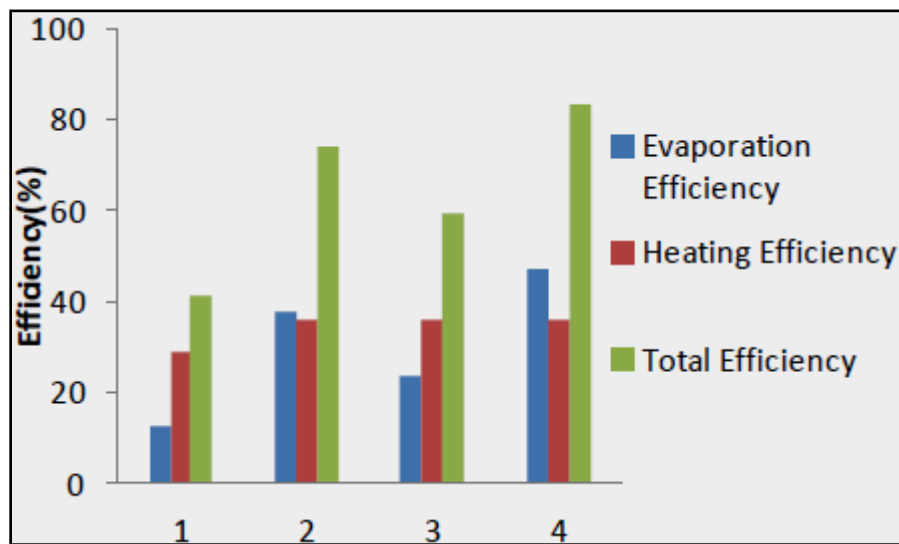


Figure 39 Efficiency values of the system for 1. Saline water, 2. Nanofluid, 3. Foam, 4. Nanofluid with forced air.

5.14 Stability of nanofluid

The stability of the nanofluid was observed for a total of 10 days as seen in figure 40. Absorbance values were measured and it is seen that the values for the sonication time of 4 hours and 3 hours give an almost equal and better result as compared to the one with sonication time of 1 and 2 hours respectively. They can be effectively used for 4 days without much hamper in performance. But the only drawback is that sonication of such a large amount of nanofluid at once is challenging.

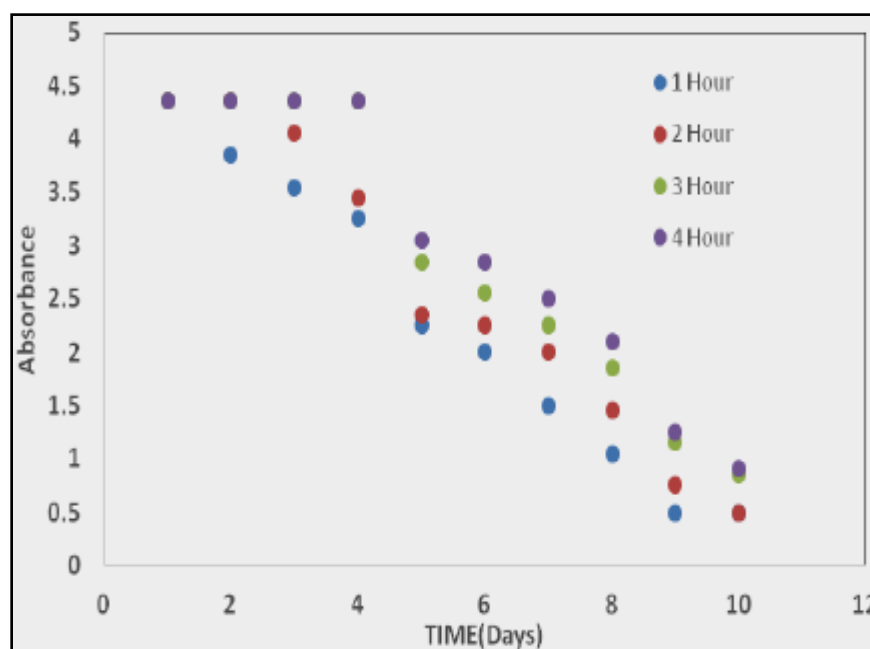


Figure 40 The comparison of stability of nanofluids sonicated for different time intervals.

5.15 Economic analysis of the setup

The payback periods for the different types of methods used have been determined and are stated in figure 41. The price for 1 L of distilled water has been taken as 0.5 \$. The amount of distillate produced has been calculated per day and the formula for $Payback = \frac{Investment}{Earning\ per\ day}$, where investment is the total amount of money spent on the system and earning is calculated by using the amount of distillate that is produced and the price for it. This is for an ideal condition but still would be very much applicable to the real world scenario.

S.I	Component	Water (\$)	Nano Fluid (\$)	Foam(\$)
1	Acrylic Glass	85	85	85
2	Pipes	3	3	3
3	Hose and connectors	5	5	5
4	Nanoparticles	---	2	7
5	Fabrication and overheads	50	50	50
	TOTAL	143	145	150
	Payback Period(days)	90	49	80

Figure 41 Cost analysis

5.16 Produced water proof of concept of evaporation and adsorption

For the initial tests performed using activated carbon nanofluid and activated carbon foam using different concentrations of oil. These are shown in Fig. 42 and we observe that the best result is obtained by the activated carbon coated polyurethane foam followed by the nanofluid. The experiments were almost comparable even when the concentration of the oil was increased to 25 % by volume from 5 % by volume. The activated carbon nanofluid did not show very convincing results for steam generation from the produced water. There was no steam generated when there was solar irradiation to the produced water suggesting that normal evaporation is not a viable option. There has to be some sort of surfactant or adsorbent that has to be used to make the process viable.

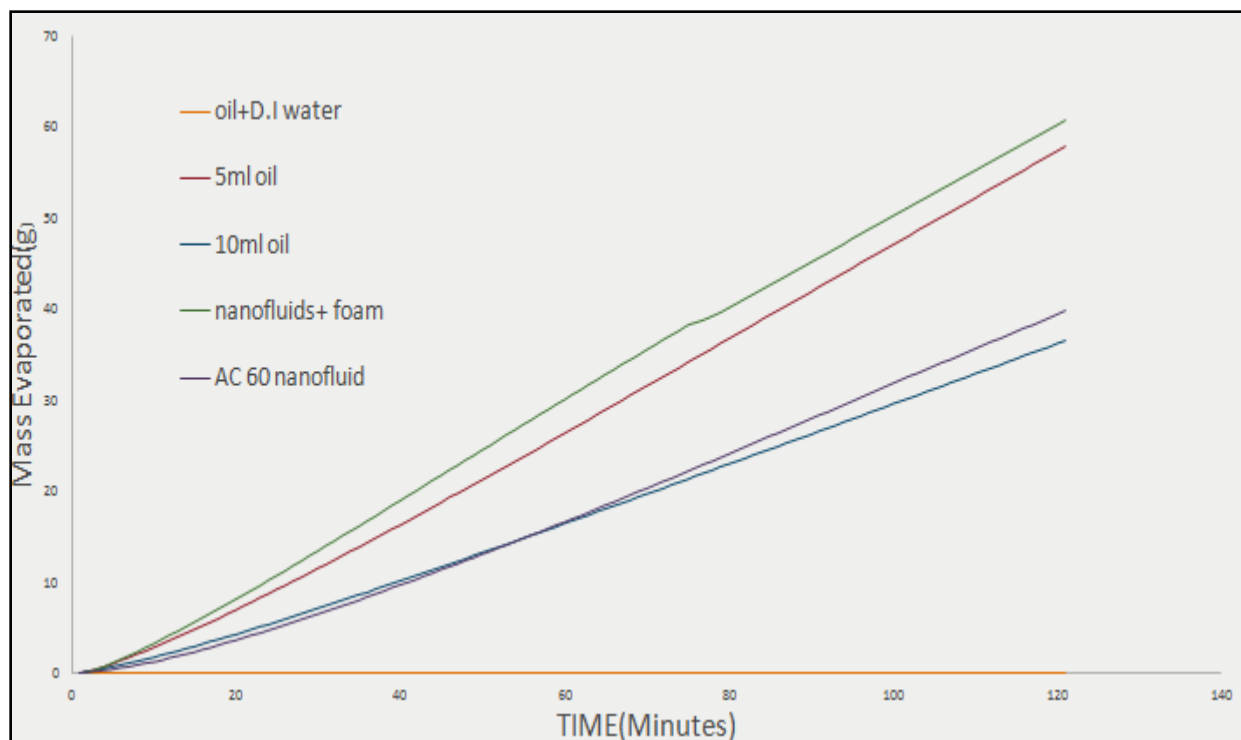


Figure 42 Steam generation results with activated carbon nanofluid and activated carbon foam.

5.17 Temperature variance

For the temperature values obtained from the setup of the produced water and the produced water with the foam. Figure 43 shows the heat localization on the produced water setup and figure 44 shows the heat localization in the produced water and the floating foam on top of it. As we observe in Figure 43 there is some heat localization on the top surface of the produced water but on the top of the foam there is higher heat localization because the foam is black in color and absorbs more heat from the incoming solar radiation. This localization causes the capillary effect and the water gets drawn up to the surface where the evaporation takes place.

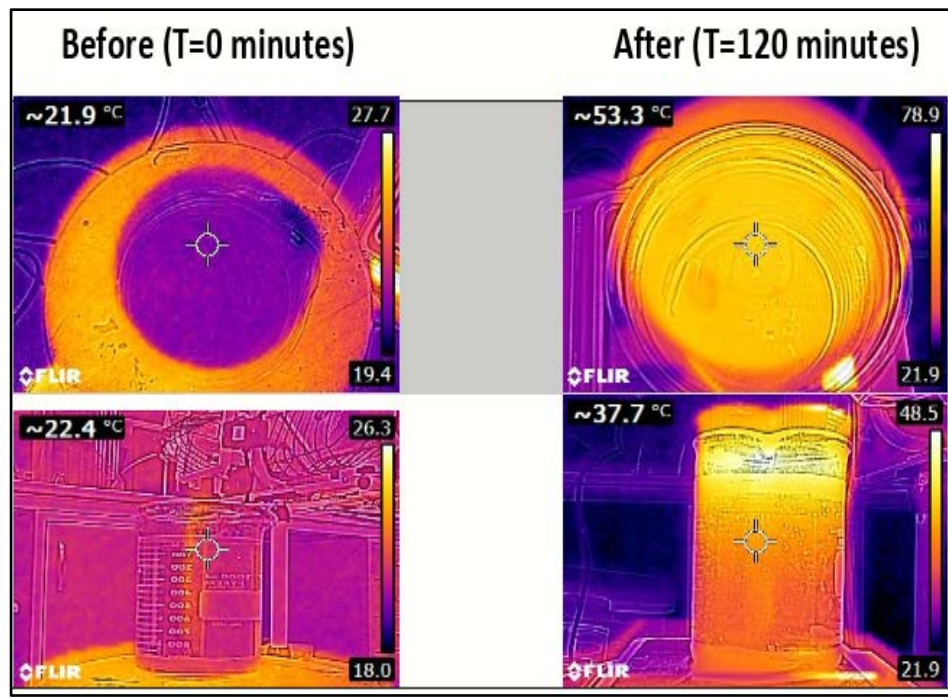


Figure 43 Heat localization in produced water.

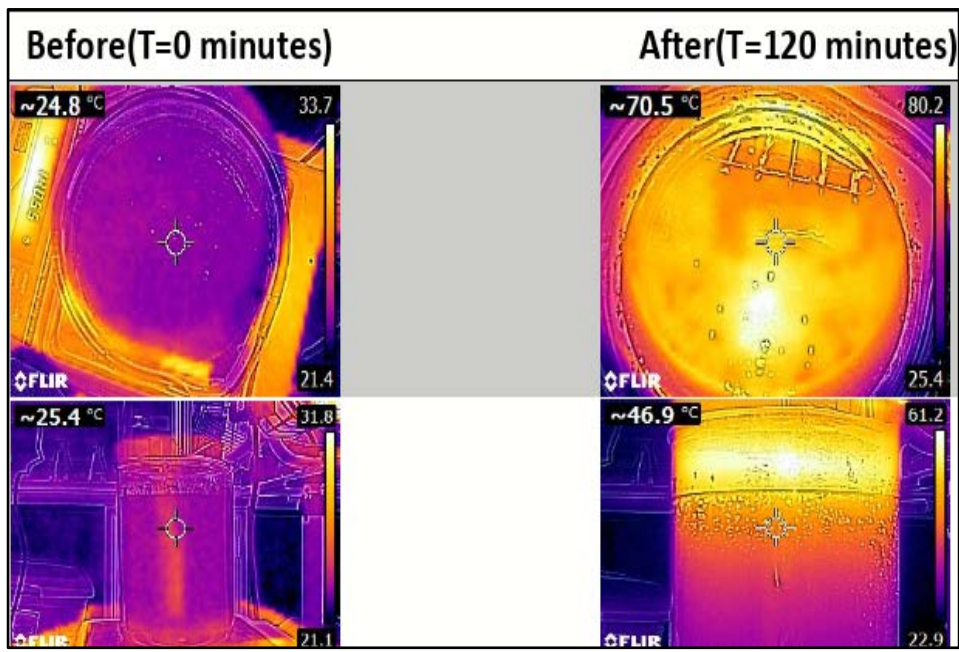


Figure 44 Heat localization in produced water and foam.

5.18 Oil absorbance by polyurethane foam

The oil absorbance of the polyurethane foam was observed for different concentration values of the oil from 10 % to 25 % by volume. We observe that the lower concentration of oil 10 % is absorbed almost 80 % in 15 minutes time whereas for the other higher concentration values it takes 25 minutes to reach the same amount of absorbance because the higher amount of oil requires a higher residence time to be adsorbed by the foam. The higher concentration values take longer time to reach the same filtered value as seen in Fig.45. We see the input oil that enters the filter and the output in Fig 46. The characteristics were also tested before and after treatment.

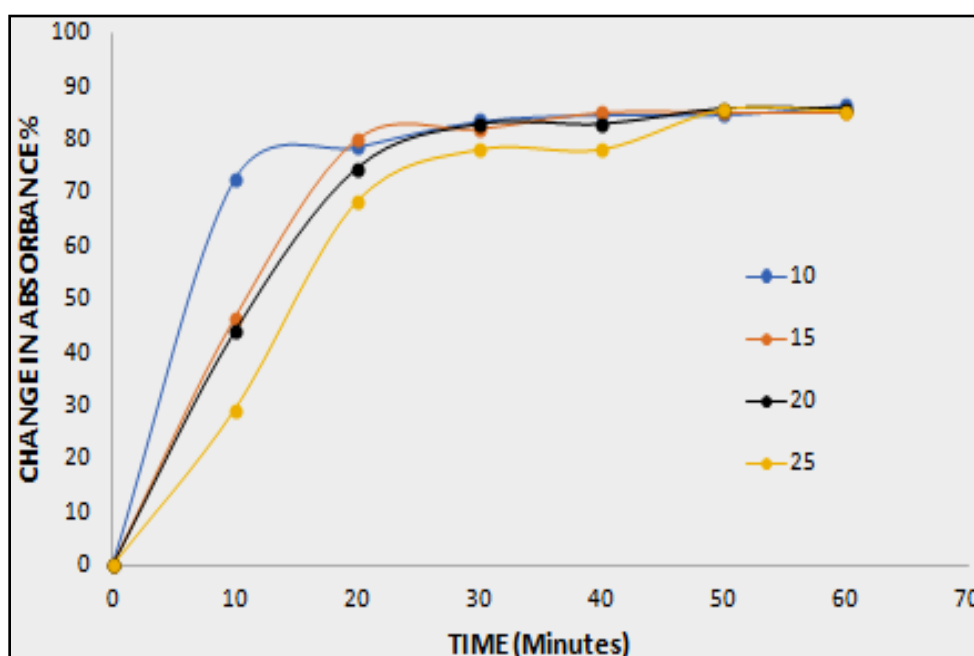


Figure 45 Comparison of different volume % of oil used

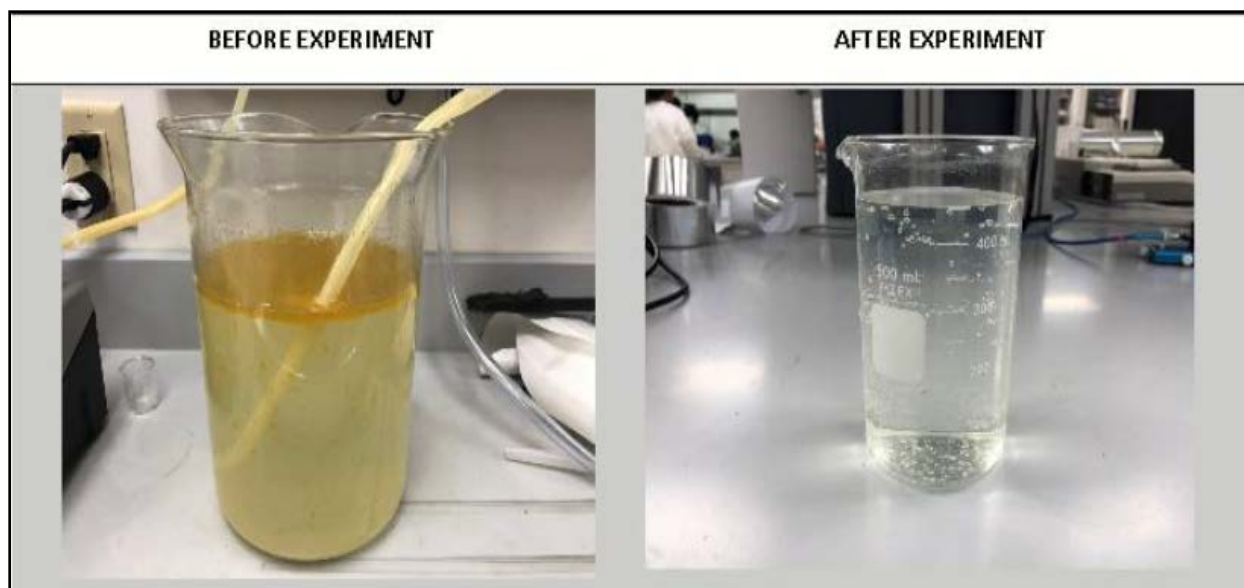


Figure 46 Produced water before and after treatment.

5.19 Oil recovery

The oil recovery capabilities were also tested for the polyurethane foam as shown in figure 47. There is a pipe that is attached to the vacuum pump via an oil collection unit. This draws in the adsorbed oil from the foam. The oil adsorbed was removed by two methods. The mechanical separation process in which the foam was mechanically pressed to remove the oil and secondly using the unit as shown in figure 46. The efficiencies are given by $\eta_{mechanical} = \frac{oil\ recovered}{oil\ adsorbed} = \frac{140}{150} = 93.33\%$ and $\eta_{vacuum} = \frac{oil\ recovered}{oil\ adsorbed} = \frac{110}{150} = 73.33\%$. So we see that the mechanical process is better than the vacuum process even when the latter uses energy. The mechanical process is better than the vacuum process because the latter is unable to penetrate the whole area of the foam to obtain all of the oil, rather just oil is obtained from the surface of the foam. The mechanical process is effective in removing both the avenues. A combination of both the methods would give the best removal of oil if it is not too contaminated. It can help get the oil back so that the foam can be reused as long as it does not degenerate, which it would not because it is a plastic.

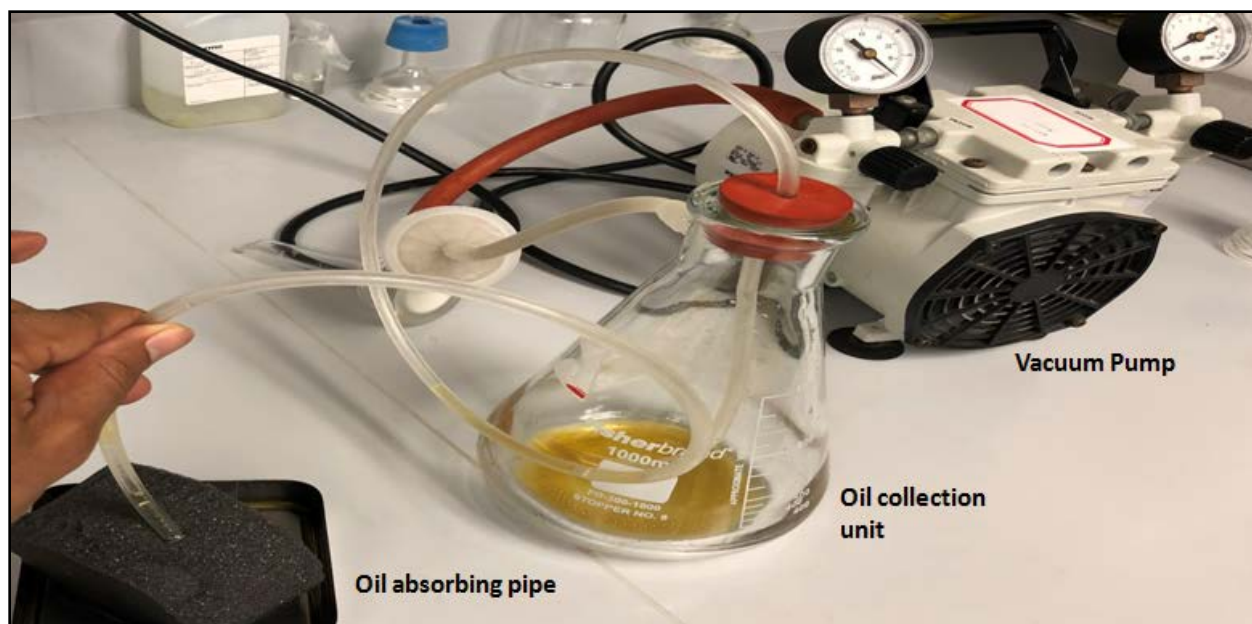


Figure 47 Oil recovery unit.

5.20 Comparison with ongoing methods

The present method was experimentally compared to some of the ongoing methods that are being undertaken to purify oil-water mixtures. There is the air diffuser method where the water is diffused to separate the oil and water mixture so that they can be effectively separated and is depicted in figure 48. The centrifuge method is used where the oil and water mixture can be separated by mixing them at high rotational speeds as shown in figure 49.

The absorbance values of the produced water was compared before and after the filtration process for the three processes as seen in figure 50. The amount of oil absorbed by the polyurethane foam is the maximum at around 85 % whereas for the diffuser and the centrifuge process is 55 % and 45 %. The foam is better at adsorbing oil because of its high adsorbing properties. It was able to adsorb 45-60 times its own volume of oil so it is very effective and efficient.

The evaporation performance was also tested for the three methods to test the feasibility of the steam collection capabilities of the purified water from them. We see that from figure 51 the best performance is observed from the polyurethane foam as it removed the maximum amount of oil which promotes rapid evaporation rather than the diffuser and the centrifuge methods.

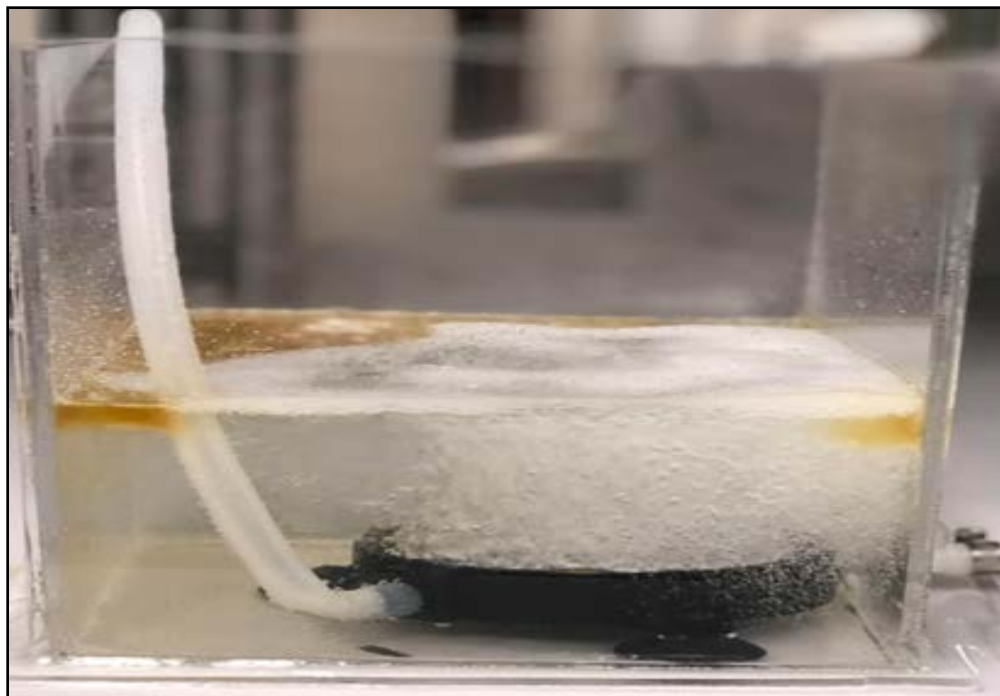


Figure 48 Air diffuser oil removal.

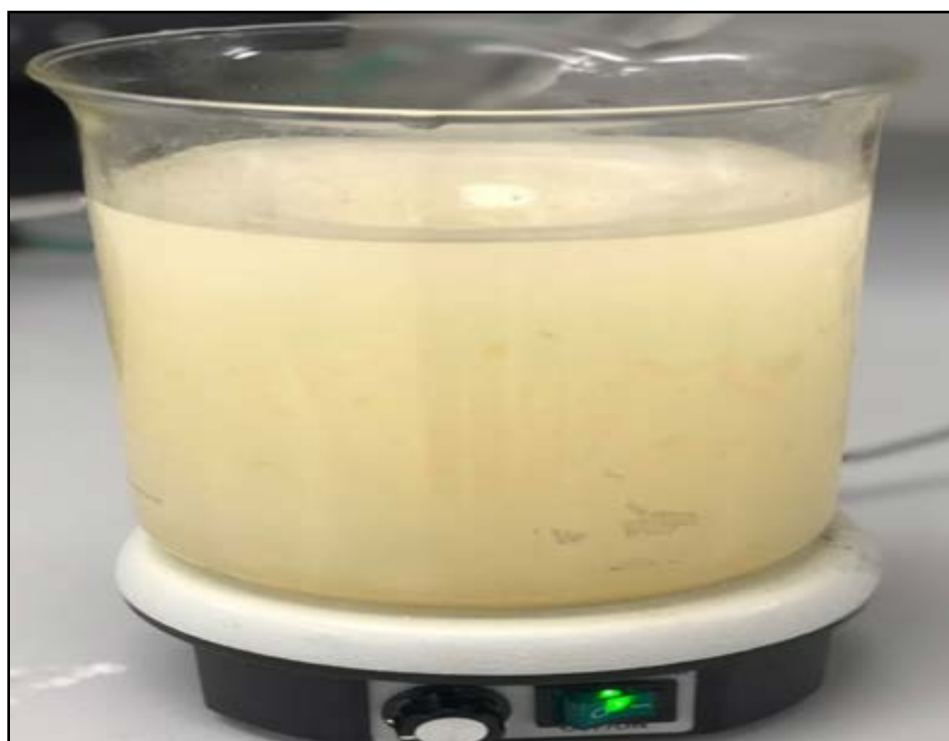


Figure 49 Centrifuge for oil removal.

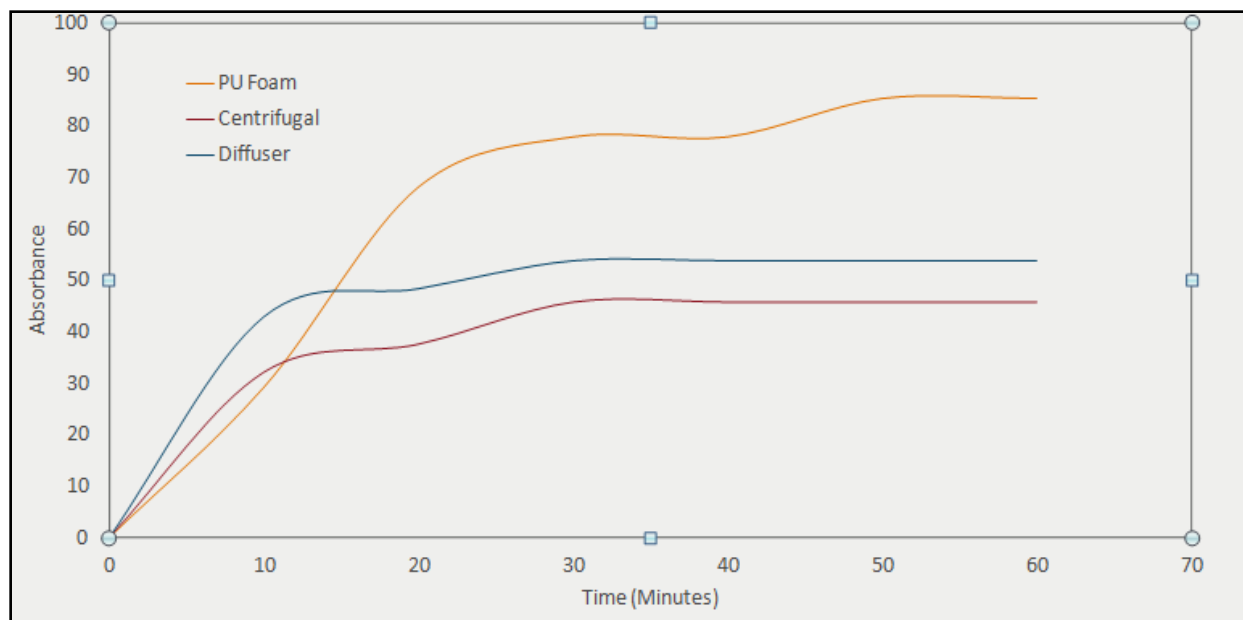


Figure 50 Comparison of oil absorbance between the three methods.

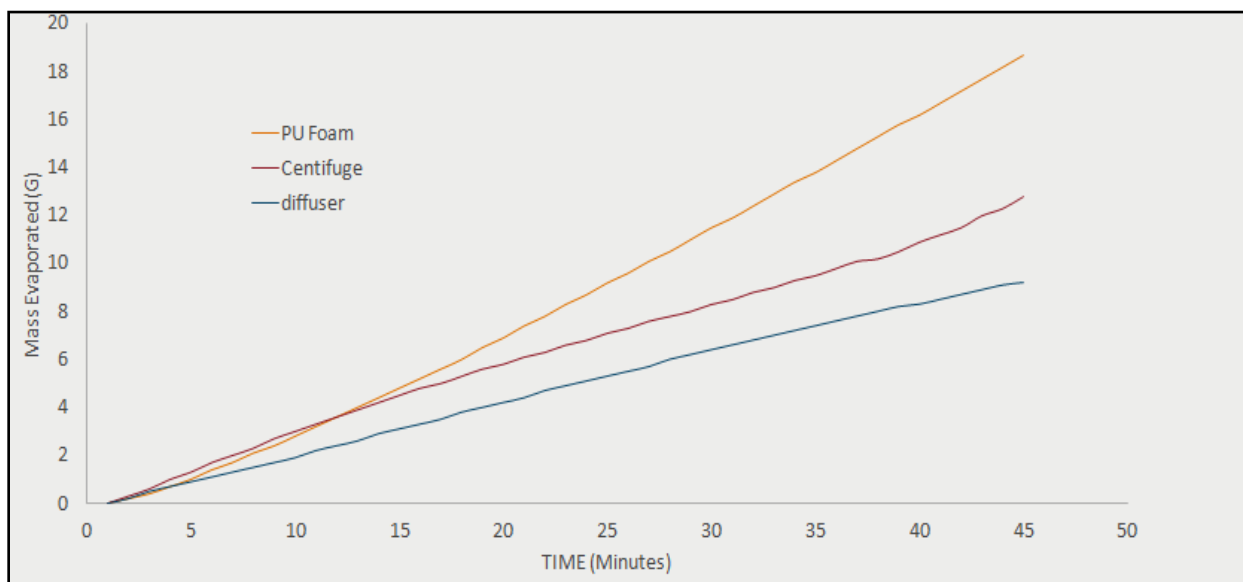


Figure 51 Comparison between the evaporation performances of the three methods.

5.21 Distillation experiments using natural and simulated solar light

The distillation was done with polyurethane foam and activated carbon foam. There was a higher output obtained with the activated carbon coated polyurethane foam than the normal polyurethane foam from Fig.52. The water obtained characteristics were also mentioned in Fig .53 we see that

the water characteristics are almost similar to the D.I water, the TOC is a bit higher but under the US-EPA standards. The distillation experiments were carried out in natural solar light as well so as to make sure that the ongoing process is applicable. So we see the activated carbon foam is better than the normal foam even under natural solar light. The water characteristics obtained were similar as the simulated solar light.

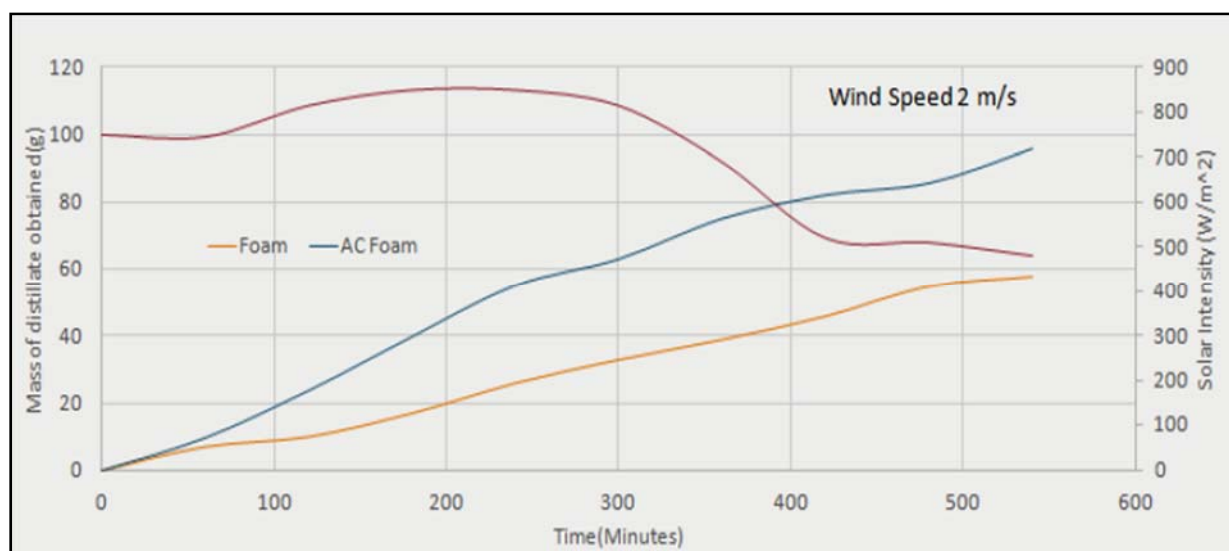


Figure 52 Distillation results in natural sunlight.

Property	D.I Water	Obtained Water from distillation
Absorbance	0	0.35
Turbidity	0.95	1.25
pH	7.00	7.52
TOC	1.4 mg/L	7.5 mg/L

Figure 53 Water characteristics of obtained water compared with D.I water.

5.22 Evaporation with fresnel lens and temperature variance

The evaporation performance was monitored for the polyurethane foam, activated carbon coated polyurethane foam and detergent membrane as seen in figure 54. The best performance is observed from the activated carbon coated polyurethane foam as it facilitates the maximum heat localization at the top surface of the foam. This causes the water to wick through the foam faster than the one in the polyurethane foam. Although the detergent coated membrane was also effective but it is not as effective in removing the oil traces from the produced water as the foam. The simultaneous adsorption and the evaporation from the top surface seems to be an effective and energy efficient method for produced water purification.

The temperature variation on the polyurethane foam was observed using a thermal camera and as well as thermocouples for different experiments as we can see in figures 56 and 57 respectively. We observe that the top surface reached high temperatures of up to 200 degrees C. Even at such high temperatures the foam being a good insulator keeps the heat out of the fluid column as we see the temperature does not increase more than 45 degrees C. So we see there is no heat transfer which increases the efficiency of the process as the bulk temperature increase is prevented. SEM analysis of the foam in figure 55 also shows there is not any visible degradation of the top surface of the foam because of such high temperatures of the order of 150-200 degrees C because the melting point of the foam is about 100 degrees C.

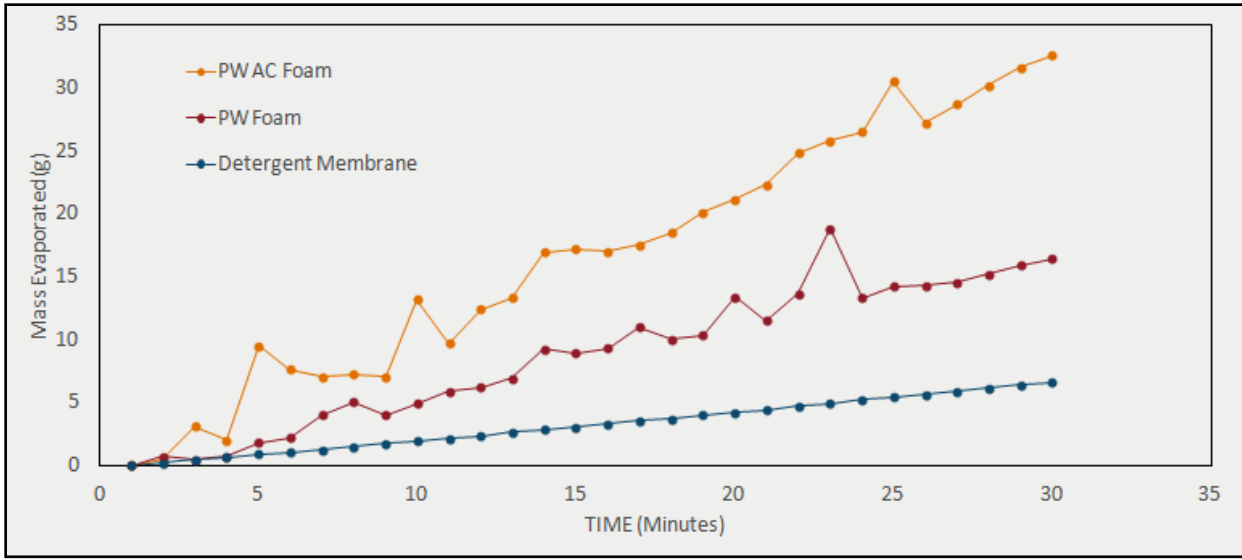


Figure 54 Evaporation performance of different methods.

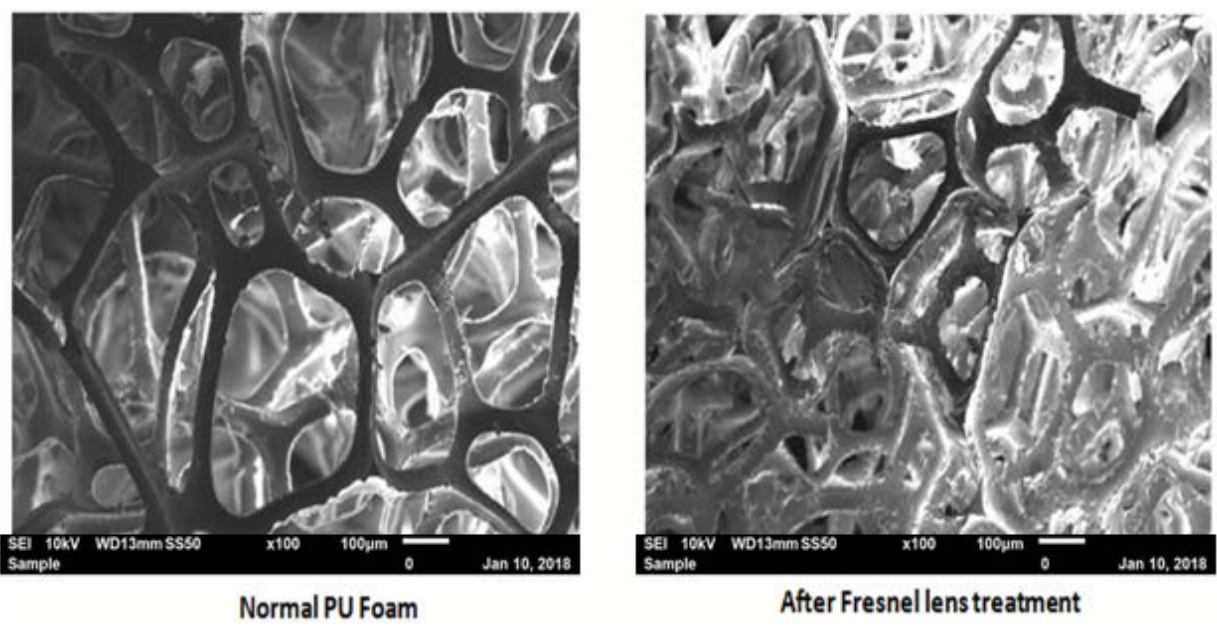


Figure 55 Before and after pictures after concentrated solar experiment.

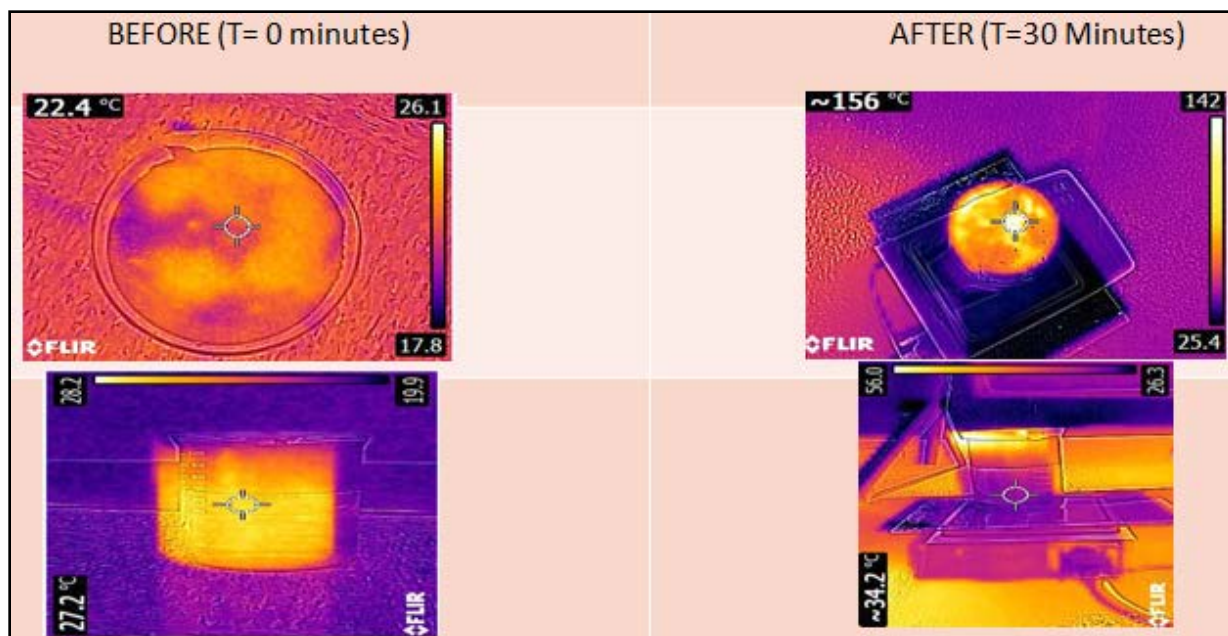


Figure 56 Heat localization on top of the foam due to concentrated solar light.

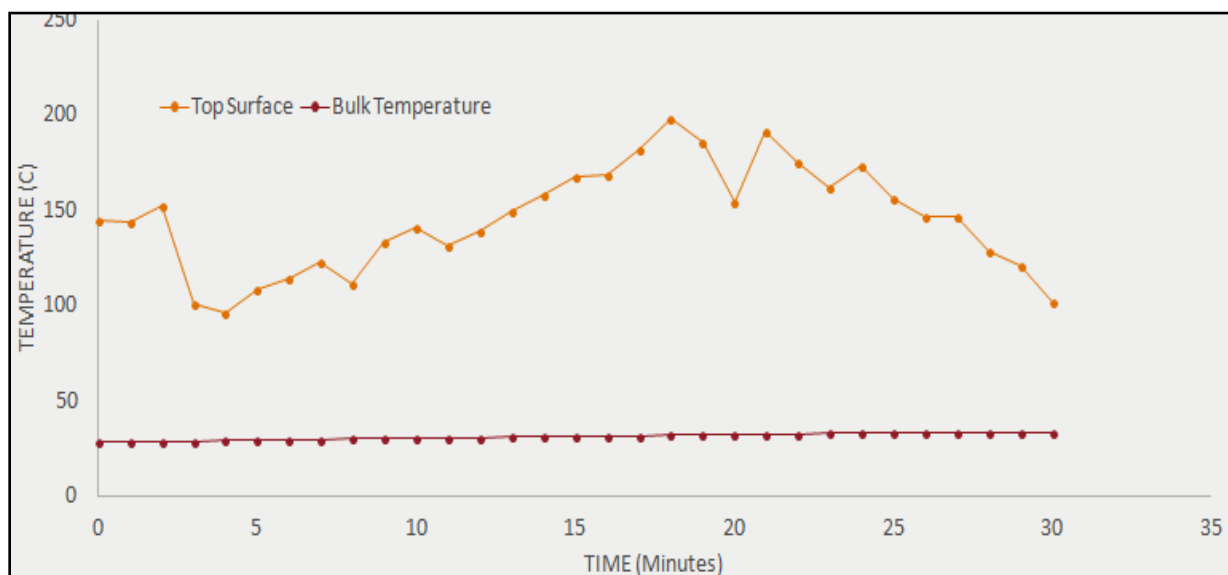


Figure 57 Temperature variation due to concentrated solar light.

5.23 Evaporation rates with impurities and effect of foam thickness

The evaporation rates were also studied with the varying thickness of the foam so as to get the optimal thickness for the polyurethane foam as seen in figure 58. We observe that the 50 mm foam is the optimal thickness where the maximum evaporation takes place. At lower thicknesses the

foam gets logged and hence there is not much evaporation through it and for the high thickness there is not enough capillary power to pull enough water to the top surface, so an optimal amount of thickness which prevents the foam from being clogged and enough capillary power to pull the water to the top surface for evaporation to occur.

The evaporation performance was also studied by adding mud and organic material to the produced water to test the feasibility of the performance of the process so that this can be applied in a real world scenario to purify produced water. We observe from figure 59 that the performance they are very similar even with the addition of the impurities showing that the process is independent of the organic material. So this can be a viable option to purify produced water with organic material.

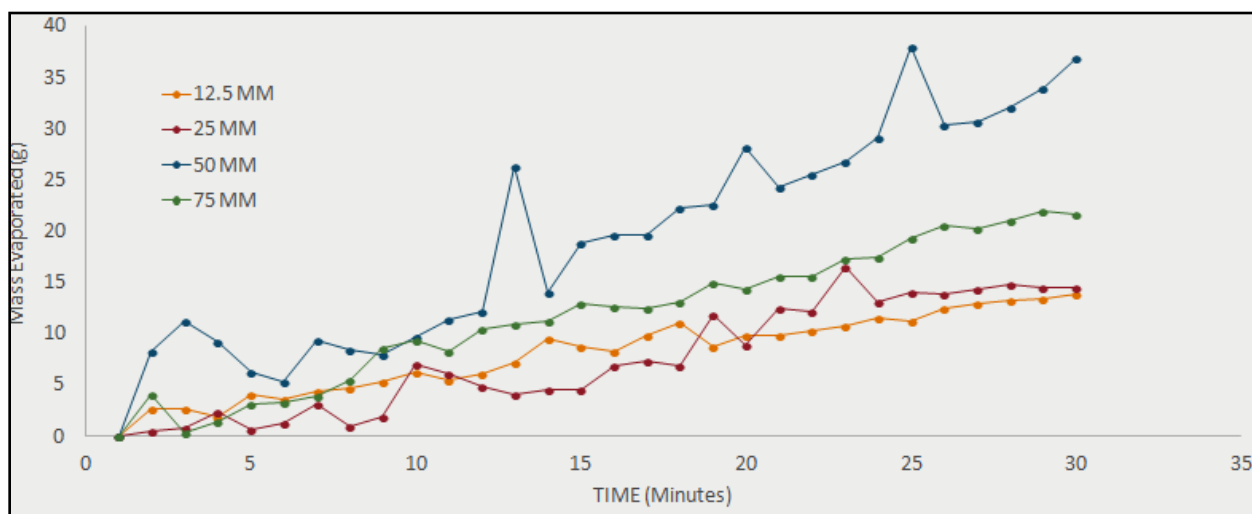


Figure 58 Evaporation performance due to various thickness of foam.

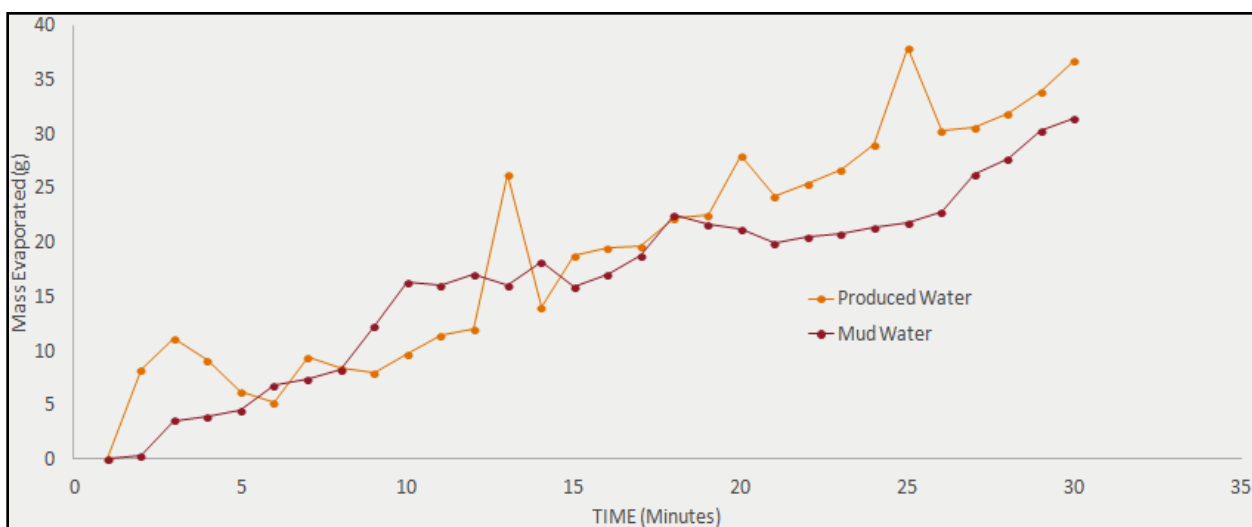


Figure 59 Evaporation performance due to organic impurities

CHAPTER 6. CONCLUSION

In this work, the activated carbon coated polyurethane foam was used to purify produced water in a simultaneous method where the oil was adsorbed by the foam and the temperature difference caused the movement of water through the pores to be evaporated by the solar light. There is a temperature variation that is observed in the nanofluids which shows that the majority of the energy that is incident on the surface is used for evaporation rather than the bulk heating phenomenon which is unnecessary and a waste of energy. The steam generation properties of activated carbon as a low cost alternative was studied and compared with conventional nanoparticles. It was observed that 60 % concentration by volume was the optimum value of concentration for this work. The thermal evaporation experiments proved that light is the major driving force in the evaporation process. The turbidity analysis reveals that the work can be done at different values of turbidity without affecting the steam generation rate. Oil concentrations up to 25 % by volume could be purified and salt concentrations up to 25000 mg/L have been treated to get pure water, which can be used in several different ways, be it household, agricultural or industrial. The oil adsorbed could also be recovered for reuse and recycling. About 95 % of all the impurities were removed from the synthetic produced water using this method. The process also shows promise under natural solar light (600-1000 W/m²), showing it can be a viable option to use as a method to purify this on a larger scale. The high volume steam generation properties also show that the process can utilize wastewater and generate steam which can be used to drive a turbine, essentially making it an efficient process from waste water. This can also be used to obtain a large amount of distilled water from the high volume steam.

REFERENCES

- [1] Philippe Gourbesville, Mingxuan Du, Elodie Zavattoni, Qiang Ma, DSS Architecture for Water Uses Management, *Procedia Engineering*, Volume 154, 2016, Pages 928-935, <https://doi.org/10.1016/j.proeng.2016.07.512>.
- [2] Antón Justes, Ramón Barberán, Begoña A. Farizo, Economic valuation of domestic water uses, *Science of The Total Environment*, Volume 472, 2014, Pages 712-718, <https://doi.org/10.1016/j.scitotenv.2013.11.113>.
- [3] Tao Cao, Saige Wang, Bin Chen, The energy-water nexus in interregional economic trade from both consumption and production perspectives, *Energy Procedia*, Volume 152, 2018, Pages 281-286, <https://doi.org/10.1016/j.egypro.2018.09.124> .
- [4] Muhammad Wakeel, Bin Chen, Tasawar Hayat, Ahmed Alsaedi, Bashir Ahmad, Energy consumption for water use cycles in different countries: A review, *Applied Energy*, Volume 178, 2016, Pages 868-885, <https://doi.org/10.1016/j.apenergy.2016.06.114> .
- [5] B. Van der Bruggen, Chapter 3 The Global Water Recycling Situation, Editor(s): Isabel C. Escobar, Andrea I. Schäfer, *Sustainability Science and Engineering*, Elsevier, Volume 2, 2010, Pages 41-62, [https://doi.org/10.1016/S1871-2711\(09\)00203-7](https://doi.org/10.1016/S1871-2711(09)00203-7) .
- [6] Zhuo Chen, Huu Hao Ngo, Wenshan Guo, A critical review on sustainability assessment of recycled water schemes, *Science of The Total Environment*, Volume 426, 2012, Pages 13-31, <https://doi.org/10.1016/j.scitotenv.2012.03.055> .
- [7] Naveen Joseph, Dongryeol Ryu, Hector M. Malano, Biju George, K.P. Sudheer, Anshuman, Estimation of industrial water demand in India using census-based statistical data, *Resources, Conservation and Recycling*, Volume 149, 2019, Pages 31-44, <https://doi.org/10.1016/j.resconrec.2019.05.036> .
- [8] Narjes Nouri, Farhad Balali, Adel Nasiri, Hamid Seifoddini, Wilkistar Otieno, Water withdrawal and consumption reduction for electrical energy generation systems, *Applied Energy*, Volume 248, 2019, Pages 196-206, <https://doi.org/10.1016/j.apenergy.2019.04.023> .

- [9] Steven J. Kenway, Ka Leung Lam, Jennifer Stokes-Draut, Kelly Twomey Sanders, Amanda N. Binks, Julijana Bors, Brian Head, Gustaf Olsson, James E. McMahon, Defining water-related energy for global comparison, clearer communication, and sharper policy., *Journal of Cleaner Production*, 2019 <https://doi.org/10.1016/j.jclepro.2019.06.333> .
- [10] X.F. Wu, G.Q. Chen, Global overview of crude oil use: From source to sink through inter-regional trade, *Energy Policy*, Volume 128, 2019, Pages 476-486, <https://doi.org/10.1016/j.enpol.2019.01.022> .
- [11] Bjarne Foss, Brage Rugstad Knudsen, Bjarne Grimstad, Petroleum production optimization – A static or dynamic problem?, *Computers & Chemical Engineering*, Volume 114, 2018, Pages 245-253, <https://doi.org/10.1016/j.compchemeng.2017.10.009> .
- [12] Nina Linn Ulstein, Bjørn Nygreen, Jan Richard Sagli, Tactical planning of offshore petroleum production, *European Journal of Operational Research*, Volume 176, Issue 1, 2007, Pages 550-564, <https://doi.org/10.1016/j.ejor.2005.06.060> .
- [13] Jiandong Chen, Jie Yu, Bowei Ai, Malin Song, Wenxuan Hou, Determinants of global natural gas consumption and import–export flows, *Energy Economics*, 2018, <https://doi.org/10.1016/j.eneco.2018.06.025> .
- [14] Mucahit Aydin, Natural gas consumption and economic growth nexus for top 10 natural Gas–Consuming countries: A granger causality analysis in the frequency domain, *Energy*, Volume 165, Part B, 2018, Pages 179-186, <https://doi.org/10.1016/j.energy.2018.09.149>.
- [15] Mehmet Akif Destek, Natural gas consumption and economic growth: Panel evidence from OECD countries, *Energy*, Volume 114, 2016, Pages 1007-1015, <https://doi.org/10.1016/j.energy.2016.08.076> .
- [16] Antonio A. Golpe, Monica Carmona, Emilio Congregado, Persistence in natural gas consumption in the US: An unobserved component model, *Energy Policy*, Volume 46, 2012, Pages 594-600, <https://doi.org/10.1016/j.enpol.2012.04.021> .
- [17] Ilhan Ozturk, Usama Al-Mulali, Natural gas consumption and economic growth nexus: Panel data analysis for GCC countries, *Renewable and Sustainable Energy Reviews*, Volume 51, 2015, Pages 998-1003, <https://doi.org/10.1016/j.rser.2015.07.005> .
- [18] Junchen Li, Xiucheng Dong, Jianxin Shangguan, Mikael Hook, Forecasting the growth of China’s natural gas consumption, *Energy*, Volume 36, Issue 3, 2011, Pages 1380-1385, <https://doi.org/10.1016/j.energy.2011.01.003> .

- [19] Naima A. Khan, Mark Engle, Barry Dungan, F.Omar Holguin, Pei Xu, Kenneth C. Carroll, Volatile-organic molecular characterization of shale-oil produced water from the Permian Basin, *Chemosphere*, Volume 148, 2016, Pages 126-136, <https://doi.org/10.1016/j.chemosphere.2015.12.116> .
- [20] Zacariah L. Hildenbrand, Doug D. Carlton, Brian E. Fontenot, Jesse M. Meik, Jayme L. Walton, Jonathan B. Thacker, Stephanie Korlie, C. Phillip Shelor, Akinde F. Kadjo, Adelaide Clark, Sascha Usenko, Jason S. Hamilton, Phillip M. Mach, Guido F. Verbeck, Paul Hudak, Kevin A. Schug, Temporal variation in groundwater quality in the Permian Basin of Texas, a region of increasing unconventional oil and gas development, *Science of The Total Environment*, Volume 562, 2016, Pages 906-913, <https://doi.org/10.1016/j.scitotenv.2016.04.144> .
- [21] Muhammad Wakeel, Bin Chen, Tasawar Hayat, Ahmed Alsaedi, Bashir Ahmad, Energy consumption for water use cycles in different countries: A review, *Applied Energy*, Volume 178, 2016, <https://doi.org/10.1016/j.apenergy.2016.06.114> .
- [22] Marc Compton, Sarah Willis, Behnaz Rezaie, Karen Humes, Food processing industry energy and water consumption in the Pacific northwest, *Innovative Food Science & Emerging Technologies*, Volume 47, 2018, Pages 371-383, <https://doi.org/10.1016/j.ifset.2018.04.001> .
- [23] Gen Li, Bing Bai, Kenneth H. Carlson, Characterization of solids in produced water from wells fractured with recycled and fresh water, *Journal of Petroleum Science and Engineering*, Volume 144, 2016, Pages 91-98, <https://doi.org/10.1016/j.petrol.2016.03.011> .
- [24] Neff J., Lee K., DeBlois E.M. (2011) Produced Water: Overview of Composition, Fates, and Effects. In: Lee K., Neff J. (eds) Produced Water. Springer, New York, NY, 2011, https://doi.org/10.1007/978-1-4614-0046-2_1 .
- [25] William Orem, Calin Tatu, Matthew Varonka, Harry Lerch, Anne Bates, Mark Engle, Lynn Crosby, Jennifer McIntosh, Organic substances in produced and formation water from unconventional natural gas extraction in coal and shale, *International Journal of Coal Geology*, Volume 126, 2014, Pages 20-31, <https://doi.org/10.1016/j.coal.2014.01.003> .

- [26] Bethany Alley, Alex Beebe, John Rodgers, James W. Castle, Chemical and physical characterization of produced waters from conventional and unconventional fossil fuel resources, *Chemosphere*, Volume 85, Issue 1, 2011, Pages 74-82, <https://doi.org/10.1016/j.chemosphere.2011.05.043> .
- [27] Fillo J.P., Koraido S.M., Evans J.M. (1992) Sources, Characteristics, and Management of Produced Waters from Natural Gas Production and Storage Operations. In: Ray J.P., Engelhardt F.R. (eds) *Produced Water*. Environmental Science Research, vol 46. Springer, Boston, M, https://doi.org/10.1007/978-1-4615-2902-6_12 .
- [28] Shepherd, M.C., Shore, F.L., Mertens, S.K., Gibson, J.S, Characterization of produced waters from natural gas production and storage operations: Regulatory analysis of a complex matrix, *Produced Water: Technological/Environmental Issues and Solutions* Pages 163-174, 1992,
- [29] James Rosenblum, Andrew W. Nelson, Bridger Ruyle, Michael K. Schultz, Joseph N. Ryan, Karl G. Linden, Temporal characterization of flowback and produced water quality from a hydraulically fractured oil and gas well, *Science of The Total Environment*, Volumes 596-597, 2017, Pages 369-377, <https://doi.org/10.1016/j.scitotenv.2017.03.294> .
- [30] Toril I. Røe Utvik, Chemical characterisation of produced water from four offshore oil production platforms in the North Sea, *Chemosphere*, Volume 39, Issue 15, 1999, Pages 2593-2606, [https://doi.org/10.1016/S0045-6535\(99\)00171-X](https://doi.org/10.1016/S0045-6535(99)00171-X) .
- [31] José M. Estrada, Rao Bhamidimarri, A review of the issues and treatment options for wastewater from shale gas extraction by hydraulic fracturing, *Fuel*, Volume 182, 2016, Pages 292-303, <https://doi.org/10.1016/j.fuel.2016.05.051> .
- [32] Z. Sheikholeslami, D. Yousefi Kebria, F. Qaderi, Nanoparticle for degradation of BTEX in produced water; an experimental procedure, *Journal of Molecular Liquids*, Volume 264, 2018, Pages 476-482, <https://doi.org/10.1016/j.molliq.2018.05.096> .
- [33] S. Shokrollahzadeh, F. Golmohammad, N. Naseri, H. Shokouhi, M. Arman-mehr, Chemical Oxidation for Removal of Hydrocarbons from Gas-Field Produced Water, *Procedia Engineering*, Volume 42, 2012, Pages 942-947, <https://doi.org/10.1016/j.proeng.2012.07.487> .

- [34] Jeffrey L. Means, Norman Hubbard, Short-chain aliphatic acid anions in deep subsurface brines: A review of their origin, occurrence, properties, and importance and new data on their distribution and geochemical implications in the Palo Duro Basin, Texas, *Organic Geochemistry*, Volume 11, Issue 3, 1987, Pages 177-191, [https://doi.org/10.1016/0146-6380\(87\)90021-0](https://doi.org/10.1016/0146-6380(87)90021-0) .
- [35] Haroldo S. Dórea, José R.L. Bispo, Kennedy A.S. Aragão, Bruno B. Cunha, Sandro Navickiene, José P.H. Alves, Luciane P.C. Romão, Carlos A.B. Garcia, Analysis of BTEX, PAHs and metals in the oilfield produced water in the State of Sergipe, Brazil, *Microchemical Journal*, Volume 85, Issue 2, 2007, Pages 234-238, <https://doi.org/10.1016/j.microc.2006.06.002> .
- [36] Donald B. MacGowan, Ronald C. Surdam, Difunctional carboxylic acid anions in oilfield waters, *Organic Geochemistry*, Volume 12, Issue 3, 1988, Pages 245-259, [https://doi.org/10.1016/0146-6380\(88\)90262-8](https://doi.org/10.1016/0146-6380(88)90262-8) .
- [37] Shan Zhao, Guohe Huang, Guanhui Cheng, Yafei Wang, Haiyan Fu, Hardness, COD and turbidity removals from produced water by electrocoagulation pretreatment prior to Reverse Osmosis membranes, *Desalination*, Volume 344, 2014, Pages 454-462, <https://doi.org/10.1016/j.desal.2014.04.014> .
- [38] José M. Estrada, Rao Bhamidimarri, A review of the issues and treatment options for wastewater from shale gas extraction by hydraulic fracturing, *Fuel*, Volume 182, 2016, Pages 292-303, <https://doi.org/10.1016/j.fuel.2016.05.051> .
- [39] Brian G. Rahm, Josephine T. Bates, Lara R. Bertoia, Amy E. Galford, David A. Yoxtheimer, Susan J. Riha, Wastewater management and Marcellus Shale gas development: Trends, drivers, and planning implications, *Journal of Environmental Management*, Volume 120, 2013, Pages 105-113, <https://doi.org/10.1016/j.jenvman.2013.02.029> .
- [40] Katherine J. Skalak, Mark A. Engle, Elisabeth L. Rowan, Glenn D. Jolly, Kathryn M. Conko, Adam J. Benthem, Thomas F. Kraemer, Surface disposal of produced waters in western and southwestern Pennsylvania: Potential for accumulation of alkali-earth elements in sediments, *International Journal of Coal Geology*, Volume 126, 2014, Pages 162-170, <https://doi.org/10.1016/j.coal.2013.12.001> .

- [41] Samuel Adams, Edem Kwame Mensah Klobodu, Alfred Apio, Renewable and non-renewable energy, regime type and economic growth, *Renewable Energy*, Volume 125, 2018, Pages 755-767, <https://doi.org/10.1016/j.renene.2018.02.135> .
- [42] Charalambos N. Elias, Vassilis N. Stathopoulos, A comprehensive review of recent advances in materials aspects of phase change materials in thermal energy storage, *Energy Procedia*, Volume 161, 2019, Pages 385-394, <https://doi.org/10.1016/j.egypro.2019.02.101> .
- [43] Suphi S. Oncel, Green energy engineering: Opening a green way for the future, *Journal of Cleaner Production*, Volume 142, Part 4, 2017, Pages 3095-3100, <https://doi.org/10.1016/j.jclepro.2016.10.158> .
- [44] Ibrahim Dincer, Calin Zamfirescu, Potential options to greenize energy systems, *Energy*, Volume 46, Issue 1, 2012, Pages 5-15, <https://doi.org/10.1016/j.energy.2011.11.061> .
- [45] Ugo Pelay, Lingai Luo, Yilin Fan, Driss Stitou, Mark Rood, Thermal energy storage systems for concentrated solar power plants, *Renewable and Sustainable Energy Reviews*, Volume 79, 2017, Pages 82-100, <https://doi.org/10.1016/j.rser.2017.03.139> .
- [46] Yaxue Lin, Yuting Jia, Guruprasad Alva, Guiyin Fang, Review on thermal conductivity enhancement, thermal properties and applications of phase change materials in thermal energy storage, *Renewable and Sustainable Energy Reviews*, Volume 82, Part 3, 2018, Pages 2730-2742, <https://doi.org/10.1016/j.rser.2017.10.002> .
- [47] Tejvir Singh, Muataz Ali Atieh Hussien, Tareq Al-Ansari, Khaled Saoud, Gordon McKay, Critical review of solar thermal resources in GCC and application of nanofluids for development of efficient and cost effective CSP technologies, *Renewable and Sustainable Energy Reviews*, Volume 91, 2018, Pages 708-719, <https://doi.org/10.1016/j.rser.2018.03.050> .
- [48] Sujit kumar verma, Arun Kumar Tiwari, Application of Nanoparticles in Solar collectors: A Review, *Materials Today: Proceedings*, Volume 2, Issues 4–5, 2015, Pages 3638-3647, <https://doi.org/10.1016/j.matpr.2015.07.121> .
- [49] Muhammad Abid, Tahir A.H. Ratlamwala, Ugur Atikol, Solar assisted multi-generation system using nanofluids: A comparative analysis, *International Journal of Hydrogen Energy*, Volume 42, Issue 33, 2017, Pages 21429-21442, <https://doi.org/10.1016/j.ijhydene.2017.05.178> .

- [50] Titan C. Paul, A.K.M. M. Morshed, Jamil A. Khan, Effect of Nanoparticle Dispersion on Thermophysical Properties of Ionic Liquids for its Potential Application in Solar Collector, *Procedia Engineering*, Volume 90, 2014, Pages 643-648, <https://doi.org/10.1016/j.proeng.2014.11.785> .
- [51] Khalil Khanafer, Kambiz Vafai, A review on the applications of nanofluids in solar energy field, *Renewable Energy*, Volume 123, 2018, Pages 398-406, <https://doi.org/10.1016/j.renene.2018.01.097> .
- [52] Owen Arthur, M.A. Karim, An investigation into the thermophysical and rheological properties of nanofluids for solar thermal applications, *Renewable and Sustainable Energy Reviews*, Volume 55, 2016, Pages 739-755, <https://doi.org/10.1016/j.rser.2015.10.065> .
- [53] J.P. Wilcoxon, Chapter 2 - Nanoparticles—Preparation, Characterization and Physical Properties, Editor(s): Roy L. Johnston, J.P. Wilcoxon, *Frontiers of Nanoscience*, Elsevier, Volume 3, 2012, Pages 43-127, <https://doi.org/10.1016/B978-0-08-096357-0.00005-4> .
- [54] Heinrich Badenhorst, A review of the application of carbon materials in solar thermal energy storage, *Solar Energy*, 2018, <https://doi.org/10.1016/j.solener.2018.01.062> .
- [55] Yoshitaka Ueki, Takashi Aoki, Kenta Ueda, Masahiko Shibahara, Thermophysical properties of carbon-based material nanofluid, *International Journal of Heat and Mass Transfer*, Volume 113, 2017, Pages 1130-1134, <https://doi.org/10.1016/j.ijheatmasstransfer.2017.06.008> .
- [56] Abdullah A.A.A. Alrashed, Maryam Soltanpour Gharibdousti, Marjan Goodarzi, Letícia Raquel de Oliveira, Mohammad Reza Safaei, Enio Pedone Bandarra Filho, Effects on thermophysical properties of carbon based nanofluids: Experimental data, modelling using regression, ANFIS and ANN, *International Journal of Heat and Mass Transfer*, Volume 125, 2018, Pages 920-932, <https://doi.org/10.1016/j.ijheatmasstransfer.2018.04.142> .
- [57] Mohammed Danish, Tanweer Ahmad, A review on utilization of wood biomass as a sustainable precursor for activated carbon production and application, *Renewable and Sustainable Energy Reviews*, Volume 87, 2018, Pages 1-21, <https://doi.org/10.1016/j.rser.2018.02.003> .
- [58] Wenyuan Qu, Tong Yuan, Guojun Yin, Shiai Xu, Qing Zhang, Hongjun Su, Effect of properties of activated carbon on malachite green adsorption, *Fuel*, Volume 249, 2019, Pages 45-53, <https://doi.org/10.1016/j.fuel.2019.03.058> .

- [59] Rodriguez-Reinoso, Francisco. (2001). Activated Carbon and Adsorption. Encyclopedia of Materials: Science and Technology. 22-34. 10.1016/B0-08-043152-6/00005-X.
- [60] Wenqing Yang, Qingyin Dong, Shili Liu, Henghua Xie, Lili Liu, Jinhui Li, Recycling and Disposal Methods for Polyurethane Foam Wastes, Procedia Environmental Sciences, Volume 16, 2012, Pages 167-175, <https://doi.org/10.1016/j.proenv.2012.10.023>.
- [61] Lee, S. , Teramoto, Y. and Shiraishi, N. (2002), Biodegradable polyurethane foam from liquefied waste paper and its thermal stability, biodegradability, and genotoxicity. J. Appl. Polym. Sci., 83: 1482-1489. doi:10.1002/app.10039 .
- [62]] Khalid Mahmood Zia, Haq Nawaz Bhatti, Ijaz Ahmad Bhatti, Methods for polyurethane and polyurethane composites, recycling and recovery: A review, Reactive and Functional Polymers, Volume 67, Issue 8, 2007, Pages 675-692, <https://doi.org/10.1016/j.reactfunctpolym.2007.05.004> .
- [63] Hua Li, Lifen Liu, Fenglin Yang, Oleophilic Polyurethane Foams for Oil Spill Cleanup, Procedia Environmental Sciences, Volume 18, 2013, Pages 528-533, <https://doi.org/10.1016/j.proenv.2013.04.071>.
- [64] Nadeem Baig, Fahd I. Alghunaimi, Hind S. Dossary, Tawfik A. Saleh, Superhydrophobic and superoleophilic carbon nanofiber grafted polyurethane for oil-water separation, Process Safety and Environmental Protection, Volume 123, 2019, Pages 327-334, <https://doi.org/10.1016/j.psep.2019.01.007> .
- [65] Amir Ahmad Nikkhah, Hamid Zilouei, Ahmad Asadinezhad, Alireza Keshavarz, Removal of oil from water using polyurethane foam modified with nanoclay, Chemical Engineering Journal, Volume 262, 2015, Pages 278-285, <https://doi.org/10.1016/j.cej.2014.09.077>.
- [66] Mohammad A. Al-Ghouti, Maryam A. Al-Kaabi, Mohammad Y. Ashfaq, Dana Adel Da'na, Produced water characteristics, treatment and reuse: A review, Journal of Water Process Engineering, Volume 28, 2019, Pages 222-239, <https://doi.org/10.1016/j.jwpe.2019.02.001>.
- [67] Jisi Zheng, Bing Chen, Worakanok Thanyamanta, Kelly Hawboldt, Baiyu Zhang, Bo Liu, Offshore produced water management: A review of current practice and challenges in harsh/Arctic environments, Marine Pollution Bulletin, Volume 104, Issues 1–2, 2016, Pages 7-19, <https://doi.org/10.1016/j.marpolbul.2016.01.004> .

- [68] Bethany Alley, Alex Beebe, John Rodgers, James W. Castle, Chemical and physical characterization of produced waters from conventional and unconventional fossil fuel resources, *Chemosphere*, Volume 85, Issue 1, 2011, Pages 74-82, <https://doi.org/10.1016/j.chemosphere.2011.05.043>
- [69] James Rosenblum, Andrew W. Nelson, Bridger Ruyle, Michael K. Schultz, Joseph N. Ryan, Karl G. Linden, Temporal characterization of flowback and produced water quality from a hydraulically fractured oil and gas well, *Science of The Total Environment*, Volumes 596–597, 2017, Pages 369-377, <https://doi.org/10.1016/j.scitotenv.2017.03.294> .
- [70] Hao Lu, Yi-qian Liu, Jing-bo Cai, Xiao Xu, Lin-sheng Xie, Qiang Yang, Yue-xi Li, Kai Zhu, Treatment of offshore oily produced water: Research and application of a novel fibrous coalescence technique, *Journal of Petroleum Science and Engineering*, Volume 178, 2019, Pages 602-608, <https://doi.org/10.1016/j.petrol.2019.03.025> .
- [71] Tiffany Liden, Doug D. Carlton, Shinji Miyazaki, Takehiko Otoyoy, Kevin A. Schug, Forward osmosis remediation of high salinity Permian Basin produced water from unconventional oil and gas development, *Science of The Total Environment*, Volume 653, 2019, Pages 82-90, <https://doi.org/10.1016/j.scitotenv.2018.10.325> .
- [72] Andrii Butkovskiy, Harry Bruning, Stefan A.E. Kools, Huub H.M. Rijnaarts, and Annemarie P. Van Wezel *Environmental Science & Technology* 2017 51 (9), 4740-4754, <https://doi.org/10.1021/acs.est.6b05640> .
- [73] Kyle J. Ferrar, Drew R. Michanowicz, Charles L. Christen, Ned Mulcahy, Samantha L. Malone, and Ravi K. Sharma, Assessment of Effluent Contaminants from Three Facilities Discharging Marcellus Shale Wastewater to Surface Waters in Pennsylvania, *Environmental Science & Technology* 2013 47 (7), 3472-3481, DOI: 10.1021/es301411q.
- [74] R. D. Vidic, S. L. Brantley, J. M. Vandenbossche, D. Yoxtheimer, J. D. Abad, Impact of Shale Gas Development on Regional Water Quality, *Science* 17 May 2013, <https://doi.org/10.1126/science.1235009>.
- [75] Elise Barbot, Natasa S. Vidic, Kelvin B. Gregory, and Radisav D. Vidic, Spatial and Temporal Correlation of Water Quality Parameters of Produced Waters from Devonian-Age Shale following Hydraulic Fracturing *Environmental Science & Technology* 2013 47 (6), 2562-2569, <https://doi.org/10.1021/es304638h>.

- [76] Yaal Lester, Imma Ferrer, E. Michael Thurman, Kurban A. Sitterley, Julie A. Korak, George Aiken, Karl G. Linden, Characterization of hydraulic fracturing flowback water in Colorado: Implications for water treatment, *Science of The Total Environment*, Volumes 512-513, 2015, Pages 637-644, <https://doi.org/10.1016/j.scitotenv.2015.01.043> .
- [77] Paul F. Ziemkiewicz, Y. Thomas He, Evolution of water chemistry during Marcellus Shale gas development: A case study in West Virginia, *Chemosphere*, Volume 134, 2015, Pages 224-231, <https://doi.org/10.1016/j.chemosphere.2015.04.040> .
- [78] Brian W. Stewart, Elizabeth C. Chapman, Rosemary C. Capo, Jason D. Johnson, Joseph R. Graney, Carl S. Kirby, Karl T. Schroeder, Origin of brines, salts and carbonate from shales of the Marcellus Formation: Evidence from geochemical and Sr isotope study of sequentially extracted fluids, *Applied Geochemistry*, Volume 60, 2015, Pages 78-88, <https://doi.org/10.1016/j.apgeochem.2015.01.004> .
- [79] Fenglian Fu, Qi Wang, Removal of heavy metal ions from wastewaters: A review, *Journal of Environmental Management*, Volume 92, Issue 3, 2011, Pages 407-418, <https://doi.org/10.1016/j.jenvman.2010.11.011> .
- [80] Katherine J. Skalak, Mark A. Engle, Elisabeth L. Rowan, Glenn D. Jolly, Kathryn M. Conko, Adam J. Benthem, Thomas F. Kraemer, Surface disposal of produced waters in western and southwestern Pennsylvania: Potential for accumulation of alkali-earth elements in sediments, *International Journal of Coal Geology*, Volume 126, 2014, Pages 162-170, <https://doi.org/10.1016/j.coal.2013.12.001> .
- [81] William Orem, Calin Tatu, Matthew Varonka, Harry Lerch, Anne Bates, Mark Engle, Lynn Crosby, Jennifer McIntosh, Organic substances in produced and formation water from unconventional natural gas extraction in coal and shale, *International Journal of Coal Geology*, Volume 126, 2014, Pages 20-31, <https://doi.org/10.1016/j.coal.2014.01.003> .
- [82] Jenna L. Luek, Michael Gonsior, Organic compounds in hydraulic fracturing fluids and wastewaters: A review *Water Research*, Volume 123, 2017, Pages 536-548, <https://doi.org/10.1016/j.watres.2017.07.012> .
- [83] William T. Stringfellow, Jeremy K. Domen, Mary Kay Camarillo, Whitney L. Sandelin, Sharon Borglin, Physical, chemical, and biological characteristics of compounds used in hydraulic fracturing, *Journal of Hazardous Materials*, Volume 275, 2014, Pages 37-54, <https://doi.org/10.1016/j.jhazmat.2014.04.040>.

- [84] Sareh Rezaei Hosein Abadi, Mohammad Reza Sebzari, Mahmood Hemati, Fatemeh Rekabdar, Toraj Mohammadi, Ceramic membrane performance in microfiltration of oily wastewater, *Desalination*, Volume 265, Issues 1–3, 2011, Pages 222-228, <https://doi.org/10.1016/j.desal.2010.07.055> .
- [85] Hongzhu Ma, Bo Wang, Electrochemical pilot-scale plant for oil field produced wastewater by M/C/Fe electrodes for injection, *Journal of Hazardous Materials*, Volume 132, Issues 2–3, 2006, Pages 237-243, <https://doi.org/10.1016/j.jhazmat.2005.09.043>.
- [86] T. Zsirai, H. Qiblawey, P. Buzatu, M. Al-Marri, S.J. Judd, Cleaning of ceramic membranes for produced water filtration, *Journal of Petroleum Science and Engineering*, Volume 166, 2018, Pages 283-289, <https://doi.org/10.1016/j.petrol.2018.03.036>.
- [87] Flannery C. Dolan, Tzahi Y. Cath, Terri S. Hogue, Assessing the feasibility of using produced water for irrigation in Colorado, *Science of The Total Environment*, Volumes 640–641, 2018, Pages 619-628, <https://doi.org/10.1016/j.scitotenv.2018.05.200> .
- [88] S. Jiménez, M.M. Micó, M. Arnaldos, F. Medina, S. Contreras, State of the art of produced water treatment, *Chemosphere*, Volume 192, 2018, Pages 186-208, <https://doi.org/10.1016/j.chemosphere.2017.10.139> .
- [89] Jisi Zheng, Bing Chen, Worakanok Thanyamanta, Kelly Hawboldt, Baiyu Zhang, Bo Liu, Offshore produced water management: A review of current practice and challenges in harsh/Arctic environments, *Marine Pollution Bulletin*, Volume 104, Issues 1–2, 2016, Pages 7-19, <https://doi.org/10.1016/j.marpolbul.2016.01.004> .
- [90] Tânia L.S. Silva, Sergio Morales-Torres, Sérgio Castro-Silva, José L. Figueiredo, Adrián M.T. Silva, An overview on exploration and environmental impact of unconventional gas sources and treatment options for produced water, *Journal of Environmental Management*, Volume 200, 2017, Pages 511-529, <https://doi.org/10.1016/j.jenvman.2017.06.002> .
- [91] Aamer Ali, Cejna Anna Quist-Jensen, Enrico Drioli, Francesca Macedonio, Evaluation of integrated microfiltration and membrane distillation/crystallization processes for produced water treatment, *Desalination*, Volume 434, 2018, Pages 161-168, <https://doi.org/10.1016/j.desal.2017.11.035> .

- [92] Salem Alzahrani, Abdul Wahab Mohammad, Pauzi Abdullah, Othman Jaafar, Potential tertiary treatment of produced water using highly hydrophilic nanofiltration and reverse osmosis membranes, *Journal of Environmental Chemical Engineering*, Volume 1, Issue 4, 2013, Pages 1341-1349, <https://doi.org/10.1016/j.jece.2013.10.002> .
- [93] Amit Bhatnagar, William Hogland, Marcia Marques, Mika Sillanpää, An overview of the modification methods of activated carbon for its water treatment applications, *Chemical Engineering Journal*, Volume 219, 2013, Pages 499-511, <https://doi.org/10.1016/j.cej.2012.12.038> .
- [94] Khaled Okiel, Mona El-Sayed, Mohamed Y. El-Kady, Treatment of oil–water emulsions by adsorption onto activated carbon, bentonite and deposited carbon, *Egyptian Journal of Petroleum*, Volume 20, Issue 2, 2011, Pages 9-15, <https://doi.org/10.1016/j.ejpe.2011.06.002> .
- [95] Ariyawathie G. Wathugala, Takao Suzuki, Yasushi Kurihara, Removal of nitrogen, phosphorus and COD from waste water using sand filtration system with *Phragmites Australis*, *Water Research*, Volume 21, Issue 10, 1987, Pages 1217-1224, [https://doi.org/10.1016/0043-1354\(87\)90173-4](https://doi.org/10.1016/0043-1354(87)90173-4) .
- [96] Haiqing Chang, Tong Li, Baicang Liu, Radisav D. Vidic, Menachem Elimelech, John C. Crittenden, Potential and implemented membrane-based technologies for the treatment and reuse of flowback and produced water from shale gas and oil plays: A review, *Desalination*, Volume 455, 2019, Pages 34-57, <https://doi.org/10.1016/j.desal.2019.01.001> .
- [97] Tero Luukkonen, Emma-Tuulia Tolonen, Hanna Runtti, Jaakko Pellinen, Tao Hu, Jaakko Rämö, Ulla Lassi, Removal of total organic carbon (TOC) residues from power plant make-up water by activated carbon, *Journal of Water Process Engineering*, Volume 3, 2014, Pages 46-52, <https://doi.org/10.1016/j.jwpe.2014.08.005> .
- [98] Kenji Takeuchi, Hidenori Kitazawa, Masatsugu Fujishige, Noboru Akuzawa, Josue Ortiz Medina, Aaron Morelos-Gomez, Rodolfo Cruz-Silva, Takumi Araki, Takuya Hayashi, Morinobu Endo, Oil removing properties of exfoliated graphite in actual produced water treatment, *Journal of Water Process Engineering*, Volume 20, 2017, Pages 226-231, <https://doi.org/10.1016/j.jwpe.2017.11.009> .

- [99] Johnny Gasperi, Bastien Laborie, Vincent Rocher, Treatment of combined sewer overflows by ballasted flocculation: Removal study of a large broad spectrum of pollutants, *Chemical Engineering Journal*, Volumes 211–212, 2012, Pages 293-301, <https://doi.org/10.1016/j.cej.2012.09.025> .
- [100] C.P. Huang, Chengdi Dong, Zhonghung Tang, Advanced chemical oxidation: Its present role and potential future in hazardous waste treatment, *Waste Management*, Volume 13, Issues 5–7, 1993, Pages 361-377, [https://doi.org/10.1016/0956-053X\(93\)90070-D](https://doi.org/10.1016/0956-053X(93)90070-D) .
- [101] A. Kirubakaran, Shailendra Jain, R.K. Nema, A review on fuel cell technologies and power electronic interface, *Renewable and Sustainable Energy Reviews*, Volume 13, Issue 9, 2009, Pages 2430-2440, <https://doi.org/10.1016/j.rser.2009.04.004> .
- [102] Folke Günther, Wastewater treatment by greywater separation: Outline for a biologically based greywater purification plant in Sweden, *Ecological Engineering*, Volume 15, Issues 1–2, 2000, Pages 139-146, [https://doi.org/10.1016/S0925-8574\(99\)00040-3](https://doi.org/10.1016/S0925-8574(99)00040-3) .
- [103] Mang Lu, Zhongzhi Zhang, Weiyu Yu, Wei Zhu, Biological treatment of oilfield-produced water: A field pilot study, *International Biodeterioration & Biodegradation*, Volume 63, Issue 3, 2009, Pages 316-321, <https://doi.org/10.1016/j.ibiod.2008.09.009> .
- [104] Qingxin Li, Congbao Kang, Changkai Zhang, Waste water produced from an oilfield and continuous treatment with an oil-degrading bacterium, *Process Biochemistry*, Volume 40, Issue 2, 2005, Pages 873-877, <https://doi.org/10.1016/j.procbio.2004.02.011> .
- [105] Borte Kose, Hale Ozgun, Mustafa Evren Ersahin, Nadir Dizge, Derya Y. Koseoglu-Imer, Burcu Atay, Recep Kaya, Mahmut Altınbas, Sema Sayılı, Pelin Hoshan, Doga Atay, Esra Eren, Cumali Kinaci, Ismail Koyuncu, Performance evaluation of a submerged membrane bioreactor for the treatment of brackish oil and natural gas field produced water, *Desalination*, Volume 285, 2012, Pages 295-300, <https://doi.org/10.1016/j.desal.2011.10.016> .
- [106] Yaxue Lin, Yuting Jia, Guruprasad Alva, Guiyin Fang, Review on thermal conductivity enhancement, thermal properties and applications of phase change materials in thermal energy storage, *Renewable and Sustainable Energy Reviews*, Volume 82, Part 3, 2018, Pages 2730-2742, <https://doi.org/10.1016/j.rser.2017.10.002> .

- [107] Soteris A. Kalogirou, Solar thermal collectors and applications, *Progress in Energy and Combustion Science*, Volume 30, Issue 3, 2004, Pages 231-295, <https://doi.org/10.1016/j.pecs.2004.02.001> .
- [108] Xinzhi Wang, Yurong He, Xing Liu, Lei Shi, Jiaqi Zhu, Investigation of photothermal heating enabled by plasmonic nanofluids for direct solar steam generation, *Solar Energy*, Volume 157, 2017, Pages 35-46, <https://doi.org/10.1016/j.solener.2017.08.015> .
- [109] Ehsanul Kabir, Pawan Kumar, Sandeep Kumar, Adedeji A. Adelodun, Ki-Hyun Kim, Solar energy: Potential and future prospects, *Renewable and Sustainable Energy Reviews*, Volume 82, Part 1, 2018, Pages 894-900, <https://doi.org/10.1016/j.rser.2017.09.094>.
- [110] Abdul Wahab, Ali Hassan, Muhammad Arslan Qasim, Hafiz Muhammad Ali, Hamza Babar, Muhammad Usman Sajid, Solar energy systems – Potential of nanofluids, *Journal of Molecular Liquids*, Volume 289, 2019, 111049, <https://doi.org/10.1016/j.molliq.2019.111049> .
- [111] Xinzhi Wang, Yurong He, Xing Liu, Lei Shi, Jiaqi Zhu, Investigation of photothermal heating enabled by plasmonic nanofluids for direct solar steam generation, *Solar Energy*, Volume 157, 2017, Pages 35-46, <https://doi.org/10.1016/j.solener.2017.08.015> .
- [112] Yang Fu, Tao Mei, Gang Wang, Ankang Guo, Guangchao Dai, Sheng Wang, Jianying Wang, Jinhua Li, Xianbao Wang, Investigation on enhancing effects of Au nanoparticles on solar steam generation in graphene oxide nanofluids, *Applied Thermal Engineering*, Volume 114, 2017, Pages 961-968, <https://doi.org/10.1016/j.applthermaleng.2016.12.054> .
- [113] Lei Shi, Yurong He, Yimin Huang, Baocheng Jiang, Recyclable Fe₃O₄@CNT nanoparticles for high-efficiency solar vapor generation, *Energy Conversion and Management*, Volume 149, 2017, Pages 401-408, <https://doi.org/10.1016/j.enconman.2017.07.044>.
- [114] Xinzhi Wang, Yurong He, Xing Liu, Jiaqi Zhu, Enhanced direct steam generation via a bio-inspired solar heating method using carbon nanotube films, *Powder Technology*, Volume 321, 2017, Pages 276-285, <https://doi.org/10.1016/j.powtec.2017.08.027> .
- [115] Haichuan Jin, Guiping Lin, Lizhan Bai, Aimen Zeiny, Dongsheng Wen, Steam generation in a nanoparticle-based solar receiver, *Nano Energy*, Volume 28, 2016, Pages 397-406, <https://doi.org/10.1016/j.nanoen.2016.08.011> .

- [116] Haoran Li, Yurong He, Ziyu Liu, Yimin Huang, Baocheng Jiang, Synchronous steam generation and heat collection in a broadband Ag@TiO₂ core-shell nanoparticle-based receiver, *Applied Thermal Engineering*, Volume 121, 2017, Pages 617-627, <https://doi.org/10.1016/j.applthermaleng.2017.04.102> .
- [117] Jian Huang, Yurong He, Meijie Chen, Baocheng Jiang, Yimin Huang, Solar evaporation enhancement by a compound film based on Au@TiO₂ core-shell nanoparticles, *Solar Energy*, Volume 155, 2017, Pages 1225-1232, <https://doi.org/10.1016/j.solener.2017.07.070> .
- [118] Hongyang Wei, Huawen Hu, Menglei Chang, Yuyuan Zhang, Dongchu Chen, Meifeng Wang, Improving solar thermal absorption of an anodic aluminum oxide-based photonic crystal with Cu-Ni composite nanoparticles, *Ceramics International*, Volume 43, Issue 15, 2017, Pages 12472-12479, <https://doi.org/10.1016/j.ceramint.2017.06.117> .
- [119] Gang Wang, Yang Fu, Xiaofei Ma, Wenbo Pi, Dengwu Liu, Xianbao Wang, Reusable reduced graphene oxide based double-layer system modified by polyethylenimine for solar steam generation, *Carbon*, Volume 114, 2017, Pages 117-124, <https://doi.org/10.1016/j.carbon.2016.11.071> .
- [120] George Ni, Nenad Miljkovic, Hadi Ghasemi, Xiaopeng Huang, Svetlana V. Boriskina, Cheng-Te Lin, Jianjian Wang, Yanfei Xu, Md. Mahfuzur Rahman, TieJun Zhang, Gang Chen, Volumetric solar heating of nanofluids for direct vapor generation, *Nano Energy*, Volume 17, 2015, Pages 290-301, <https://doi.org/10.1016/j.nanoen.2015.08.021> .
- [121] Xinzhi Wang, Yurong He, Gong Cheng, Lei Shi, Xing Liu, Jiaqi Zhu, Direct vapor generation through localized solar heating via carbon-nanotube nanofluid, *Energy Conversion and Management*, Volume 130, 2016, Pages 176-183, <https://doi.org/10.1016/j.enconman.2016.10.049> .
- [122] Roberto Gómez-Villarejo, Elisa I. Martín, Javier Navas, Antonio Sánchez-Coronilla, Teresa Aguilar, Juan Jesús Gallardo, Rodrigo Alcántara, Desiré De los Santos, Iván Carrillo-Berdugo, Concha Fernández-Lorenzo, Ag-based nanofluidic system to enhance heat transfer fluids for concentrating solar power: Nano-level insights, *Applied Energy*, Volume 194, 2017, Pages 19-29, <https://doi.org/10.1016/j.apenergy.2017.03.003> .

- [123] Vishal Bhalla, Himanshu Tyagi, Parameters influencing the performance of nanoparticles-laden fluid-based solar thermal collectors: A review on optical properties, *Renewable and Sustainable Energy Reviews*, Volume 84, 2018, Pages 12-42, <https://doi.org/10.1016/j.rser.2017.12.007> .
- [124] Dawid Janas, Stefanie K. Kreft, Krzysztof K.K. Koziol, Steam reforming on reactive carbon nanotube membranes, *Journal of Industrial and Engineering Chemistry*, Volume 25, 2015, Pages 222-228, <https://doi.org/10.1016/j.jiec.2014.10.038> .
- [125] Bindu Sharma, M.K. Rabinal, Plasmon based metal-graphene nanocomposites for effective solar vaporization, *Journal of Alloys and Compounds*, Volume 690, 2017, Pages 57-62, <https://doi.org/10.1016/j.jallcom.2016.07.330> .
- [126] Zhaolong Wang, Xiaojun Quan, Zhuomin Zhang, Ping Cheng, Optical absorption of carbon-gold core-shell nanoparticles, *Journal of Quantitative Spectroscopy and Radiative Transfer*, Volume 205, 2018, Pages 291-298, <https://doi.org/10.1016/j.jqsrt.2017.08.001> .
- [127] Desong Fan, Qiang Li, Weibing Chen, Jia Zeng, Graphene nanofluids containing core-shell nanoparticles with plasmon resonance effect enhanced solar energy absorption, *Solar Energy*, Volume 158, 2017, Pages 1-8, <https://doi.org/10.1016/j.solener.2017.09.031> .
- [128] Muhammad Amjad, Ghulam Raza, Yan Xin, Shahid Pervaiz, Jinliang Xu, Xiaoze Du, Dongsheng Wen, Volumetric solar heating and steam generation via gold nanofluids, *Applied Energy*, Volume 206, 2017, Pages 393-400, <https://doi.org/10.1016/j.apenergy.2017.08.144> .
- [129] Jianhua Zhou, Yufei Gu, Ziyang Deng, Lei Miao, Hui Su, Pengfei Wang, Jiaqi Shi, The dispersion of Au nanorods decorated on graphene oxide nanosheets for solar steam generation, *Sustainable Materials and Technologies*, Volume 19, 2019, e00090, <https://doi.org/10.1016/j.susmat.2018>.
- [130] Xinzhi Wang, Yurong He, Xing Liu, Jiaqi Zhu, Enhanced direct steam generation via a bio-inspired solar heating method using carbon nanotube films, *Powder Technology*, Volume 321, 2017, Pages 276-285, <https://doi.org/10.1016/j.powtec.2017.08.027> .
- [131] Haichuan Jin, Guiping Lin, Lizhan Bai, Aimen Zeiny, Dongsheng Wen, Steam generation in a nanoparticle-based solar receiver, *Nano Energy*, Volume 28, 2016, Pages 397-406, <https://doi.org/10.1016/j.nanoen.2016.08.011> .

- [132] Haoran Li, Yurong He, Ziyu Liu, Yimin Huang, Baocheng Jiang, Synchronous steam generation and heat collection in a broadband Ag@TiO₂ core-shell nanoparticle-based receiver, *Applied Thermal Engineering*, Volume 121, 2017, Pages 617-627, <https://doi.org/10.1016/j.applthermaleng.2017.04.102> .
- [133] Jian Huang, Yurong He, Meijie Chen, Baocheng Jiang, Yimin Huang, Solar evaporation enhancement by a compound film based on Au@TiO₂ core-shell nanoparticles, *Solar Energy*, Volume 155, 2017, Pages 1225-1232, <https://doi.org/10.1016/j.solener.2017.07.070> .
- [134] Hongyang Wei, Huawen Hu, Menglei Chang, Yuyuan Zhang, Dongchu Chen, Meifeng Wang, Improving solar thermal absorption of an anodic aluminum oxide-based photonic crystal with Cu-Ni composite nanoparticles, *Ceramics International*, Volume 43, Issue 15, 2017, Pages 12472-12479, <https://doi.org/10.1016/j.ceramint.2017.06.117> .
- [135] Gang Wang, Yang Fu, Xiaofei Ma, Wenbo Pi, Dengwu Liu, Xianbao Wang, Reusable reduced graphene oxide based double-layer system modified by polyethylenimine for solar steam generation, *Carbon*, Volume 114, 2017, Pages 117-124, <https://doi.org/10.1016/j.carbon.2016.11.071> .
- [136] George Ni, Nenad Miljkovic, Hadi Ghasemi, Xiaopeng Huang, Svetlana V. Boriskina, Cheng-Te Lin, Jianjian Wang, Yanfei Xu, Md. Mahfuzur Rahman, TieJun Zhang, Gang Chen, Volumetric solar heating of nanofluids for direct vapor generation, *Nano Energy*, Volume 17, 2015, Pages 290-301, <https://doi.org/10.1016/j.nanoen.2015.08.021> .
- [137] Xinzhi Wang, Yurong He, Gong Cheng, Lei Shi, Xing Liu, Jiaqi Zhu, Direct vapor generation through localized solar heating via carbon-nanotube nanofluid, *Energy Conversion and Management*, Volume 130, 2016, Pages 176-183, <https://doi.org/10.1016/j.enconman.2016.10.049> .
- [138] Roberto Gómez-Villarejo, Elisa I. Martín, Javier Navas, Antonio Sánchez-Coronilla, Teresa Aguilar, Juan Jesús Gallardo, Rodrigo Alcántara, Desiré De los Santos, Iván Carrillo-Berdugo, Concha Fernández-Lorenzo, Ag-based nanofluidic system to enhance heat transfer fluids for concentrating solar power: Nano-level insights, *Applied Energy*, Volume 194, 2017, Pages 19-29, <https://doi.org/10.1016/j.apenergy.2017.03.003> .

- [139] Sainan Ma, Chun Pang Chiu, Yujiao Zhu, Chun Yin Tang, Hui Long, Wayesh Qarony, Xinhua Zhao, Xuming Zhang, Wai Hung Lo, Yuen Hong Tsang, Recycled waste black polyurethane sponges for solar vapor generation and distillation, *Applied Energy*, Volume 206, 2017, Pages 63-69, <https://doi.org/10.1016/j.apenergy.2017.08.169> .
- [140] Jian Huang, Yurong He, Li Wang, Yimin Huang, Baocheng Jiang, Bifunctional Au@TiO₂ core-shell nanoparticle films for clean water generation by photocatalysis and solar evaporation, *Energy Conversion and Management*, Volume 132, 2017, Pages 452-459, <https://doi.org/10.1016/j.enconman.2016.11.053> .
- [141] Panpan Zhang, Qihua Liao, Houze Yao, Yaxin Huang, Huhu Cheng, Liangti Qu, Direct solar steam generation system for clean water production, *Energy Storage Materials*, Volume 18, 2019, Pages 429-446, <https://doi.org/10.1016/j.ensm.2018.10.006> .
- [142] Heinrich Badenhorst, A review of the application of carbon materials in solar thermal energy storage, *Solar Energy*, 2018, <https://doi.org/10.1016/j.solener.2018.01.062> .
- [143] Yoshitaka Ueki, Takashi Aoki, Kenta Ueda, Masahiko Shibahara, Thermophysical properties of carbon-based material nanofluid, *International Journal of Heat and Mass Transfer*, Volume 113, 2017, Pages 1130-1134, <https://doi.org/10.1016/j.ijheatmasstransfer.2017.06.008> .
- [144] John Collins, Gerald Gourdin, Deyang Qu, Chapter 3.23 - Modern Applications of Green Chemistry: Renewable Energy, Editor(s): Béla Török, Timothy Dransfield, *Green Chemistry*, Elsevier, 2018, Pages 771-860, <https://doi.org/10.1016/B978-0-12-809270-5.00028-5> .
- [145] Roberto C. Dante, 7 - Carbon materials, Editor(s): Roberto C. Dante, *Handbook of Friction Materials and their Applications*, Woodhead Publishing, 2016, Pages 93-103, <https://doi.org/10.1016/B978-0-08-100619-1.00007-9> .
- [146] Mauro C. dos Santos, Marlon C. Maynart, Luci R. Aveiro, Edson C. da Paz, Victor dos Santos Pinheiro, *Carbon-Based Materials: Recent Advances, Challenges, and Perspectives*, Reference Module in Materials Science and Materials Engineering, Elsevier, 2017, <https://doi.org/10.1016/B978-0-12-803581-8.09262-6>.